The Complex *Kaposin* Locus of Kaposi's Sarcoma-Associated Herpesvirus: Defining a New Role in the Lytic Viral Replication Cycle

by

Grant MacNeil

Submitted in partial fulfilment of the requirements
for the degree of Master of Science

at

Dalhousie University
Halifax, Nova Scotia
March 2019

TABLE OF CONTENTS

LIST OF TABLES

LIST OF FIGURES

ABSTRACT

Kaposi's sarcoma-associated herpesvirus (KSHV) is the etiologic agent of the endothelial cell (EC) cancer, Kaposi's sarcoma, and two B-cell malignancies. In infected cells, the virus exists in two states; the latent program alters cell morphology and inflammatory gene expression, while the lytic cycle produces new virus and promotes tumorigenesis in a paracrine manner. The kaposin locus, located in the latent gene cluster, generates multiple transcripts and gene products in both viral states; however, its function remains unclear. I developed a library of novel recombinant viruses to mutagenize kaposin coding capacity and investigate protein-specific effects during each viral life cycle. I found that while entry and latent gene expression were unaffected by kaposin mutagenesis, the ability to reprogram ECs may be impaired. Furthermore, I identified defects in lytic viral gene expression and virion production in some kaposin-mutant viruses, leading me to suggest new roles for the kaposins in lytic cycle progression.

LIST OF ABBREVIATIONS USED

AIDS	Acquired immunodeficiency syndrome
AP-1	Activator protein-1
ARE	AU-rich element
BAC	Bacterial artificial chromosome
BCBL	Body cavity-based lymphoma
BEC	Blood vascular endothelial cell
bp	Base pairs
CAMK	Ca^{2+}/calmodulin-dependent protein kinase
cART	Combination antiretroviral therapy
CDK	Cyclin-dependent kinase
C/EBPα	CCAAT/enhancer-binding protein α
CGEB	Centre for Comparative Genomics and Evolutionary Bioinformatics
CHIP	Chromatin immunoprecipitation
DAPI	4',6-diamidino-2-phenylindole, dihydrochloride
dsDNA	Double-stranded deoxyribonucleic acid
DMEM	Dulecco's minimal essential medium
DMVEC	Dermal vascular endothelial cells
Dox	Doxycycline
DR	Direct repeats
DTT	1,4-Dithiothreitol
EBV	Epstein-Barr virus
FBS	Fetal bovine serum

FLICE	Fas-associated protein with death domain-like interleukin-1β-converting enzyme
FLIP	FLICE/caspase-8-inhibitory protein
FSC	Forward scatter
gB,gH/L	Glycoproteins B, H/L
GFP	Green fluorescent protein
GM-CSF	Granulocyte/macrophage colony-stimulating factor
GTPase	Guanosine triphosphatase
HAT	Histone acetylase
HDAC	Histone deacetylase
HEK	Human embryonic kidney
HHV	Human herpesvirus
HI-FBS	Heat-inactivated FBS
HIV	Human immunodeficiency virus
hpi	Hours post-induction, hours post-infection
HRP	Horseradish peroxidase
HUVEC	Human umbilical vein endothelial cells
HVS	Herpesvirus saimiri
IE-, E-, L-	Immediate early-, early-, late-genes
IKK	IκB kinase
IL-1α, -1β, -6	Interleukin-1alpha, -1beta, -6
IMR	Integrated Microbiome Resource
INF-γ	Interferon-gamma
IRES	Internal ribosome entry site

KapA, B, C	Kaposin A, B, C
kb	Kilobase pairs
KS	Kaposi's sarcoma
KSHV	Kaposi's sarcoma-associated herpesvirus
LANA	Latency-associated nuclear antigen
LB	Luria broth
LEC	Lymphatic endothelial cell
LT_d	Downstream latent promoter
MAPK	Mitogen-activated protein kinase
MCD	Multicentric Castleman's disease
MCM	Mini-chromosome maintenance
MCP	Major capsid protein
MHV	Murine gamma-herpesvirus
mRNA	Messenger-RNA
miRNA, miR-	Micro-RNA
MSM	Men who have sex with men
NaB	Sodium butyrate
NF- κB	Nuclear factor-kappa B
Ori-(Lyt)	Origin of (lytic) replication
ORC	Origin replication complex
ORF	Open reading frame
PAA	Phosphonoacetic acid
PAGE	Polyacrylamide gel electrophoresis

PAN	Polyadenylated nuclear RNA
PB	Processing body
PBS	Phosphate-buffered saline
PCR	Polymerase chain reaction
PEL	Primary effusion lymphoma
PFGE	Pulsed-field gel electrophoresis
PKC	Protein kinase C
PSQ	Penicillin/streptomycin/glutamine
qPCR	Quantitative PCR
RBP-Jκ	Recombinant signal sequence-binding protein-J kappa
RFP	Red fluorescent protein
RNA	Ribonucleic acid
RRE	RTA-responsive element
RTA	Replication and transcription activator
SCP	Small capsid protein
SDS	Sodium dodecyl sulfate
SSC	Side scatter
TBE	Tris/borate/EDTA
TBS-T	Tris-buffered saline/Tween-20
TGF-β	Transforming growth factor-beta
TGN	*Trans*-Golgi network
TNF	Tumour necrosis factoor
TRE	Tetracycline-responsive element

TPA	12-O-tetradecanoylphorbol-13-acetate
TR	Terminal repeats
TREx	Tetracycline-responsive element
UTR	Untranslated region
vCCL-1, -2, -3	Viral CC-chemokine ligand-1, -2, -3
vFLIP	Viral FLIP
vIL-6	Viral IL-6
VEGF	Vascular endothelial growth factor
YAC	Yeast artificial chromosome

ACKNOWLEDGEMENTS

I have been blessed to have been surrounded by many people throughout the course of my degree to whom I am very grateful; this work would not have been possible without them.

There are not enough words with which to express my gratitude to my supervisor, Dr. Jennifer Corcoran. Her unwavering support, guidance and dedication to provide nothing but the best in learning opportunities have made this experience exceptionally special. Thank you for being an amazing source of inspiration and for teaching me to reach for goals that are never beyond my own 'control'.

I am very appreciative to have a passionate and thoughtful supervisory committee. A big thank you to my co-supervisor, Dr. Craig McCormick, for his invaluable expertise and an enthusiasm for new ideas that is truly infectious. Thank you to Dr. Jan Rainey and Dr. David Langelaan, both of whom provided a wealth of knowledge, keen eyes, and kind support to my project.

I have had the pleasure to meet many amazing people throughout my time in Halifax. A huge thank you to the Corcoran-Weeks lab, especially Gill, Kathleen, Carolyn, and Beth for not only providing a positive work environment, but also great friendship. Thank you to the McCormick lab, with special thanks to Eric Pringle, for his advice, patience, and eagerness to help with my project. Jordan and Jamie, thank you for your encouragement and for always being there to help me enjoy the melody amidst a racket.

Lastly, I would like to thank my family who have always believed in me and have been a steady stream of support. To my parents, Gary and Sue, who have and always will be my greatest teachers, I am deeply indebted to you.

CHAPTER 1: INTRODUCTION

1.1 The Human Herpesviruses

Herpesviruses are known to establish long-lasting and complex relationships with their hosts and have evolved over time to infect a diverse range of species, including humans. This evolution has provided an advantageous capacity for these intracellular obligate parasites to manipulate their hosts in order to evade immune detection as well as sequester and prioritize host machinery for their own persistence. Viruses that establish such a relationship with their hosts are relatively clinically benign, however, as is the case with human herpesviruses, infections may be life-long with symptoms that can vary from mild to severe, depending on the virus-host interactions (Grinde, 2013).

As a part of their genomes, herpesviruses encode many unique features to subvert their hosts and ensure their persistence and replication. However, replication of the virus is kept in check by innate cell and host immunity. This presents a complex balance that must exist between the virus and immune surveillance (Grinde, 2013). All herpesviruses have the characteristic ability to enter a biphasic life cycle; this allows them to enter either a period of latency, where no progeny virus is produced and immune detection is limited, or a stage of lytic production, where virus replication is activated. Each herpesvirus has a unique set of circumstances that it must overcome, such as cell tropism and intracellular conditions, to orchestrate both virus life cycles successfully, presenting a diverse range of disease associated with human herpesviruses. Nevertheless, these viruses have conserved structures and mechanisms for entry and egress that have provided us with a better understanding of their pathogenicity.

Within the *Herpesviridae* family are three phylogenetic subfamilies that are classified based on their biological properties: alpha-, beta-, and gamma-herpesvirinae (Pellett & Roizman, 2013). Alpha-herpesviruses preferentially establish latency in neurons, while beta- and gamma-herpesviruses show a tropism for lymphoid tissue and establish latency in T or B lymphocytes with varying ranges of specificity (Pellett & Roizman 2013). Classified accordingly within these subfamilies are the eight human herpesviruses (HHVs). While the human alpha- and beta-herpesviruses are associated with prevalent diseases, the primary focus of this study will be the gamma-herpesviruses, which include human herpesviruses-4 and -8 (HHV-4, HHV-8), more commonly known as Epstein-Barr virus (EBV) and Kaposi's sarcoma associated herpesvirus (KSHV).

1.1.1 Structure

Herpesviruses characteristically have large (124-295 kilobase pair [kb]), linear double-stranded DNA (dsDNA) genomes and are packaged inside an icosahedral protein coat, called the capsid (Pellett & Roizman, 2013). Surrounding the capsid is a lipid bilayer envelope derived from cellular membranes, embedded in which are viral glycoproteins that serve as virus-host attachments during entry (Pellett & Roizman, 2013). Distributed between the capsid and envelope is a dense tegument compartment; this partially ordered structure varies in size and is composed of both viral and cellular encoded proteins acquired during assembly and release of the virus from its previous infected host (Pellett & Roizman, 2013; reviewed in Guo et al., 2010). Tegument proteins have the potential to act immediately upon membrane fusion with newly infected cells and are involved in multiple processes of the virus life cycle such as capsid transport to the nucleus and modulation of

host signaling and innate immunity (Guo et al., 2010). Each ~200 nm infectious unit, termed the virion, is relatively conserved across all human herpesviruses, with slight variations providing functional and pathogenic differences specific to each virus (Pellett & Roizman, 2013).

1.1.2 Cell Tropism and Entry

Entry of herpesviruses into their host cell is determined by interactions between cell surface receptors and the attachment glycoproteins embedded in the viral lipid envelope (reviewed in Heldwein & Krummenacher, 2008). The core machinery for all herpesviruses to mediate attachment and fusion of the viral envelope with host membranes are glycoprotein B (gB) and a heterodimer of glycoprotein H and L (gH/gL) (Heldwein & Krummenacher, 2008). Herpesvirus entry mechanisms differ slightly depending on cell type, but generally follow a stepwise progression of: 1) initial reversible attachment with heparan sulfate on cell surface proteoglycans, 2) irreversible binding between specific types of host integrins and glycoproteins, 3) cell signaling events leading to endocytosis of the bound virion, and 4) conformational changes to gB and/or gH/gL that are triggered by receptor-binding or low pH from endosomal acidification (Figure 1.1) (Heldwein & Krummenacher, 2008). This step-wise progression leads to the release of viral capsids into the cell cytoplasm, readying the capsid for delivery of its genome to the correct subcellular compartment required for latency.

Retrograde transport of viral capsids to the nucleus is necessary for the establishment of latency; this process is dependent on microtubules and their associated motor proteins, dyneins (Figure 1.1) (reviewed in Miranda-Saksena et al., 2018). Docking

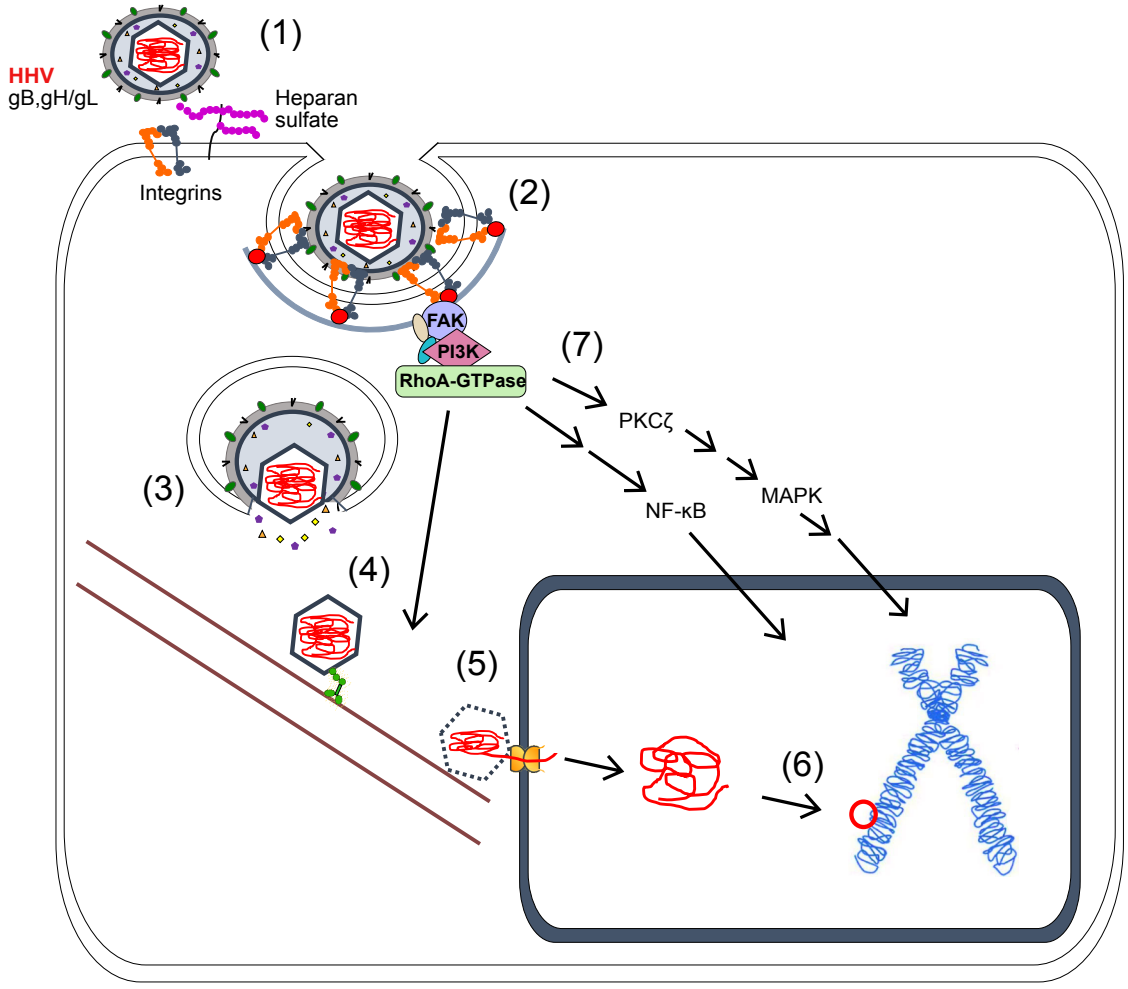

Figure 1.1: Entry and capsid delivery of herpesviruses. Schematic diagram depicting the attachment and uncoating steps of viral entry for human herpesviruses (HHVs). (1) Weak initial attachment with heparan sulfate leads to stronger interaction between viral glycoproteins, gB and gH/gL, with cell surface receptors, such as integrins. (2) Clathrin-mediated endocytosis leads to the vesicular internalization of the virion. (3) Fusion of the virion envelope with the endocytic membrane occurs via conformational changes in receptor and/or irreversibly-bound glycoprotein, initiated by acidification of the endocytic vesicle. (4) Trafficking of the viral capsid to the nucleus is facilitated by dyneins, microtubules, and viral tegument proteins released during fusion; this results in (5) docking of the capsid at the nuclear pore complex, capsid disassembly, and release of the viral genome into the nucleus where it (6) establishes latency as a circular episome attached to host chromatin. (7) Receptor binding leads to the activation of cell signaling pathways, such as FAK, PI3K, and RhoA-GTPases, that facilitate trafficking and viral gene expression through the activation of effector molecules, including factors that induce transcriptional activity, such as the NF-κB and MAPK pathways. Adapted from Kumar and Chandran, 2016.

of the capsid with the nuclear pore complex leads to capsid disassembly and delivery of the viral dsDNA genome into the nucleus where it can establish a latent infection (Figure 1.1) (reviewed in Fay & Panté, 2015). During entry, herpesviruses also activate host signaling events that can facilitate trafficking to the nucleus; for example, integrin receptor binding by human herpesvirus-8 (HHV-8) leads to the activation of RhoA- guanosine triphosphatases (GTPases), causing acetylation and aggregation of microtubules, and accelerating transport to the nucleus (Naranatt et al., 2005). This activity is mediated by many host signaling pathways that are activated by gB-integrin binding; these include focal adhesion kinase (FAK), phosphatidylinositol-3-kinase (PI3K), and protein kinase C-zeta (PKCζ), which in turn also lead to the downstream induction of transcription factors that modulate host gene expression in preparation for the establishment of latency (Figure 1.1) (reviewed in Kumar & Chandran, 2016). Transcriptional activity following entry has been associated with induction of both the mitogen-activated protein kinase (MAPK) and nuclear factor kappa B (NF-κB) pathways (Figure 1.1) (Kumar & Chandran, 2016).

Upon delivery to the nucleus, the linear viral genome is circularized to form an episome that becomes tethered to host chromatin (Figure 1.1) (Deshmane & Fraser, 1989). The virus then enters a latent program that is characterized by the limited expression of viral genes and a reliance on cellular machinery for episome persistence (Grinde, 2013). Mechanisms for the establishment of latency are virus- and cell-type specific; while some processes are generally conserved amongst most herpesviruses, additional details that are specific to HHV-8 latency will be discussed in later sections.

1.1.3 Assembly & Egress

A key characteristic of all herpesviruses is the ability to reactivate from latency; this program, herein referred to as the lytic cycle, involves the replication of the viral genome, assembly of capsid-enclosed linear dsDNA structures, and anterograde trafficking to the cell plasma membrane for virion release (Figure 1.2). Throughout the lytic cycle, viral gene expression is significantly upregulated from latency such that all viral genes are expressed to facilitate the complex processes of replication, assembly, and egress. Lytic gene function is temporally regulated by a cascade of viral gene expression; the sequential transcription of three distinct classes, immediate-early, early, and late viral genes, leads to successful production of herpes-virions (Honess & Roizman, 1974). These three classes will be discussed in specific detail as they pertain to HHV-8 in later sections.

Generally, lytic genome replication proceeds through a combination of mechanisms that result in the exponential accumulation of viral DNA (reviewed in Rennekamp & Lieberman, 2010). Similar to Lambda-bacteriophage, a dual-mechanism has been proposed by which replication initiates in a bi-directional manner that later transitions to a rolling-circle mechanism (Figure 1.2) (Rennekamp & Lieberman, 2010). This model is evidenced by intermediates with multiple replication forks and the production of head-to-tail repeats of the linear viral genome, termed concatemers (Bermek et al., 2015; Poffenberger & Roizman, 1985). Successful replication involves concatemeric DNA being cleaved into individual virion DNA subunits that can then be packaged into capsids (Deiss & Frenkel, 1986).

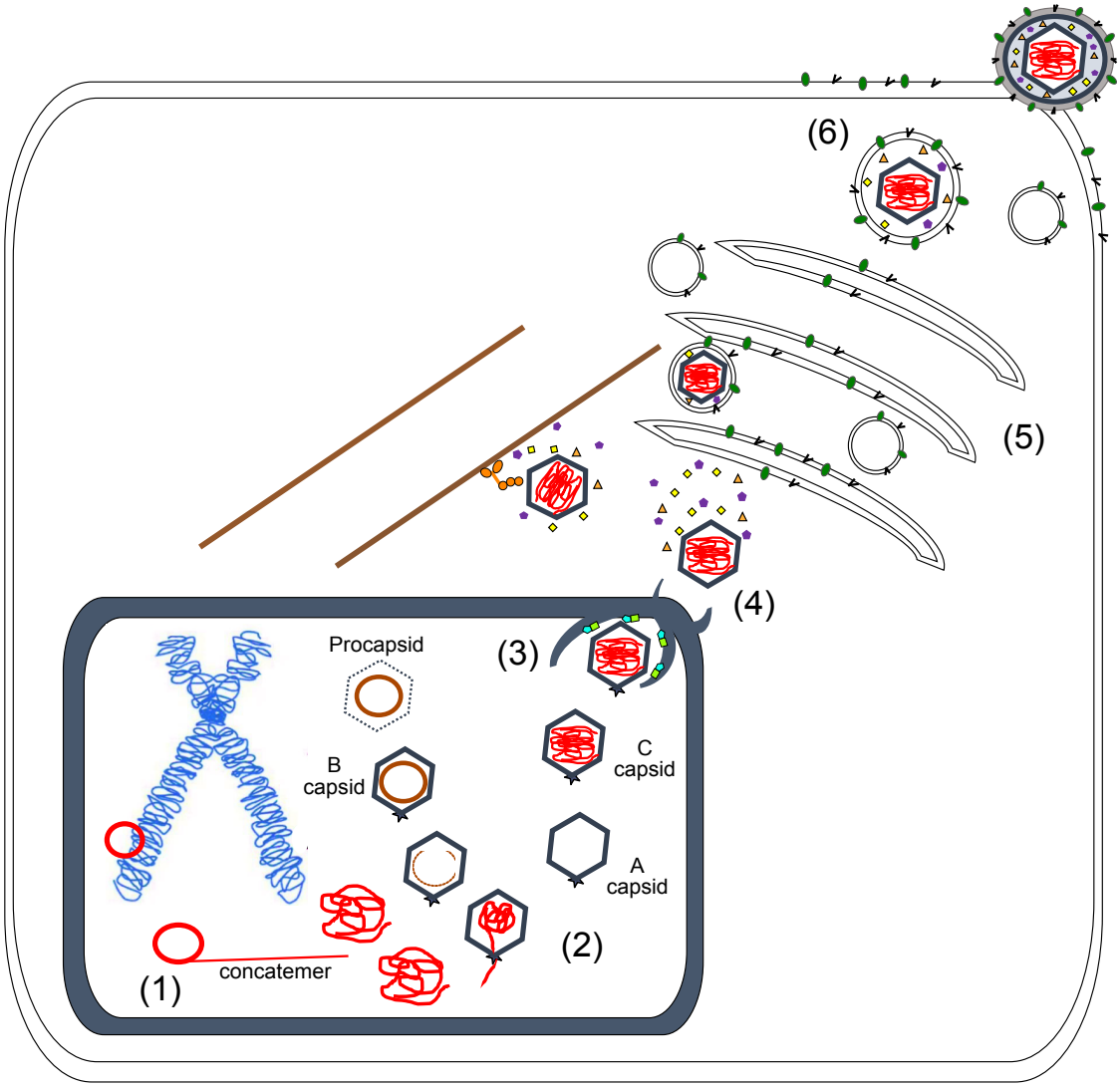

Figure 1.2: Assembly and egress of herpesviruses. Schematic diagram depicting the steps of genome replication, capsid assembly, and egress of human herpesviruses during the lytic cycle. (1) Lytic viral genome replication initiates in a bi-directional manner that transitions to a rolling circle mechanism, generating long head-to-tail repeats of viral dsDNA, called concatemers. (2) Cleavage of concatemeric DNA into single genome units allows for them to be injected into capsids via the portal vertex. Procapsids and B-capsids must be processed to remove the scaffold protein prior to DNA packaging. (3) C-capsids containing viral DNA accumulate at evaginations of the inner nuclear membrane caused by the heterodimer nuclear egress complex. (4) Envelopment and de-envelopment through the nuclear membrane releases the capsids into the cytoplasm where it interacts with tegument proteins. (5) The capsids traffic via microtubules and vesicles of the *trans*-Golgi network to the plasma membrane, acquiring along the way a glycoprotein-containing membrane envelope. (6) The assembled virion is released from the plasma membrane to infect a new cell either by direct cell-to-cell spread or release into the extracellular environment.

Assembly of all non-enveloped capsids begins in the nucleus. In infected cells, capsids can exist in three forms: A-, B-, and C-capsids; the distinction between capsid classifications indicates whether proper capsid assembly and genome packaging has occurred (Figure 1.2) (Nealson et al., 2001; Pellett & Roizman, 2013). The assembly pathway, which also resembles that of dsDNA bacteriophages, initiates by the formation of a spherical 'procapsid' intermediate in the nucleus of the host cell (Newcomb et al., 1996). A core of scaffold protein interacts with major capsid proteins that compose the sides, faces, and vertices of the icosahedron (Newcomb et al., 1996). The portal complex assembles at one of the 12 vertices of the icosahedron and is responsible for injecting the viral dsDNA into the capsid (Newcomb et al., 2003). Stabilization of the capsid shell leads to the scaffold being degraded and ejected from the procapsid, allowing for subsequent entry of the viral DNA through the portal complex and formation of a complete capsid (Newcomb et al., 1996; reviewed in Homa & Brown, 1997). C-capsids are the result of proper packaging and contain viral DNA, whereas A- and B-capsids are considered failed and immature versions of capsids, respectively, due to their lack of DNA (Perdue et al., 1975; Newcomb & Brown, 1991). B-capsids, which still contain the cleaved scaffold protein, are thought to be able to package DNA and mature into infectious virions, whereas A-capsids that do not contain either DNA or the scaffold protein are thought to result from failures in DNA packaging (Newcomb & Brown, 1991).

Final assembly of virions occurs in the cell cytoplasm; in order to achieve this, the large ~125nm nucleocapsid, which cannot fit through nuclear pores, must be moved across the nuclear membrane (Johnson & Baines, 2011). This process involves a complex rearrangement and dissolution of the nuclear lamina, formation of a heterodimer nuclear

egress complex, and the generation of vesicles that facilitate budding from the inner nuclear membrane, all of which is orchestrated by viral-encoded proteins (Figure 1.2) (reviewed in Johnson & Baines, 2011; Roller & Baines, 2017). At this stage of primary envelopment, the capsid undergoes de-envelopment through fusion of the virion envelope with the outer nuclear membrane, releasing the capsid into the cytoplasm (Johnson & Baines, 2011). It is here that the capsid accumulates tegument proteins and undergoes secondary envelopment by budding into the *trans*-Golgi network (TGN), using cellular machinery for exocytosis and vesicular traffic to the plasma membrane for final virion release (Figure 1.2) (Johnson & Baines, 2011). Again, this process is facilitated by viral-encoded proteins that extensively alter TGN composition and trafficking to favour the accumulation of membranes that contain embedded virion glycoproteins (Campadelli, et al. 1993).

Despite some differences in cell tropism and certain aspects of their life cycles, herpesviruses demonstrate conserved mechanisms to ensure the successful establishment and progression of their latent and lytic life cycles, respectively. These viruses use a unique combination of cellular- and viral-encoded machinery to achieve a balance between inactive and active periods of virion production, presenting a complex relationship between herpesviruses and host innate immune surveillance.

1.2 Kaposi's Sarcoma-associated Herpesvirus

1.2.1 Disease Associations

1.2.1.1 Kaposi's Sarcoma

The classic form of Kaposi's sarcoma (KS) was first described by Moritz Kaposi in 1872 as a clinical condition that affected men over forty years of age and presented as

"idiopathic multiple pigmented sarcomas of the skin" in the lower limbs (Antman & Chang, 2000). KS tumours were primarily seen in elderly men of Eastern European (Ashkenzai) Jewish and Mediterranean origins; the condition commonly initiated as purple-blue or red-brown flat lesions on hands and feet but could progress to affect the mucosa, gastrointestinal tract, and lymph nodes (Antman & Chang, 2000; Vangipuram & Tyring, 2018). An endemic form of KS was described in the 1960s in Sub-Saharan Africa, affecting men, women and children, and ranging in severity from benign cutaneous nodules, similar to classic KS, to aggressive invasion of the viscera and lymphoreticular system (Taylor et al., 1971; Antman & Chang, 2000). Soon after, KS tumours were being observed in patients elsewhere in the world that were undergoing solid-organ transplants and receiving immunosuppressive agents, suggestive of an association between KS and immunodeficiency (Klepp et al., 1978; Stribling et al., 1978). What had once been a rare malignancy in North America and Europe, KS was beginning to be reported as an aggressive disease with rising incidence in young homosexual men in the United States circa the early 1980s (Friedman-Kien, 1981; Centers for Disease Control, 1981). The increased prevalence of KS paralleled the rise in acquired immunodeficiency syndrome (AIDS) cases among populations of men having sex with men (MSM). A relationship was shortly established between KS and infections involving the newly discovered human immunodeficiency virus (HIV); however, the incidence of KS was much higher in HIV-infected MSM than in other HIV risk groups, such as injection drug users, inciting the search for an alternative sexually-transmitted agent (Bhutani et al., 2015).

Human herpesvirus 8 (HHV-8), also known as Kaposi's sarcoma-associated herpesvirus (KSHV), was identified as the causative agent of KS; 95% of cells in KS

lesions, regardless of clinical subtype, were identified as having viral DNA-sequences that were absent in normal tissue (Chang et al., 1994; Antman & Chang, 2000). While KSHV infection is necessary for KS development, it is insufficient to cause tumourigenesis. Co-infection with HIV-1 and immunodeficiency have been shown to be sufficient cofactors for the development of KS; in the era of combination antiretroviral therapies (cART) that reduce HIV-1 viremia and restore CD4+ T-cell counts depleted by HIV-1 pathogenesis, KS incidences have decreased significantly (Labo et al., 2015). Despite the reduction in KS cases, the proportion of non-AIDS related KS patients is increasing, and likely represents incidences resulting from senescence and aging in KSHV-infected populations, analogous to classic KS (Thakker & Verma, 2016).

Histologically, KS lesions are characterized by KSHV-infected, spindle-shaped endothelial cells, abnormal slit-like blood vessels and chronic inflammatory cell infiltrate (Nickoloff & Griffiths, 1989; Douglas et al., 2010). These lesions are heterogeneous and are not considered outgrowths of a single cell type as in most cancers; the progression of disease is often delineated by different stages that are defined by differing cell-type composition (Regezi et al., 1993; reviewed in Ganem, 2010). Lesions begin as flat *patches* that contain high numbers of inflammatory cells (T and B cells), extensive vascularization, and some elongated spindle-shaped cells (Ganem, 2010). As the spindle cells proliferate, the lesions progress to *plaque* and *nodular* stages in which visible masses of spindle cells develop, accompanied by inflammatory cells, such as marcrophages, monocytes, and dendritic cells (Kaaya et al., 1995; Douglas et al., 2010).The purple-blue colour of lesions results from the leakage of fluid from newly-formed, abnormal blood vessels, the

extravasation of red blood cells, and the accumulation of hemosiderin in macrophages (Ganem, 2010).

The origin of spindle cells has been controversial; while initial studies identified them as deriving from lymphatic endothelial cells (LECs) (Beckstead et al., 1985), others have shown that blood vascular endothelial cells (BECs) may be the origin and undergo KSHV-induced reprogramming to express LEC-specific markers (Hong et al., 2004). Spindle cells are considered to be the proliferative subunit of KS, however they are highly dependent on extracellular growth factors and fail to thrive in regions devoid of lymphatics, such as the brain or *ex vivo* (Ensoli & Stürzl, 1998; Herndier & Ganem, 2001). Furthermore, KS lesions tend to arise at sites of inflammation and trauma, (Potouridou et al., 1997), suggesting a not-well defined relationship between KSHV-infected cells, immune cell recruitment, and the establishment of a pro-inflammatory, tumour-promoting environment (Douglas et al., 2010). KSHV-induced reprogramming of endothelial cells is evidenced by the upregulated expression of cellular cytokines in spindle cells that promote angiogenesis and a pro-inflammatory niche. Vascular endothelial growth factor (VEGF), interleukins -1alpha, -1beta, and -6 (IL-1α, IL-1β, IL-6), interferon-gamma (INF-γ) and tumor necrosis factor (TNF) are examples of inflammatory cytokines expressed by spindle cells; collectively, these cytokines are capable of acting in an autocrine and paracrine manner to promote KS-like lesions in nude mice (Ensoli & Stürzl, 1998; Samaniego et al., 1997). Additionally, KSHV encodes its own homologues of chemokines, including viral IL-6 (vIL-6) and three viral CC-chemokine ligands, vCCL-1, -2, and -3, that serve pro-angiogenic and pro-survival functions (Chen et al., 2009; Choi & Nicholas, 2008).

This complex relationship between KSHV-reprogrammed cells and the immune system is an important aspect in the development and persistence of KS tumours. Since the seminal discovery of KSHV as the etiologic agent of Kaposi's sarcoma in 1994, it was found that the virus was associated with two lymphoproliferative disorders: multicentric Castleman's disease (MCD) and primary effusion lymphoma (PEL) (Soulier et al., 1995; Cesarman et al., 1995). These findings further highlight the relationship between KSHV, immune cells, and tumorigenesis.

1.2.1.2 Multicentric Castleman's Disease

Multicentric Castleman's disease (MCD) is a B-cell lymphoproliferative disorder and is characterized by flares of inflammation, fever, enlarged spleen and lymphoadenopathy (Oksenhendler et al., 2018). These cells are infected with KSHV and show characteristics of polyclonal B-cells undergoing differentiation toward plasmablasts, thus resembling mature B-cells (Du et al., 2001). KSHV infection appears to drive B-cell differentiation independent of normal processes that would normally occur in the germinal centers of secondary lymphoid tissue (Du et al., 2001). Consistent with KS, inflammatory symptoms and disease progression of MCD are related to increased viral loads and high expression levels of cytokines such as human and viral IL-6 (Oksendhendler et al., 2000). Taken together, KSHV is responsible for reprograming B-cells toward a specific pro-inflammatory state that contributes to the severity of lymphoproliferative disorders.

1.2.1.3 Primary Effusion Lymphoma

Primary effusion lymphomas (PELs) are relatively rare tumours that are generally seen in HIV- and AIDS-related patients; although they may account for less than 4% of AIDS-related non-Hodgkin's lymphomas, the prognosis is often poor, with a median survival of approximately 6 months (Simonelli et al., 2003; Narkhede et al., 2018). PEL is a distinct clinicopathologic subtype of diffuse large B-cell lymphomas and are generally characterized by large numbers of circulating malignant B-cells and effusions of fluid in body cavities such as the pleural, pericardial, and abdominal spaces (Nador et al., 1996). Similar to MCD, PEL cells have characteristics of differentiated post-germinal center B-cells (Jenner et al., 2003); however, they differ in that PEL cells are commonly co-infected with both KSHV and another human gamma-herpesvirus, Epstein-Barr Virus (EBV) (Cesarman, 2014).

EBV is capable of immortalizing B-cells *in vitro* and is associated with the malignant disease, Burkitt's lymphoma (Kempkes et al., 1995). It is possible that EBV infection may provide a proliferative advantage to KSHV. B-cells single-infected with KSHV were found to increase in the number of KSHV genome copies per cell when infected with exogenous EBV (Bigi et al., 2018). Furthermore, EBV co-infection of a humanized mouse model led to increased KSHV persistence and tumorigenesis that were not observed with KSHV infection alone (McHugh et al., 2017). While the majority of PELs are co-infected with EBV and KSHV, the fact that some are only KSHV-infected demonstrates that EBV is not required for development of the cancer. Nevertheless, the tumorigenic potential of both human gamma-herpesviruses is evident in their ability to reprogram B-cells toward lymphomagenesis.

1.2.2 KSHV Pathogenesis

1.2.2.1 Genome & Virion Structure

The size of the KSHV DNA genome is approximately 160-170-kb and exists in linear form in KSHV virions but is found as a circular episome maintained in the nucleus of latent-infected B lymphoma cell lines (Renne et al., 1996b). A unique coding region of approximately 140-kb is flanked by ~30-50 copies of 801-base pair (bp) GC-rich, tandem repeats at its termini with no coding or transcription potential, herein referred to as the terminal repeats (TR) (Figure 1.3) (Russo et al., 1996). Of the >86 open reading frames (ORFs) encoded by KSHV, many are conserved in other herpesviruses, especially with other primate gamma-herpesviruses, namely EBV and herpesvirus saimiri (HVS); these include proteins and enzymes involved in viral DNA replication (DNA polymerase, ORF9), nucleotide synthesis (thymidylate synthase, ORF70), and transcriptional gene regulation (ORF50) (Russo et al., 1996). Additionally, a number of ORFs that are unique to KSHV, denoted with a 'K' such as K1 and K15, have been found to serve important purposes for viral pathogenicity (Russo et al., 1996; Steinbrück et al., 2015).

Enclosing the dsDNA are the four main classes of proteins that comprise herpesvirus capsids (Figure 1.3). The icosahedron shape consists of 161 capsomeres (150 hexamers and 11 pentamers) that are composed entirely of the major capsid protein (MCP), ORF 25 (Nealson et al., 2001; Pellett & Roizman, 2013). These capsomeres are held together in groups of three by a heterotriplex of proteins composed of ORF62 and ORF26 (Nealson et al., 2001). A small-capsid protein (SCP), ORF65, interacts with the capsomeres and is thought to be an important antigenic determinant for KSHV; unlike other herpesvirus

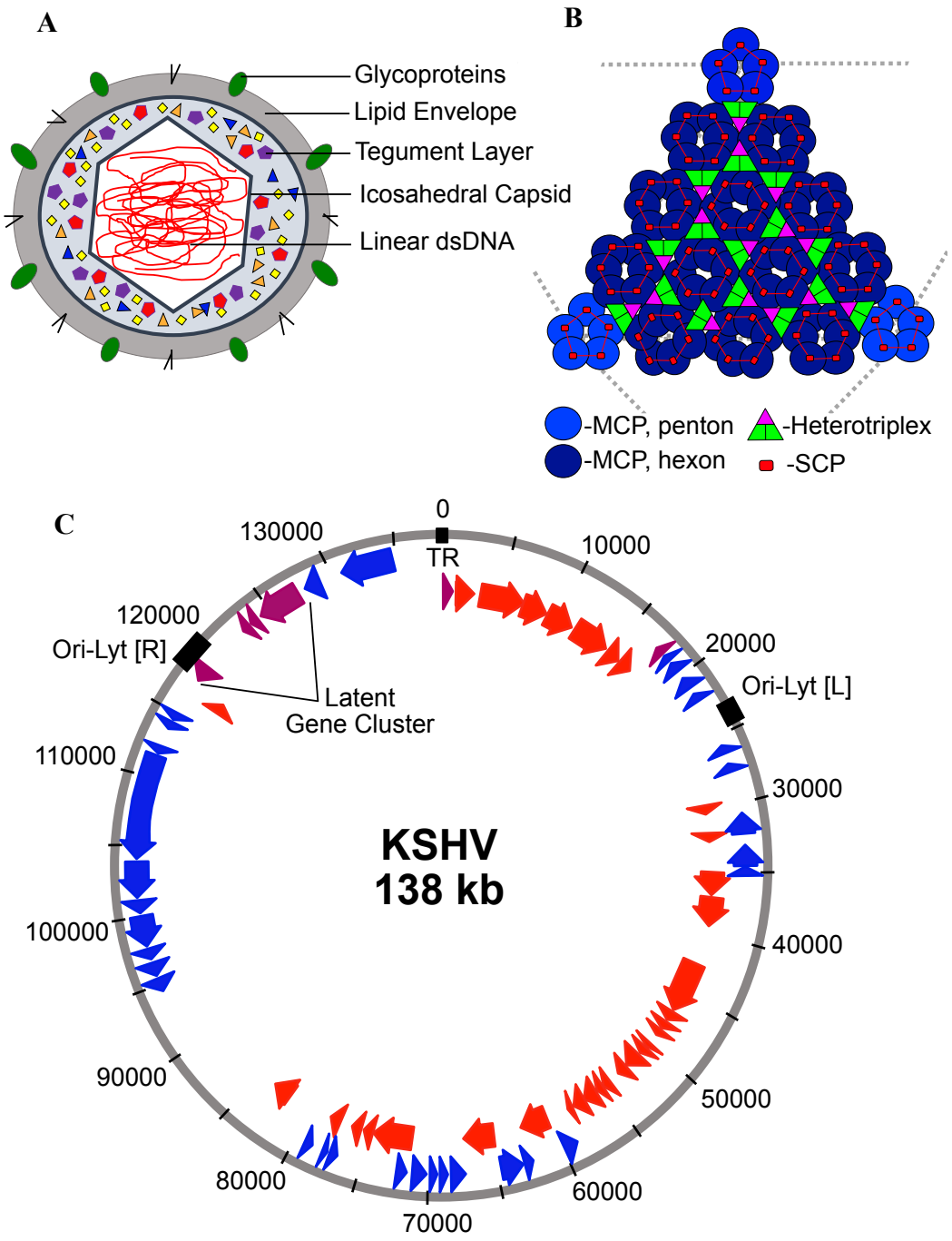

Figure 1.3: KSHV virions are composed of dsDNA genomes with a large coding capacity. (A) Diagram depicting the enveloped KSHV virion consisting of an icosahedron capsid, tegumentous matrix, and linear dsDNA-genome. (B) Image depicting one face of the icosahedron capsid comprising pentons and hexons composed of major capsid protein (MCP), heterotrimer complexes, and small capsid proteins (SCP). Adapted from Dai et al., 2018. (C) Schematic diagram of the unique coding region of KSHV. Antisense (blue), sense (red), and latent (purple) ORFs are indicated along with origins of lytic replication (Ori-Lyt). Terminal repeats (TR) are omitted from this diagram. Adapted from Arias et al., 2014.

small capsid proteins, ORF65 is essential for KSHV assembly (Nealson et al., 2001; Trus et al., 2001; Perkins et al. 2008).

Occupying the space between capsid and envelope is a tegument matrix of proteins that have multifaceted roles; one of which is structure, evidenced by ordered protein-protein interactions (Dai et al., 2014). These proteins have been shown to have important regulatory functions during entry, assembly, and egress of the virus. For example, ORF45 has been shown to associate with virions in the tegument (Zhu & Yuan, 2003) and inhibit type I interferon (INF) induction upon entry (Zhu et al., 2002). Furthermore, ORF45 has been shown to interact with a microtubule associated kinesin motor protein and is believed to be involved in trafficking of capsid-tegument complexes during assembly and egress (Sathish et al., 2009). The multifunctional role of the viral proteins is a key characteristic of herpesviruses, and in particular KSHV, the result of which is tight regulation of both infectious life cycles.

1.2.2.2 Establishment of Latency

In both human gamma-herpesviruses, EBV and KSHV, the latent program predominates in infected lymphocytes and persists both *in vitro* and *in vivo*, while the lytic cycle is relatively short-lived (Renne et al., 1996). This default latent program relies heavily on the host's cell cycle and regulatory processes to passively replicate the viral genome during cell division; such co-option of host mechanisms ensures viral persistence, cell survival, and evasion of immune responses (Purushothaman et al., 2016).

During latency, the viral genome is maintained in the nucleus as a circular, non-integrated, episome from which viral gene expression is limited and no progeny virus is

produced (Ballestas et al., 1999). The dsDNA associates with cellular histones and is maintained as a mini-chromosome during latency (Toth et al., 2010). DNA methylation and histone acetylation have been shown to play an important regulatory role in the expression of KSHV genes. Using chromatin immunoprecipitation (ChIP) assays, methylation of CpG nucleotides and specific repressive histone H3 modifications lead to the suppression of lytic gene expression and the establishment of latency (Toth et al., 2010; Günther & Grundhoff, 2010). Conversely, demethylation of the dsDNA at specific promoters in the genome can cause the virus to lytic reactivate from latency (Chen et al., 2001).

As a result, latent viral gene expression originates from discrete clusters in the viral genome and is limited to a small proportion of total encoded genes (Figure 1.3). A small region of the genome is responsible for the transcription of messenger RNAs (mRNAs) spanning ORF73 (latency-associated nuclear antigen [LANA]), ORF72 (viral cyclin D homolog [vCyclin]), and ORF71 (viral FLICE inhibitory protein [vFLIP]), which have been reported as being abundantly expressed in KS tumors and uninduced PEL cell lines (Dittmer et al., 1998). Slightly downstream of this region is a sequence from which the most abundant RNAs in latently infected KS lesion cells originate; this region is the kaposin locus, which encodes three protein products, Kaposins A (K12), B, and C (Zhong et al., 1996; Sadler et al., 1999). Most of the microRNAs (miRNAs) encoded by KSHV originate from these regions of the genome; 10 of the 12 encoded pre-miRNAs are located between ORF 71 and K12, while miR-K10 and miR-K12 are located in the K12 ORF and at its 3' untranslated region (UTR), respectively (Pfeffer et al., 2005; Cai et al., 2005; Grundhoff et al., 2006). These pre-miRNAs are processed similar to eukaryotic cellular

pre-miRNAs, thus generating 22-nucleotide-long non-coding RNAs, or mature miRNAs, that can be incorporated into the RNA-induced silencing complex (RISC) and inhibit gene expression by binding to complementary sequences in host or viral mRNAs (reviewed in Bartel, 2004).

In addition to the proteins and miRNAs that originate from the above-described latent gene cluster are two transcripts that were identified in low abundance in several latent KSHV-infected cell lines; these RNAs encode K1 and vIL-6 and have been shown to play important roles in B-cell signaling and pro-survival gene expression (Chandriani & Ganem, 2010). Difference in viral protein expression may depend on the context of the infected cell-type. For example, vIL-6 was found to be constitutively expressed in infected B cells *in vitro* and in MCD lymph nodes *in vivo*; however, its expression was restricted in KS biopsies (Parravicini et al., 2000). Many functions and cellular targets have been identified for the latently expressed viral proteins and miRNAs, respectively (reviewed in Giffin & Damania, 2014), yet many still have not been elucidated. The continued discovery of new roles for these gene products provides a better understanding of their role in KSHV pathogenesis, disease, and immunity.

1.2.2.3 Latent Viral Gene Function

LANA is a large, multifunctional protein that is required for the stable maintenance of episomal DNA during latency. One of the key capabilities of LANA is the ability to oligomerize and bind GC-rich sites in the TR region of the circular episome while simultaneously binding histones of host chromatin, thus tethering the episome to host DNA (Cotter 2nd & Robertson, 1999; Schwam et al., 2000). This event was evidenced by LANA

antibodies that were found to produce a nuclear punctate immunofluorescence pattern in spindled-cells from KS lesions (Rainbow et al., 1997). This perfect colocalization of viral DNA with LANA dots allowed for a rough estimate of the number of KSHV episomal copies in the cell, which can range from 50 to 100 viral copies per cell in KSHV-associated lymphomas (Cotter 2nd & Robertson, 1999; Asahi-Ozaki et al., 2006).

LANA has also been shown to have roles as a transcriptional activator and repressor, depending on the context of the neighbouring promoter, including autoregulation of its own promoter (Renne et al., 2001). In addition to binding histones, the N-terminal proline-rich region of LANA is known to interact with many chromatin associated proteins (Ballestas & Kaye, 2011). Identification of LANA-interacting partners that are involved in epigenetic regulation, such as methyl transferases and CpG nucleotide binding proteins, highlight LANA's role as an important point of control for gene expression during latency (Sakakibara et al., 2004).

The significance of LANA binding to the TRs is important in terms of providing a mechanism for viral genome persistence in dividing cells. Proteins of the origin replication complex (ORC) and mini-chromosome maintenance (MCM) complex were found to bind to the TRs in a cell-cycle dependent manner in latently infected PEL cells (Stedman et al., 2004). Recruitment of these complexes to the TRs forms a pre-replication complex that licenses use of the sequence as an origin or replication, termed ori-P, in late G1 phase of the cell cycle (reviewed in Purushothaman et al., 2016). Interactions between LANA and MCM proteins during G1/S phase have been shown to be an important component of ensuring latent viral DNA replication and episome segregation to daughter cells during mitosis (Dabral et al., 2019; Hu et al., 2002). Furthermore, expression of KSHV LANA

alone in cell culture is sufficient for replication of TR-containing synthetic plasmids and episomes (Grundhoff & Ganem, 2003). Despite LANA being a viral-encoded protein, it is clear that latent genome replication relies heavily on the subversion of cellular machinery to successfully ensure viral genomes are not diluted out of dividing cell populations.

Other latent viral proteins that play participatory roles in genome maintenance and the establishment of a tumorigenic and inflammatory latent state are vCyclin and vFLIP. vCyclin is a homolog of cellular cyclin D and has been shown to bind several Cyclin-dependent kinases (CDKs) in latent PEL cells, thus having a regulatory effect on cell-cycle progression (Child & Mann, 2001) For example, vCyclin-CDK6 interaction results in phosphorylation events leading to the bypass of G1/S checkpoint blockades (Järviluoma et al., 2006). The ability of vCyclin to induce cell-cycle progression presents its oncogenic potential; in a transgenic mouse model, vCyclin overexpression results in the induction of tumours, while deletion of the gene decreases tumor incidence and extends animal survival (Verschuren et al., 2002; Jones et al., 2014).

vFLIP is a cellular homolog of FLICE/caspase-8-inhibiting proteins and has been shown to contribute to both the pro-inflammatory and proliferative state of KSHV-infected cells (Grossmann et al., 2006). vFLIP is capable of interacting with IκB kinase (IKK) complexes in PEL cells, leading to the constitutive activation of the transcription factor, NF-κB (Chaudhary et al., 1999; Field et al., 2003). The resultant phenotypes of vFLIP-induced NF-κB-activation in endothelial cells is spindling and upregulated expression of proinflammatory cytokines, including IL-6, both of which are characteristics of KS lesion cells (Grossmann et al., 2006). Furthermore, vFLIP protein contains two death-effector domains that are capable of directly inhibiting apoptotic signaling events (Thome et al.,

1997). This provides vFLIP with tumorigenic potential that may contribute to KSHV-oncogenesis; lymphomagenesis and vascular abnormalities have each been shown *in vivo* in mice genetically engineered to express vFLIP in B-cells (Ballon et al., 2011) and endothelial cells (Ballon et al., 2015), respectively.

1.2.2.4 Lytic Reactivation

In KS tumours and PELs, only a small proportion of cells are undergoing lytic reactivation; less than approximately 1-3% of cells express lytic transcripts, while 98% express exclusively latent transcripts (Staskus et al., 1997). This proportion of latent to lytic cells has been shown to play an important role in the development and progression of KS-like tumours in a transgenic mouse model *in vivo*, suggestive of a cooperative role between latent and lytic life cycles (Montaner et al., 2003). The transition between latency and lytic reactivation is controlled by LANA and its counterpart, the replication and transcription activator, RTA (ORF50), for lytic gene expression (Sun et al., 1998). RTA is able to activate the promoters of lytic genes by binding directly to DNA sequences, termed RTA response elements (RRE), or by interacting with sequence-specific cellular DNA-binding proteins that promote transcription, such as recombinant signal sequence-binding protein-J kappa (RBP-Jκ) and CCAAT/enhancer-binding protein alpha (C/EBPα) (Liang et al., 2001; Wang et al., 2003) The interplay between LANA and RTA proteins is an important mode of control that allows for the default establishment of latency during *de novo* KSHV infection; following entry, LANA expression leads to repression of the RTA promoter as well as RTA-responsive elements, thus preventing lytic gene transcription (Li et al., 2008).

However, certain stimuli have been shown to induce lytic reactivation from the repressive latent state in KSHV-infected cells; these include co-infections, immune suppression, hypoxia, and oxidative stress (reviewed in Ye et al., 2011). Additionally, epigenetic modulation has been shown to play a role in chromatin reorganization and thus influencing gamma-herpesvirus reactivation (reviewed in Poudyal et al., 2017). Treatment of PEL cells with histone deacetylase (HDAC) inhibitors, such as *n*-butyrate, have been shown to strongly activate lytic gene expression by preventing the removal of acetyl groups from histone lysines, resulting in relaxed chromatin (Miller et al., 1997). Chromatin remodelling has been found to specifically occur at the RTA promoter in response to sodium butyrate treatment; this event was dependent on the recruitment of cellular chromatin regulatory proteins, such as histone acetyltransferases (HATs), that mediate these rearrangements (Lu et al., 2003).

Treatment of KSHV-infected cells with phorbol esters, such as 12-*O*-tetradecanoylphorbol-13-acetate (TPA), has been another standard reagent for the induction of lytic gene expression and virion production (Renne et al., 1996; Miller et al., 1997). TPA treatment has been shown to stimulate binding of cellular transcription factors, such as C/EBPα, to the KSHV genome leading to the activation of RTA-induced lytic gene expression (Wang et al., 2003). This induction was abrogated in the presence of PKCζ inhibitors, suggesting that TPA-induced lytic reactivation is PKC-dependent (Zoeteweij et al., 2001). PKCζ is known to activate many cellular signaling pathways associated with cellular proliferation, such as the MAPK signaling cascade, and is thus believed to play an important regulatory role in gamma-herpesvirus pathogenesis (Ueda et al., 1996; Gao et al., 2001).

Activation of RTA initiates a temporal cascade of lytic gene expression leading to the replication of viral genomes and production of infectious virions: lytic genes fall into one of three classes: immediate early (IE), early (E), and late (L) genes (Sun et al., 1999). The distinction between early and late gene classification is the timing of their expression pre- or post-lytic genome replication, respectively. Experimentally this is determined by the sensitivity of gene expression to treatment with cycloheximide and phosphonoacetic acid (PAA) (Sun et al., 1999). Cycloheximide is an inhibitor of peptidyl-tRNA transfer in ribosomes and blocks protein synthesis of E- and L-genes (McKeehan & Hardesty, 1969; Sun et al., 1999). PAA has been shown to specifically inhibit herpesvirus DNA polymerase activity and thus blocks lytic genome replication and L-gene expression (Overby et al., 1977; Sun et al., 1999). IE-gene expression does not require prior viral protein synthesis; therefore, RTA, which is the only gene partly resistant to both cycloheximide and PAA treatment, is an IE-gene (Sun et al., 1999). Genes expressed earlier in the lytic cycle are in general functionally essential for genome replication, whereas late transcripts usually code for virion structural proteins or factors required for assembly and egress (Schulz & Chang, 2007).

ORF57 and ORFK8 (K-bZIP) are early genes both expressed shortly after lytic induction with TPA- and HDAC inhibitor-treatment; both are RTA-binding proteins and are essential for virion production (Majerciak et al., 2006; Lefort & Flamand, 2009). ORF57 has been shown to enhance the transport and splicing of viral transcripts, thus affecting the expression of lytic genes and progression of the temporal cascade (Han & Swaminathan, 2006). K-bZIP has been shown to stabilize the transcription factor C/EBPα, thus promoting RTA-induced transcription by enhancing RRE-binding (Wang et al., 2003).

1.2.2.5 Lytic Genome Replication

Genome replication is one of the key events that define lytic reactivation and it differs from that during latency, largely due to the participating proteins and exponential amplification of viral genomes; while latent genome replication is principally a passive process driven by host enzymatic activities, lytic replication is predominantly accomplished by virus-encoded proteins. Lytic replication of the viral DNA genome initiates at two origins (ori-Lyts); these ori-Lyts are inverted duplications of one another and are located at opposite ends of the genome, one between K4.2 and K5 (ori-Lyt [L]) and the other between K12 and ORF71 (ori-Lyt [R]) (Figure 1.3) (Aucoin et al., 2002; Lin et al., 2003). The ori-Lyts are composed of near identical core sequences that include a 600-bp GC rich direct repeat region (DR); the complete 1.7-kb sequence is sufficient to act as a *cis*-signal for DNA replication (Lin et al., 2003) (Figure 1.4). Within the core sequence is a long AT-palindromic region with binding sites for transcription factors, such as C/EBPα and activator protein 1 (AP-1), as well as promoter elements such as a TATA box and an RRE (Figure 1.4) (Lin et al., 2003; Aucoin et al., 2004). The AT-palindromes are thought to be sites of DNA unwinding and serve as K-bZIP binding sites, while the RRE serves to recruit RTA to the ori-Lyt (Figure 1.4) (Lin et al., 2003; Aucoin et al., 2004). In addition to RTA and K-bZIP binding, virus-encoded core replication proteins, such as a DNA polymerase, polymerase processivity factor, single-stranded DNA binding protein, and trivalent helicase-primase complex are recruited to the ori-Lyt along with many other host regulatory proteins such as topoisomerases and cellular repair and recombination factors (Figure 1.4) (Wu et al., 2001; Wang et al., 2008).

The presence of *cis*-regulatory elements that serve as a promoter at each of the ori-Lyts suggests that transcription within this region is required for DNA replication (Wang et al., 2004). Evidence was observed for EBV where a G-rich long non-coding RNA (lncRNA), BHLF1, was generated from the EBV ori-Lyt promoter during lytic reactivation (Gao et al., 1997). This transcript was found to bind DNA, forming an RNA-DNA hybrid that is required for proper lytic DNA replication (Rennekamp & Lieberman, 2011). DNA replication was reduced when either the transcript or its promoter was truncated; additionally, reductions in the G-nucleotide content, but not the removal of the ATG translation initiation codon of the BHLF1 ORF, attenuated DNA replication (Rennekamp & Lieberman, 2011). This suggests that the RNA transcript and not its translation products are required for DNA replication. In KSHV, similar analyses showed that DNA replication was inhibited when RTA-transcription through the GC-rich tandem repeat of ori-Lyt[L] was prematurely terminated, suggesting that generation of a GC-rich transcript is essential for proper loading of core replication machinery (Figure 1.4) (Wang et al., 2006). Furthermore, this transcript was found to interact with K-bZIP and facilitate its binding to the ori-Lyt DNA, an event necessary for subsequent recruitment of the replication complex (Liu et al., 2018).

Genetic recombination is also believed to play a role in lytic replication; recombination at repetitive sequences in alpha-herpesviruses has been well established and is an important mechanism for genetic diversity (reviewed in Umene et al., 1999). The GC-rich tandem and inverted repeats in the KSHV genome are likely regions for homologous recombination and DNA-repair responses (Brown, 2014). While the importance of these features has yet to be proven for lytic replication, DNA recombination-like structures have

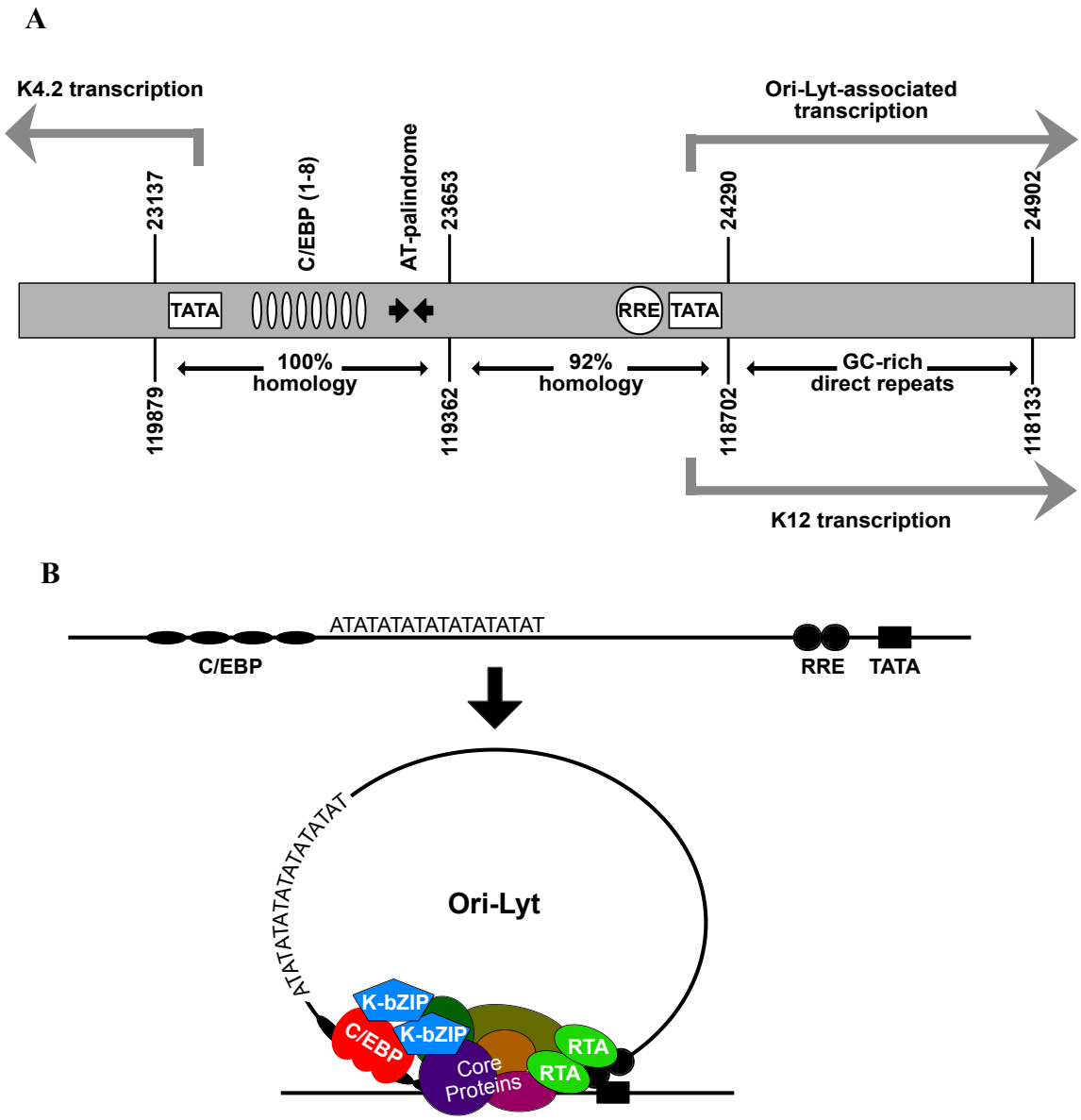

Figure 1.4: Origins of lytic genome replication in KSHV. (A) Schematic diagram of the two origins of lytic replication of KSHV, Ori-Lyt[L] (nucleotides 23137-24902) and Ori-Lyt[R] (nucleotides 118133-119879); nucleotide numbers refer to the KSHV genome position according to Russo et al., 1996. The ori-Lyts are inverted duplications of each other and share significant homology. Each is composed of multiple C/EBP binding sites, an AT-rich palindrome region, an RTA-responsive element (RRE), promoter elements (TATA), and GC-rich direct repeat regions. (B) These *cis*-elements recruit viral (K-bZIP and RTA) and cellular (C/EBP) proteins to act as transcriptional activators for gene expression and possibly ori-Lyt function. These t*rans*-factors also recruit core replication proteins to initiate genome replication. Adapted from Aneja & Yuan, 2017.

been shown to occur at TRs during cell division, which is believed to provide stability to the repeat regions during latency (Dheekollu et al., 2003).

1.2.3 The Kaposin Locus

1.2.3.1 Gene Organization & Expression

In a study conducted by Zhong et al. (1996), two RNA transcripts, referred to as T1.1 and T0.7, were identified in high abundance by Northern blot hybridization of total RNA from KS pulmonary tissue that were not observed in normal tissue. The polyadenylated T1.1 transcript would be identified as PAN (polyadenylated nuclear RNA), a multifunctional long non-coding RNA accounting for 80% of the viral transcriptome that plays an important role in KSHV replication and growth (reviewed in Rossetto & Pari, 2014).

Within the T0.7 transcript, Zhong et al. (1996) identified a short 60 amino acid long coding region that initiated from an AUG codon with no known homologs and extreme hydrophobicity, consistent with a transmembrane domain; this ORF is now known as kaposin A or K12 (Appendix A, Figure A.1) (Zhong et al., 1996). Upon further study, the T0.7 transcript was predominantly found to be much larger than the initially reported 0.7-kb, varying between ~1.5 and 2.5-kb (Figure 1.5) (Sadler, 1999). The 5'end of the transcript contained two additional sets of 23-bp, GC-rich direct repeats (DRs) (DR1 and DR2); this region is the same GC-rich locus described for ori-Lyt[R] (Sadler, 1999). Although these repeats lacked AUG translation initiation codons, they were found to be translated as a result of initiation at non-canonical start codons, such as CUG and GUG (Figure 1.5) (Sadler, 1999). The coding potential of the DR sequences is such that identical polypeptides composed of 23 amino acid tandem repeats could be produced from all three open reading

frames (Figure 1.5) (Sadler, 1999). The major translation product in TPA-induced and uninduced PEL cells was a 48 kDa protein, identified as kaposin B, derived entirely from DR sequences (Appendix A, Figure A.1) (Sadler, 1999). Initiation from alternative CUG codons allows for translation of DR-K12 fusion proteins that are expressed with less relative abundance; called kaposin C. Of note is that due to the variability of the number of repeats in DR sequences among KSHV isolates, the sizes of kaposin B and C proteins can vary (Sadler, 1999). Furthermore, the expression of either kaposin B or C is dependent on which non-canonical initiation codon is used for translation; this was made apparent by a study conducted by Li et al. (2002), where they reported that kaposin B was absent in PEL tumour cells.

Latent transcripts for the kaposins are believed to originate from a unique downstream constitutive latent promoter (LT_d) separate from the promoter proposed to control all latent genes (LT_c) (Figure 1.5) (Pearce et al., 2005). The LT_d is positioned in the intergenic region between LANA (ORF73) and vCyclin (ORF72), and produces two mRNAs: an un-spliced, bicistronic transcript encoding ORFs 72 and 71, and a spliced kaposin transcript (Figure 1.5) (Li et al., 2002; Pearce et al., 2005). Kaposin transcript and protein levels are significantly increased following lytic reactivation; this is a result of an additional promoter that becomes activated by direct RTA binding to an RRE immediately upstream of the kaposin B translation initiation codon, also described above for the ori-Lyt [R] (Figure 1.5) (Chang et al., 2002). This RRE shares 20-bp homology with an RTA binding site at ori-Lyt [L] that directs transcription of a 1.4-kb RNA that similarly contains GC-rich tandem repeats at its 5'end and an ORF of 75 amino acids at its 3'end (Chang et

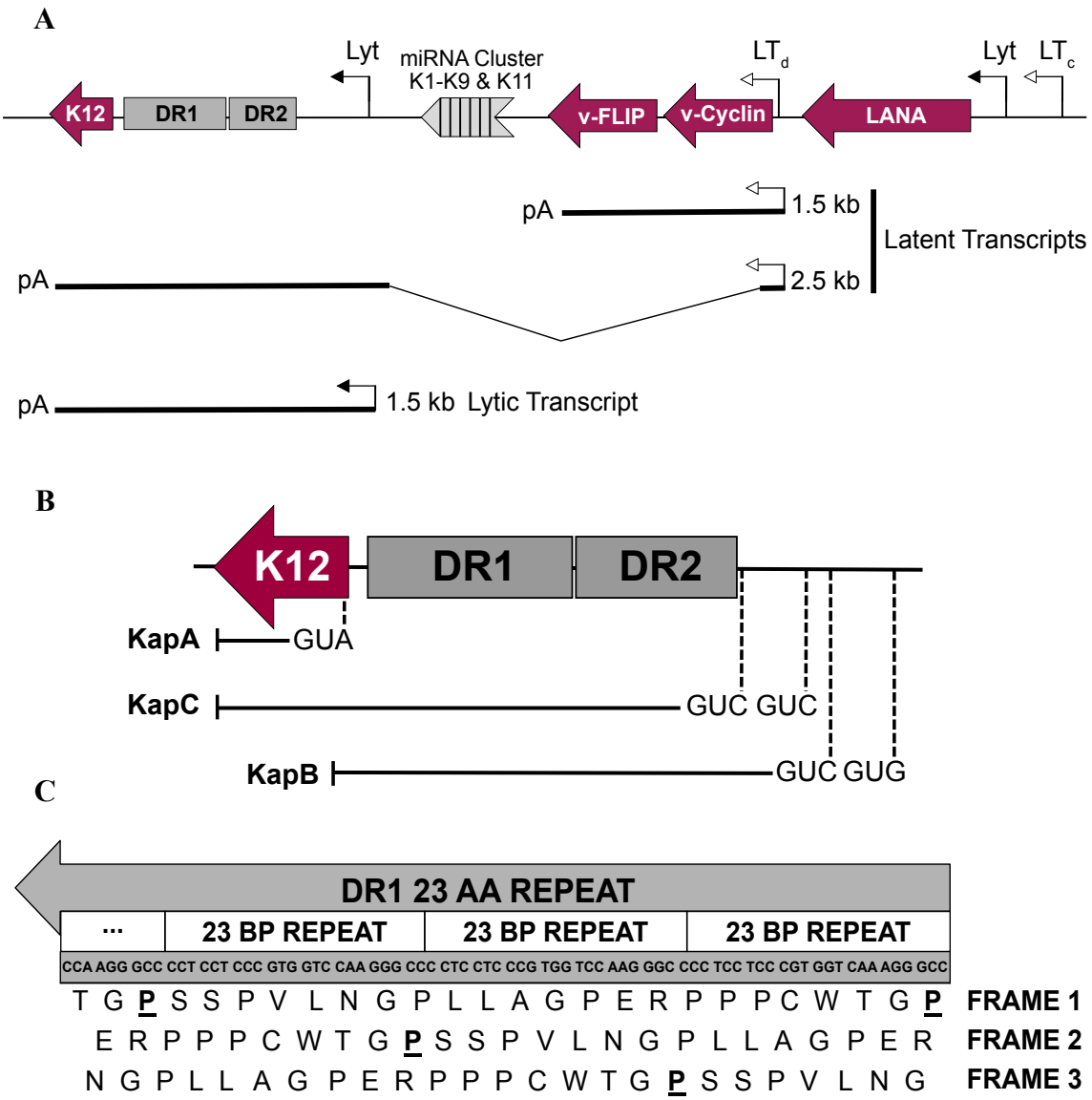

Figure 1.5: Kaposin transcription and translation. (A) Schematic diagram of the latent gene cluster of KSHV. Constitutive latent (LT) and lytic (Lyt) promoters are indicated. Kaposin transcription originates from the downstream (LT_d) promoter during latency and a proximal RTA-responsive element (RRE) during the lytic cycle. Adapted from Pearce et al., 2005. (B) Translation of kaposins B and C (KapB, KapC) initiate at non-canonical CUG and GUG start codons upstream of the K12 (KapA) ORF and include the GC-rich 23-base-pair (bp) direct repeat regions, DR2 and DR1. (C) Each repeat region has the translation potential to generate a polypeptide composed of 23-amino acid (aa) direct repeats in all three reading frames. The bolded and underlined proline arbitrarily denotes the beginning of each repeat. Adapted from Sadler et al., 1999.

al., 2002; Wang et al., 2004). While the function of each kaposin protein during the latent and lytic cycle is still being elucidated, the information gathered thus far suggests that these proteins play important roles in the establishment of a tumorigenic niche for KSHV-infected cells.

1.2.3.2 Kaposin A (K12) & Kaposin C

The oncogenic potential of kaposin A (KapA) was characterized shortly after the discovery of the T0.7 transcript. Transfection of Rat-3 cells with plasmids expressing T0.7 or KapA protein resulted in morphological changes that, upon subcutaneous injection into athymic nude (nu/nu) mice, were capable of inducing vascular, high-grade sarcomas (Muralidhar et al., 1998). Further characterization of these cells showed that KapA co-localized with Golgi membrane proteins by immunofluorescence assay and that kinase activity, specifically the activity of PKC and Ca^{2+}/calmodulin-dependent protein kinase (CAMK), was increased as seen by phospho-spot analysis (Muralidhar et al., 2000). Both CAMK and PKC signaling have been implicated in cell-cycle regulation and the initiation of DNA synthesis, supporting the idea that KapA promotes cancer progression (Skelding et al., 2011; Nishizaka, 1992).

KapA is able to mediate changes in cell morphology by its interaction with cytohesin-1, a guanine nucleotide exchange factor, at phospholipid membranes; KapA recruits cytohesin-1 which in turn increases relative GTPase activity *in vitro* (Kliche et al., 2001). The phenotypic outcome is a rearrangement in cellular F-actin in KapA-expressing rat fibroblasts; this is characterized by the lack of actin bundle structures, known as stress fibers, that are much more apparent in control cells (Kliche et al., 2001).

Analysis of the KapA coding sequence has led to suggested motifs that may be responsible for its ascribed transformative properties. Mutation of the LXXLL amino acid motif of KapA correlated with a loss in the ability to transform cells in culture and altered the protein's subcellular localization from the nuclear and plasma membrane to the cytoplasm (Tomkowicz et al., 2005). However, this mutation did not impair KapA's ability to activate AP-1-dependent transcriptional activity; in addition to its role in ori-Lyt replication, AP-1 is known to be upregulated by MAPK-signaling in KSHV-infected cells and is an important mediator of cellular IL-6 induction and tumourigenesis (Tomkowicz et al., 2005; Xie et al., 2005).

Analysis of the coding sequence for KapA showed that RNA editing occurs at nucleotide 117990 (Genbank accession no. U75698) within the KapA ORF; adenosine deamination and an A-to-G disparity was observed between the DNA sequence and the associated cDNA generated from resultant KapA RNA (Gandy et al., 2007). This specific posttranscriptional modification, which causes a serine-to-glycine mutation in KapA, was found to eliminate the transformative potential of KapA in Rat-3 cells *in vitro* and *in vivo* in athymic nude mice (Gandy et al., 2007). Furthermore, the level of RNA editing at this position was regulated by the virus replicative state; editing was increased upon sodium butyrate and phorbol ester treatment to induce lytic replication (Gandy et al., 2007).

RNA editing occurs in the seed sequence of a miRNA encoded in the KapA ORF, miR-K10, which is differentially processed to produce multiple miRNAs during latency (Umbach & Cullen, 2010). As a result, miR-K10 has been suggested to be the source of the oncogenic properties of the KapA transcript (Forte et al., 2015). miR-K10a has been shown to transform murine fibroblast cells independent of KapA protein expression; it was

found to specifically repress known inhibitors of transforming genes, such as the CDK-inhibitor, p27 (Forte et al., 2015). Other processes that are targeted for repression by miR-K10a include transforming growth factor-beta (TGF-β) signaling (Lei et al., 2012) and cytokine signaling from tumor necrosis factor-like weak inducer of apoptosis receptor (TWEAKR), (Abend et al., 2012), both of which can contribute to a proliferative cell phenotype. This evidence supports the notion that the phenotypic effects attributed to KapA may be mediated by its RNA transcript instead of the encoded protein, however this notion is still up for debate in the field.

While no known functions have yet been attributed to kaposin C (KapC), it is believed that many of the properties ascribed to KapA may also pertain to KapC since it is a fusion protein of both the DRs and K12. It is believed that the membrane targeting potential of KapA may still play a role in KapC function; however, it is unknown how the additional N-terminal DR region, which more than triples the amino acid sequence of KapA, impacts the function of KapC (Kliche et al., 2001).

1.2.3.3 Kaposin B

The function of kaposin B (KapB), which is composed of the DRs and unique N- and C-terminal peptides, has not been associated with tumorigenesis *in vivo;* however, the effects of KapB expression suggest that this protein has important implications in KSHV pathogenicity and KS-associated phenotypes. Using a yeast-two hybrid system, the DR regions that comprise KapB (DR2 and DR1) were each used to screen a library of infected cell cDNAs for potential interaction partners; one of the hits from this screen was MAPK-associated protein kinase 2 (MK2), which was found to bind to the DR2 polypeptide

(McCormick & Ganem, 2005). This binding event was found to activate MK2, leading to the stabilization of cellular RNA transcripts containing AU-rich elements (AREs) in their 3' untranslated regions (3'UTRs) (McCormick & Ganem, 2005). The presence of AREs is known to destabilize the transcript leading to its rapid degradation (reviewed in Chen & Shyu, 1995). Activation of a signaling cascade involving MK2 and the cytoskeletal regulator, RhoA GTPase, leads to the dispersal of ribonucleoprotein granules, called processing bodies (PBs); these are known sites of degradation for ARE-containing mRNAs (Corcoran et al., 2015). Increased stability of the ARE-mRNA transcript leads to its upregulated expression; examples of ARE-containing genes that are up-regulated in KapB-expressing cells include the proto-oncogene, granulocyte/macrophage colony-stimulating factor (GM-CSF), and inflammatory cytokine, IL-6 (McCormick & Ganem, 2005). ARE-mRNA stabilization was found to be maintained, albeit at attenuated levels, with only one copy each of DR2 and DR1 regions, called the miniprotein, but not with complete removal of either repeat region, suggesting that both DRs are required for KapB activity, and that an increased number of repeats amplifies their function (McCormick & Ganem, 2006). Consistent with its role in altering signaling cascades, KapB was found to promote aberrant phosphorylation and activation of STAT3 in endothelial cells; induction of this transcription factor was found to further upregulate inflammatory gene expression, including IL-6 and the chemokine CCL5 (King, 2013).

Another ARE-containing mRNA that was found to be upregulated in KSHV-infected cells is PROX1 (Wang et al., 2004b). PROX1 is a homeodomain transcription factor that was found to induce BEC-to-LEC reprogramming of endothelial cells by repressing and upregulating the expression of BEC- and LEC-specific markers,

respectively (Hong et al., 2002). KapB-mediated activation of the MK2 pathway stimulates the cytoplasmic accumulation of an ARE-binding protein, HuR, which leads to the stabilization of PROX1 mRNA (Yoo et al., 2010). This study highlighted the important role that KapB plays in endothelial reprogramming toward a spindle morphology that is characteristic of KS lesion cells. The correlation between cell elongation and upregulated inflammatory gene expression is further evidenced by pronounced actin-rearrangement and stress-fiber formation in KapB-expressing endothelial cells in a RhoA-dependent manner (Corcoran et al., 2015).

There is growing evidence to suggest that KapB may also be able to act as a novel transcriptional cofactor. KapB expression was found to repress the promoter activity of a cellular miRNA cluster, miR-221/miR-222 in lymphatic endothelial cells, whose targets include genes involved in cell migration (Wu et al., 2011). Since KapB does not possess any DNA-binding domains of its own, this activity must be dependent on KapB-binding partners. c-Myc is a cellular transcription factor that was found to bind to KapB and upregulate several essential genes and miRNA clusters that promote angiogenesis and tumor progression (Chang et al., 2016). Small RNA sequencing and chromatin immunoprecipitation (ChIP) assays have identified several promoters of miRNAs that are either upregulated or repressed in KapB-expressing endothelial cells, suggesting that KapB may control the transcriptional activity of host and viral genes in an ARE-independent manner to cause endothelial cell reprogramming (Chang et al., 2016).

1.3 Molecular Tools for KSHV Research

1.3.1 Reliance on *In Vitro* Cell Lines

Much of the current understanding of KSHV biology has been gathered from *in vitro* experiments using patient-derived cell lines and primary samples; this is in large part due to the absence of a small animal model to study KSHV persistence and pathogenicity *in vivo.* Previous models have involved the use of the naturally occurring murine gamma-herpesvirus 68 (MHV68) in rodents for its related genomic structure and association with lymphoproliferative disease resembling human gamma-herpesviruses (reviewed in Dong et al., 2017). However, MHV68 sequences for latency- and transformation-associated genes diverge from EBV and KSHV, making the model less than ideal (Virgin 4th et al., 1997). Alternative methods to study tumourigenesis have involved the use of transgenic nude mice; these animals have been used to show the development of KS-like tumours following endothelial-specific expression of viral oncogenes or transfection of viral genomes (Montaner et al., 2003; Mutlu et al., 2007). More recently, mouse models with human immune components have being used as an alternative to study transmission, replication, and tumorigenesis of KSHV, both in the absence and presence of EBV (Wang et al., 2014; McHugh et al., 2017). Since primary samples and cell lines are more readily accessible to research groups, these continue to be a standard in the field.

1.3.1.1 Patient-Derived Cell Lines

PEL cells have been invaluable for the establishment of *in vitro* cell lines for KSHV research, both for studying latent-infected lymphocyte populations and the generation of virus stocks (Cesarman et al., 1995b; Renne et al., 1996). Two AIDS-associated body-

cavity based lymphoma (BCBL) cell lines were established from PEL patients; these cells maintained KSHV restriction digest pattern over multiple passages and were found to harbor ~40-80 copies of KSHV per cell, approximately 60-fold more DNA than in KS lesion endothelial cells (Cesarman et al., 1995b). However, most AIDS-BCBL cases, including the isolated cell lines, were found to contain EBV DNA in tumour cells in addition to KSHV (Cesarman et al., 1995; 1995b). In a subsequent study by Renne et al. (1996), DNA extracted from AIDS-BCBL patient tumours were found to be negative for EBV coinfection. One lymphoma cell line, referred to as BCBL-1, was found to harbor predominantly latent episomes of KSHV, but could release extracellular KSHV particles upon TPA-induction of the lytic replication cycle (Renne et al., 1996), While only ~5-10% of cells showed an accumulation of virus particles by electron microscopy, this cell line provided the first means for a reliable source of KSHV virions for research (Renne et al., 1996).

1.3.1.2 Permissive Cell Models

The BCBL-1 cell line has since been used for KSHV-infection and -transmission experiments *in vitro* and *in vivo*, with variable success (Renne et al., 1998; Picchio et al., 1997). Using cell-free supernatants from TPA-induced BCBL-1 cells, Renne et al. (1998) tested a variety of cell lines of different origin for susceptibility to infection; they found that fibroblasts, epithelial, endothelial and lymphoid cells can support KSHV infection, however only in a limited manner. Infections were found to be highly inefficient; most cell lines could support viral entry and gene expression, but none were fully permissive to support lytic virus production and likely represent abortive lytic cycles (Renne et al., 1998).

Transformed human embryonic kidney cells (HEK 293) were found to be the most competent at eliciting patterns of lytic viral gene expression following infection; however, these cells were still inefficient at lytic virus propagation and could only support limited serial transfer of virus (Renne et al., 1998; Friborg et al., 1998). Work with a more productive PEL cell line, JSC-1, showed higher KSHV-virion yields in supernatants that were found to infect and cause spindling in human dermal vascular endothelial cells (DMVECs) with high efficiency (Cannon et al., 2000). However, the same issue persisted; the field lacked a latently-infected endothelial cell model that could sustain productive lytic reactivation.

1.3.2 Recombinant KSHV Infection

1.3.2.1 Inducible Lytic Reactivation

The difficulty in establishing early transmission models of KSHV is that latency is the default pathway after *de novo* infection *in vitro*. However, it was soon discovered that in addition to chemical treatment, such as TPA, this default could be overcome by ectopic overexpression of the viral lytic switch protein, RTA (Renne et al., 1996; Bechtel et al., 2003). Blocks in lytic reactivation were bypassed by adenovirus delivery and expression of RTA in *trans*; this allows the virus to overcome the suppression of native RTA that occurs during latency (Bechtel et al., 2003).

To better study the switch between latent and lytic viral life cycles, Vieira & O'Hearn (2004) developed a recombinant KSHV strain, called rKSHV.219, using virus from the JSC-1 lymphoma cell line. The recombinant virus differentially expressed fluorescent proteins according to the viral life cycle; green fluorescent protein (GFP) was

constitutively expressed from a human elongation factor 1-α promoter and therefore represented latency, while red fluorescent protein (RFP) was expressed during the lytic cycle from a promoter initiated by the lytic PAN RNA (Vieira & O'Hearn, 2004). This virus was able to productively undergo lytic reactivation in multiple cell types following treatment with sodium butyrate in combination with ectopic RTA expression (Vieira & O'Hearn, 2004). This system allowed latent- and lytic-infected cells to be readily detected in cell populations during *de novo* infections.

Ectopic RTA expression systems were further refined by the addition of tetracycline-responsive elements (TREx) to their respective promoters; this allowed for tight control of RTA expression, and therefore induction of the lytic cycle, in a tetracycline- or doxycycline-dependent manner (Nakamura et al., 2003). This proved to be a highly efficient way to produce KSHV stocks in both the BCBL-1 cell line (TREx BCBL-1) (Nakamura et al., 2003) and an SLK epithelial cell line infected with the rKSHV.219 system (Myoung & Ganem, 2011a; Stürzl et al., 2013).

1.3.2.2 BACs and Mutagenesis

Recombinant viral mutants are traditional ways of determining herpesvirus gene function; cloning of genomes into bacterial artificial chromosomes (BACs) has proven to be an effective method for directed mutagenesis and the identification of unknown gene function (reviewed in Warden et al., 2011). BACs facilitate the insertion of large herpesvirus genomes, which are too big for regular plasmids, and allow them to be stably propagated in *Escherichia coli* (*E. coli*); this strategy is favoured over yeast artificial chromosomes (YACs) which are unnecessarily large and more prone to undesired genomic

rearrangements or contamination of yeast DNA (Warden et al., 2011). However, rearrangements are not exclusive to YACs; repetitive elements in viral DNA can also cause unwanted rearrangements in BACs resulting in mutations (Yakushko et al., 2011).

Two KSHV BACs have been generated to date: BAC36 and BAC16; each was constructed by inserting BAC vector sequences into the KSHV DNA of BCBL-1 and rKSHV.219 sequences, respectively (Zhou et al., 2002; Brulois et al., 2012). These BAC sequences are generally 10-kb long and include elements necessary for propagation in bacteria, such as an origin of replication, and antibiotic resistance markers (Warden et al., 2011). Both constructs were designed such that the BAC vector also contained a positive selection marker and elements for fluorescent protein expression, such as GFP, in eukaryotic cells; in rKSHV.219 this resulted in the loss of the GFP-RFP cassette that allowed differential fluorescence during the lytic cycle (Zhou et al., 2002; Brulois et al., 2012). The BAC36 and BAC16 constructs were capable of producing virus by inducible-lytic reactivation with either TPA in 293 cells, or doxycycline in iSLK cells that contain the tetracycline-responsive RTA system, respectively (Zhou et al., 2002; Brulois et al., 2012). However, the BAC36 vector was found to include a duplication of a 9-kb fragment spanning six ORFs located in the TR region by full-genome sequencing, thus highlighting the potential for recombination to occur in BAC-containing *E. coli* (Yakushko et al., 2011). This duplication highlights the potential for BACs to mutate unexpectedly.

Nevertheless, BACs are important tools for the creation of herpesvirus mutants for functional study. Recombinant mutants can be generated by two methods: 1) random transposon-inserted mutagenesis, and 2) site-directed mutagenesis of the viral BAC. Transposons are mobile genetic segments of DNA that can randomly insert themselves into

genomes and in so doing disrupt genes (reviewed in McGregor, 2003). Transfection of a transposon-carrying plasmid into BAC-containing *E. coli* can quickly generate a large number of mutations in BACs (Warden et al., 2011). Some disadvantages to this method are: 1) certain ORFs can be disrupted by multiple insertions, therefore making it time-consuming to create a library of mutants for every ORF, and 2) insertion may occur in the middle of an ORF and thus create a partial functioning protein (Warden et al., 2011).

Alternatively, site-directed mutagenesis has become a popular method for generating recombinant BACs; this procedure is known as 'recombineering' (reviewed in Sharan et al., 2009). *E. coli* are generally inefficient at homologous recombination due to the presence of RecBCD exonuclease that degrades linear DNA; in recombineering methods, this degradation is circumvented by providing genes from a defective Lambda Red prophage, making homologous recombination more efficient (Yu et al., 2000; Lee et al., 2001). Temperature-sensitive expression of Lambda Red genes leads to three main functions: 1) repression of RecBCD by the *gam* gene, 2) specific degradation of foreign DNA from the 5'end of double-strand breaks by the *exo* gene, and 3) protection of the 3' end of linear DNA from further degradation by the *beta* gene (Sharan et al., 2009). This process generates overhangs on DNA exogenously introduced into the bacterium and facilitates recombination with the viral BAC (Sharan et al., 2009). One advantage to the Lambda Red system for recombineering is that homology sequences between the exogenous DNA and the viral BAC used for recombination need only be 40-bp in length (Lee et al., 2001).

Selectable markers are usually included during recombineering methods to identify successfully mutagenized clones; these can be in the form of positive or negative selectable

markers, such as antibiotic resistance genes or metabolic genes, respectively (Warden et al., 2011). Following site-directed insertion of exogenous DNA into the viral BAC, selection markers can be removed by a second round of recombination. One method takes advantage of Cre and Flp recombinase proteins that can be induced to act on loxP or Flp-recognition target (FRT) sequences, respectively, flanking the selection marker (Lee et al., 2001). Recombinases facilitate recombination between the flanking target sequences, resulting in removal of the selection marker and leaving behind a single loxP or FRT site; for this reason, this is referred to as the 'scarred' method (Sharan et al., 2009). Alternatively, incorporation of an I-SceI endonuclease recognition site within the selection marker can allow for a 'scarless' mutagenesis (Tischer et al., 2006). The endonuclease cleaves adjacent to the selection marker, and through an intramolecular Lambda Red recombination event leads to its removal (Tischer et al., 2006).

1.4 Rationale and Objective

The limited number of viral genes expressed during KSHV latency demonstrate a unique characteristic in the ability to interact with signaling and regulatory molecules to cause altered cell morphology, upregulated inflammatory cytokine expression, and cell proliferation that are signatures of KS tumourigenesis. The kaposin locus represents a complex region within the latency-associated gene cluster; it contains elements for the generation of transcripts that have implications in both the latent and lytic viral life cycles. To date, the three kaposin proteins have been associated with predominantly latent phenotypes. KapB has been shown to upregulate inflammatory cytokine signaling and alter

cell morphology (Corcoran et al., 2015), while KapA has been shown to have transformative properties, both *in vitro* and *in vivo* (Gandy et al., 2007).

However, all phenotypic analyses conducted for the kaposin transcripts and proteins have used ectopic expression models; as a result, this raises a number of questions. First, what is the relevance of transcript abundance during different stages of the virus life cycle? Due to an adjacent RRE, kaposin transcript levels are significantly increased following lytic RTA-induction compared to latency (Chang et al., 2002). However, no distinction has been made as to whether the kaposin proteins play different roles during each virus life cycle. Second, does the function of each of the kaposin proteins differ according to the viral gene expression profile during latent and lytic virus life cycles? The kaposin transcript has the potential to express three possible proteins: KapA, B, and C (Sadler et al., 1999). While many studies have addressed KapA or KapB function independently, it is unclear whether this complex translational program allows for alternate functions when the proteins are co-expressed from the same transcript. Furthermore, these roles may differ when expressed in the context of other viral proteins. Lastly, are kaposin-related phenotypes a result of protein function or are they mediated by RNA activity? According to work conducted by Wang et al. (2006), generation of a GC-rich transcript, similar to that of the kaposin, likely has a role in proper recruitment of replication machinery at the ori-Lyt. It is still unknown whether kaposin-associated phenotypes are mediated at the transcript or protein level, and whether either has a role in the lytic replication cycle.

In this study, I sought to investigate the role of the kaposin proteins in the lytic virus life cycle. Herein I use two models that have become standards in the field for KSHV gene

characterization, TREx BCBL-1 cells and BAC16 mutagenesis, to interrogate the role of the kaposin locus. The complexity of this work is highlighted by two aspects: 1) multiple kaposin proteins are produced from a single transcript, and 2) the transcript is highly GC-rich and repetitive. These issues were addressed by taking a multi-pronged approach to characterize the effect on lytic cycle progression in the absence of kaposin protein expression. In each case, the virus was assessed in its ability to produce progeny virions following induction of the lytic cycle; this was done in the context of shRNA-mediated knockdown of the kaposin transcript in BCBL-1 cells and directed mutagenesis of individual kaposin ORFs using the BAC16 clone of KSHV. Additionally, the virions produced during the lytic cycle were examined for their ability to successfully enter and express viral genes as an assessment of virion quality; this allowed me to make inferences regarding the ability to establish latency following *de novo* infection.

This work led to the generation of a novel library of recombinant BAC16 viruses with mutations in the coding capacity of the kaposin locus, a tool that has yet to be reported in the field. These viruses were used to identify deficiencies in lytic cycle progression and the establishment of latency for a subset of kaposin mutations. I report here the first evidence for the kaposin transcript and proteins in the lytic cycle of KSHV, adding another level of complexity to the mechanism and regulation of tumorigenesis for this oncogenic virus.

CHAPTER 2: MATERIALS & METHODS

2.1 Plasmids and Cloning

The second-generation lentiviral transduction system was used in this study to express shRNAs to knockdown the kaposin transcript (Mochizuki et al., 1998). pMD.2G (envelope) and pSPAX2 (packaging) plasmids were purchased from Addgene. pIPZ vectors used for shRNA constructs were previously created in the lab of Craig McCormick from a pGIPZ vector purchased from Open Biosystems and kindly gifted to us. Briefly, this vector lacks the open reading frame (ORF) for green fluorescent protein (GFP) and places the promoter proximal to an internal ribosome entry site (IRES) (Corcoran et al., 2015). Two shRNA sequences targeting the K12 ORF of the kaposin locus were provided to us in pIPZ vectors; the 21-mer sequences for shKap1 and shKap2 were: 5'-ACGGTGTTTGTGGCAGTTCAT-3' and 5'-GTCCCGGATGTGTTACTAAAT-3, respectively. The shRNA constructs were cloned into the pIPZ backbone using MluI and XhoI cut sites. pLJM1 lentiviral vectors used for gene expression were purchased from Addgene. A 636-bp nucleotide sequence of Kaposin B (KapB), originally obtained from a pulmonary KS isolate of KSHV and kindly provided by Dr. Craig McCormick in a pCR3.1 expression vector (Invitrogen) (McCormick & Ganem, 2005), was cloned into the pLJM1 backbone by BamHI- and EcoRI- restriction digest.

2.2 Cell Culture

The KSHV-positive PEL-derived cell line, BCBL-1 (Renne et al., 1996), and the renal-cell carcinoma cell line, iSLK (Stürzl et al., 2012), were kind gifts from Craig McCormick, originally obtained from D. Ganem (University of California San Francisco). Both cell lines had been transduced with vectors to allow inducible expression of the viral

replication and transcription activator (RTA, ORF50) under control of a tetracycline-responsive (TREx) promoter; RTA-transduced cells were selected and maintained by culturing the cells in media supplemented with 1 μg/mL puromycin (Invitrogen) (Nakamura et al., 2003; Myoung and Ganem, 2011a). SLK cells were additionally selected and cultured in media containing 800 μg/mL geneticin (G418; Invitrogen) to select for cells transduced with the inducible expression system, pRetroX-Tet-On (Myoung and Ganem, 2011a). BCBL-1 cells were maintained in Roswell Park Memorial Institute (RPMI) 1640 medium (Invitrogen) supplemented with 10 percent (%) heat-inactivated fetal bovine serum (HI-FBS; Invitrogen), 100 U/mL penicillin, 100 μg/mL streptomycin, 2 mM L-glutamine (1% PSQ; Invitrogen), and 55 μM of β-mercaptoethanol (Invitrogen). These cells were maintained at a density of $2x10^5$ to $1x10^6$ cells/mL. SLK cell lines (and all derivatives) and Human Embryonic Kidney (HEK) 293T cells were cultured in Dulbecco's Minimal Essential Medium (DMEM) (Invitrogen) supplemented with 10% HI-FBS, and 1% PSQ. Medium was refreshed every 2-3 days and cells were sub-cultured once they became 80-90% confluent. Primary human umbilical vein endothelial cells (HUVECs) were obtained from Lonza and cultured in EGM-2 medium (Lonza) using tissue culture plates coated with 0.1% (wt/vol) gelatin in phosphate-buffered saline (PBS pH 7.4; Thermo Fisher Scientific). Media was refreshed every 48 hours and cells were sub-cultured once they became 80-90% confluent. HUVECs were sub-cultured in a ratio of 1:4 confluent wells of a 6-well tissue culture plate to new wells of a 6-well plate, or a ratio of 1:6 for confluent well of a 6-well plate to new wells of a 12-well plate. HUVECs were used between passages 6 and 8 for experiments. All cell lines were incubated at 37°C in a humidified chamber with 5% CO_2 content.

2.3 Recombinant lentivirus production

HEK 293Ts were used as a packaging cell line for recombinant lentivirus production. Cells were seeded in a 10 cm culture dish and incubated for 24 hours. The next day, once cells reached 70-80% confluence, cells were washed with PBS (Thermo Fisher Scientific) and subsequently cultured in 4mL of serum-free, antibiotic-free DMEM. The following reaction mixture was added to the medium dropwise: 2 μg of pSPAX2 (packaging) and 1 μg of pMD2.G (envelope) lentiviral vectors (Addgene), 3.3 μg of each shRNA-containing lentiviral transfer vector, pIPZ, and 18 μL of polyethylenimine (PEI, Sigma-Aldrich) diluted in 500 μL of Opti-MEM I reduced serum medium (Thermo-Fisher Scientific). To make KapB-expressing lentivirus, the pIPZ vector was instead replaced with a pLJM1 lentiviral expression vector containing the 636-bp KapB ORF. After 6 hours of transfection, the medium was replaced with DMEM containing 10% FBS, but absent of antibiotic, and incubated for 48 hours. Virus-containing supernatants were harvested, filtered through a 0.45 μm polyethersulfone (PES) membrane filter (VWR), and stored at -80°C in 1 mL aliquots.

2.4 Lentiviral Transduction

Prior to use, lentiviruses were thawed in a water bath at 37°C. BCBL-1 cells were transduced with shRNA-expressing lentivirus by mixing cells at a density of $2x10^5$ cells/mL with 1/10 diluted-virus and culturing in antibiotic-free medium supplemented with 5 μg/mL hexadimethrine bromide (polybrene; Sigma-Aldrich) for 24 hours at 37°C. Following transduction, cells were subjected to centrifugation at 300xg for 5 min at room temperature, washed with 1X PBS (Thermo Fisher Scientific) and selected for positive

transduction by culturing in complete medium supplemented with 1 μg/mL puromycin (Invitrogen) for 2 days at 37°C. Cells were recovered from selection by centrifugation, washed as above, and cultured in complete medium for 24 hours at 37°C.

iSLK-BAC16 cells were seeded at a density of $1x10^5$ cells/mL in a 6-well plate and the next day transduced by mixing with pLJM1-expressing lentivirus diluted to 1/10 final volume in antibiotic-free medium supplemented with 5 μg/mL polybrene. Cells were transduced for 24 hours at 37°C, after which successfully-transduced cells were selected by culturing in complete medium containing 5 μg/mL blasticidin (Invitrogen) for 4 days at 37°C. Selected cells were recovered by replacing the medium with complete medium and cultured for 24 hours at 37°C.

2.5 Production and Titration of BCBL-1 KSHV

KSHV was prepared from TREx BCBL-1-RTA cells by inducing the cells to express RTA, and therefore trigger lytic reactivation. Briefly, cells were seeded at a density of $2x10^5$ cells/mL in antibiotic-free culture medium. Medium was replaced after 24 hours with fresh medium containing 1 μg/mL of doxycycline, which induced the expression of RTA, and cells were cultured at 37°C and 5% CO_2. At 2 days post-induction, cells were pelleted by centrifugation at 4000xg for 5 min at room temperature in a Beckman Coulter Microfuge 20 Centrifuge and the virus-containing supernatant was stored at -80°C in 1 mL aliquots.

For titration, naïve iSLK cells were seeded at a density of $2.5x10^5$ cells/well of a 12-well tissue-culture plate on to coverslips coated with 0.1% gelatin in PBS. The next day, viral aliquots were thawed in a 37°C water bath and subjected to centrifugation at

4000xg for 5 mins at room temperature prior to use to pre-clear cell debris. Virus was diluted in serum-free and antibiotic-free medium in the presence of 8 μg/mL hexadimethrine bromide (polybrene; Sigma-Aldrich). Virus-containing medium was added to the iSLK cells and the cells were subjected to centrifugation at 800xg for 2 hours at 30°C, a process hereby referred to as 'spinoculation'. The medium was immediately replaced after centrifugation to antibiotic-free DMEM and cells were cultured at 37°C. The next day, cells were washed once with PBS and fixed onto coverslips with treatment of 4% paraformaldehyde in PBS for 30 mins at 37°C. Fixing reagent was washed away thoroughly and coverslips were stored in PBS at 4°C until staining for immunofluorescence; maximum time of storage was 1 month.

2.6 Quantification of Intracellular Viral Genome Copy Number

The following reagents and protocol were shared as a generous gift by Eric Pringle from the lab of Craig McCormick. DNA was harvested from cells using a DNeasy Blood and Tissue Minikit (Qiagen) as per the manufacturer's protocol and stored at -20°C. qPCR was performed using the GoTaq qPCR Master Mix (Promega) with primers designed to amplify ORF26 and β-actin (Table 2.1). Each qPCR reaction well was set up in duplicate as follows: 4 μL of DNA sample in nuclease-free water was added to 6 μL of working master mix containing 5 μL of 2X Go-Taq qPCR Master Mix (Promega) for every 1 μL of forward and reverse primers diluted in nuclease-free water [each at 2 μM]. Primer efficiencies were determined by Eric Pringle for the following qPCR cycling conditions: 1 cycle of initial denaturation (95ºC for 3 min), 40 cycles of denaturation (95ºC for 10 sec), annealing, and extension (60ºC for 30 sec), and 1 cycle of final extension (65ºC for 5 sec;

TABLE 2.1: List of qPCR primers

Primer	Primer Sequence
qPCR ORF26 – Forward	5'-CAGTTGAGCGTCCCAGATGA-3'
qPCR ORF26 – Reverse	5'-GGAATACCAACAGGAGGCCG-3'
qPCR β-actin – Forward	5'-CTTCCAGCAGATGTGGATCA-3'
qPCR β-actin – Reverse	5'-AAAGCCATGCCAATCTCATC-3'
qPCR Luc – Forward	5'-TGCGCAAGAATAGCTCCTCC-3'
qPCR Luc – Reverse	5'-TTCGGCAACCAGATCATCCC-3'

95ºC for 5 sec). KSHV genome copy number is represented as the fold change given by

$$\text{Fold change} = 2^{-[\Delta C_{T(Wild-type)} - \Delta C_{T(kaposin-mutant)}]}$$

where the average amount of target, ORF26, was normalized to an endogenous reference gene, β-actin, for each condition to determine the ΔC_T value (Livak & Schmittgen, 2001).

2.7 Quantification of Extracellular, DNase-Protected Viral Genome Copy Number

The following protocol was provided by Eric Pringle from the lab of Craig McCormick. Briefly, virus stocks from lytic TREx BCBL-1-RTA were thawed in a water-bath at 37°C and centrifuged at 4000xg for 5min at room temperature to pellet residual cell debris. An aliquot of 180 μL of virus was treated with 10U of DNase I prepared with 10X reaction buffer [100 mM Tris pH7.5, 25 mM $MgCl_2$, and 5 mM $CaCl_2$] (Invitrogen) and nuclease-free water (Invitrogen) for 30 minutes at 37°C. DNA was extracted from virions using a DNeasy Blood and Tissue Minikit (Qiagen) as per the manufacturer's protocol with the following modifications: lysis buffer AL was supplemented with 10 mg/sample of salmon sperm DNA (Invitrogen) and 1 ng/sample of pGL4.26 plasmid containing a luciferase (*luc2*) gene (Clonetech). Amplification of ORF26 and *luc2* was conducted using specific primers (Table 2.1) for qPCR using the Go-Taq Master Mix (Promega), as previously described. This allowed for detection of viral genomes, which were represented as fold change normalized to *luc2* quantity using the $2^{-\Delta\Delta C_T}$ method.

2.8 BAC16 Kaposin-Mutagenesis

A recombinant full-length KSHV genome containing a red fluorescent protein (RFP) cassette under control of a constitutively active EF1α-promoter was supplied as a

bacterial artificial chromosome (BAC) clone, BAC16, in the GS1783 *Escherichia coli* (*E.coli*) strain (Brulois et al., 2012); this genome was a generous gift from Craig McCormick and was used as the backbone for all mutagenesis described herein. Previously established kaposin mutants (ΔKapBΔKapC double mutant and ΔKapABC triple mutant and ΔKapBC double mutant) were generated by Julie Ryu using the same method described herein to generate other mutants; this method involves a two-step homologous recombination protocol relying on Lambda Red and I-SceI activities supplied by the GS1783 strain, as previously described (Tischer et al., 2010). Details of this protocol are as follows.

Genes encoding kanamycin resistance and levansucrase enzyme activity (KanSacB) were amplified as a selection cassette by PCR from the pGEM-T vector (Promgea). The amplification reaction used oligonucleotide primers to add 40bp sequences flanking the KanSacB cassette; these regions were homologous to the K12 sequence found downstream of the DR region within the BAC16 genome. The amplification reaction also incorporated BamHI and NotI restriction endonuclease sites into the product from the forward and reverse primers, respectively (Table 2.2). This PCR product was sub-cloned into a pcDNA3.1+ vector (Addgene) by restriction enzyme digest with BamHI and NotI-endonucleases (Figure 2.1).

Two gene blocks comprised of alternatively coded sequence for the DR regions were synthesized and provided in a pUC57 backbone (BioBasic). In the first gene block, the KapC ORF was recoded in order to maintain the amino acid sequence of KapC, while the KapB ORF was disrupted by insertion of multiple pre-termination codons. In the second gene block, the nucleotide sequence was recoded to disrupt the KapC protein-

TABLE 2.2: List of BAC16 mutagenesis primers

Primer	**Primer Sequence**
Fwd. is forward primer *Rev. is reverse primer*	*Restriction enzyme recognition sites are bolded.* *BAC16 homology regions are underlined.* *Complementary target sequences are italicized.*
KanSacB Homology – Fwd.	5'-ATACAT**GGATCC***AGGATGACGACGATAA GTAGGGATAACAGGGTAAT*-3'
KanSacB Homology – Rev.	5'-ATTAGT**GCGGCCGC**GGACATGAACTGCC ACAAACACCGTTAAGCCTCTATCCAT*CAACC AATTAACCAATTCTGAT*-3'
altKapC Homology – Fwd.	5'-ATACAT**GCTAGC**CGGAGGACGGATCTCT TGGATTTACACGTATCGAGGAGCG*GTAGCA CCCCAGGAACCCGTCCTAGCACACCCCA*-3'
altKapC Homology – Rev.	5'-TGATTA**GGATCC**GGACATGAACTGCCAC AAACACCGTTAAGCCTCTATCCATA*CACTGA GATTGAAGAG*-3'
altKapB Homology – Fwd.	5'-ATACAT**GCTAGC**CGGAGGACGGATCTCT TGGATTTACACGTATCGAGGAGCG*GTGGCA CCCCAGGAACCCGT*-3'
altKapB Homology – Rev.	5'-TGATTA**GGATCC**GGACATGAACTGCCAC AAACACCGTTAAGCCTCTATCCAT*GCATAGG TATAGGTGGTAGA*-3'
Kaposin Screening – Fwd.	5'-*CAGGAAACGCTATAAAGAAGAGG*-3'
Kaposin Screening – Rev. (K12 primer)	5'-*ACAGACAAACGAGTGGTGGTATC*-3'
altKapC Screening – Rev.	5'-*ATTACCTGGAAGCAATGCACC*-3'
altKapB Screening – Rev.	5'-*TGATGAAGGAACTAGATTGCCAG*-3'
KanSacB Screening – Fwd.	5'-*GCGACAACCATACGCTGAGAG*-3'
Revertant Screening – Rev. (Homology primer)	5'-*ACACCGTTAAGCCTCTATCCAT*-3'
Revertant Screening – Rev. (Revert primer)	5'- *TGCATTGGGATTGGAGTGAGGA*-3'

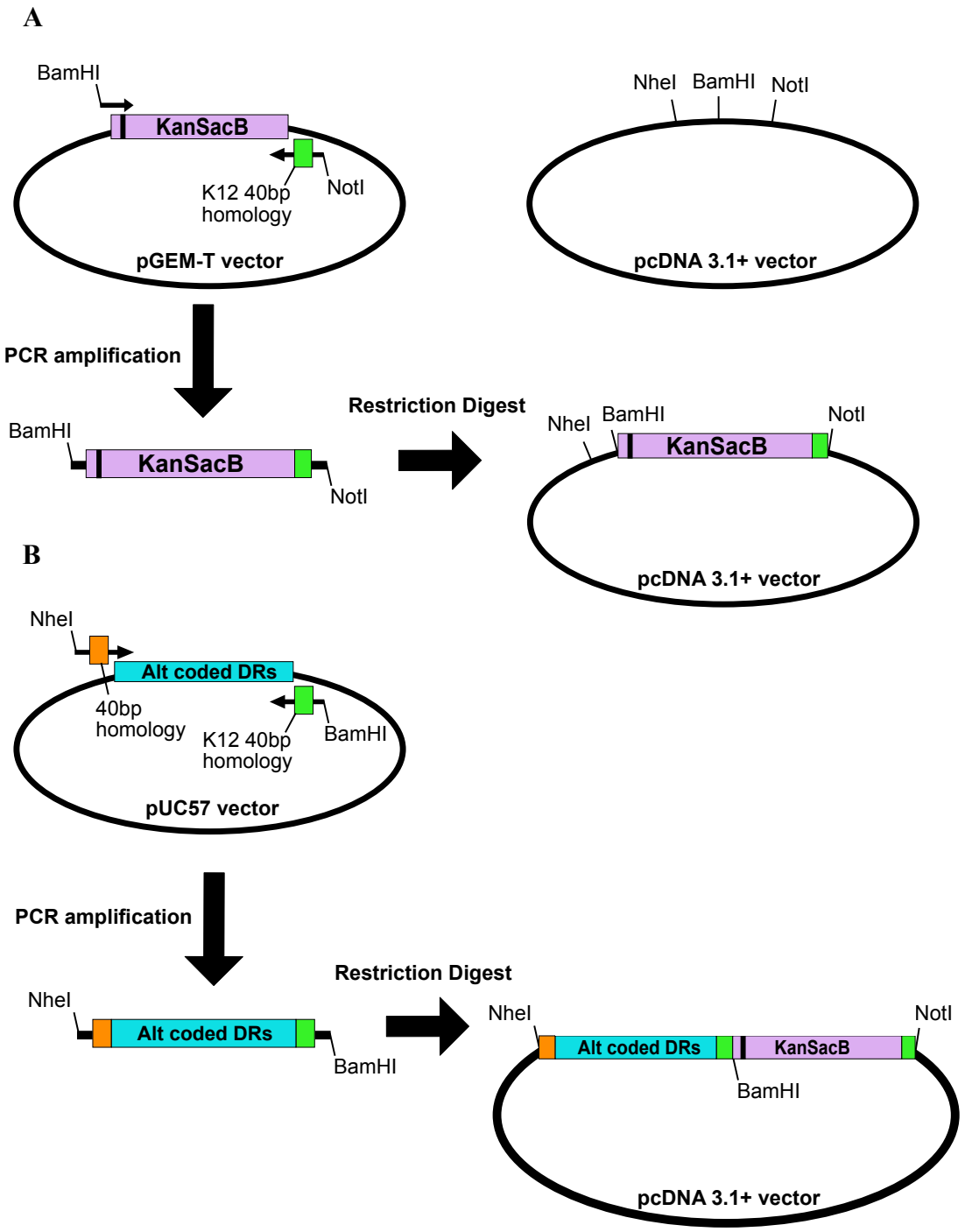

Figure 2.1: Cloning strategy for constructs used in BAC16 mutagenesis. (A) Genes encoding kanamycin resistance and levansucrase enzyme activity (KanSacB) were amplified by PCR to add restriction enzyme recognition sites and a region of homology matching the first 40-bp of the K12 ORF. PCR products were subcloned into a pcDNA3.1+ vector by BamHI- and NotI-restriction digest. (B) PCR amplification of a gene block containing alternatively coded direct repeat (alt coded DRs), which were synthesized and provided by BioBasic in a pUC57 vector, was conducted to add 40-bp homology regions and restriction enzyme recognition sites. PCR products were subcloned into the pcDNA3.1+ vector produced in (A) by NheI- and BamHI-restriction digest.

coding capacity with early termination codons, while maintaining KapB primary amino acid sequence.

Both gene blocks were amplified by PCR using primers to add 40bp sequences that flank the gene block and are homologous to upstream (forward primer) and downstream (reverse primer) regions of the DRs in the BAC16 genome (Table 2.2 for primer sequences). This PCR product was sub-cloned into the pcDNA 3.1+ KanSacB vector described above using NheI and BamHI restriction sites added by the forward and reverse primers, respectively (Figure 2.1).

Lamda Red recombination of the gene blocks was conducted in the BAC16-containing GS1783 *E.coli.* Bacteria were cultured in Miller Luria broth (LB)(Sigma-Aldrich) containing 30 μg/mL chloramphenicol to select for the BACmid. Upon reaching an optical density (OD_{600}) of 0.6-0.8, the culture was incubated in a 42°C water bath to induce expression of the Lambda Red genes. Linear DNA fragments were generated from the gene blocks & KanSacB containing plasmids by restriction digest with NheI and NotI enzymes; the DNA fragment used for recombination was purified by 1% agarose gel electrophoresis and gel extraction of the DNA band using the QIAquick Gel Extraction kit (QIAGEN). DNA fragments were electroporated (2.5 kV, 25 μF, BioRad Gene Pulser® II) into 50 μL of concentrated Lambda Red-induced GS1783 bacteria and recovered in 1 mL of LB for 1 hour at 30°C. Recombinant clones were selected at 30°C on LB plates containing 50 μg/mL kanamycin. The resulting colonies were analyzed by colony PCR using screening primers listed in Table 2.2.

Positive clones were cultured at 30°C in LB containing 1% arabinose for 1 hour to induce I-SceI expression and subsequently cultured at 42°C for 30 min to induce

recombination genes. Induction of I-SceI linearizes the BACmid allowing for an intramolecular recombination event to remove the positive selection marker, KanSacB. The bacteria were recovered in 1 mL LB for 2 hours at 30°C and then selected overnight at 30°C on LB plates containing 30 μg/mL chloramphenicol and 5% sucrose, which selects for removal of SacB. Positive colonies were replicate-plated on LB containing 50 μg/mL kanamycin; colonies sensitive to kanamycin were screened by colony PCR and verified by Sanger DNA sequencing (GENEWIZ©). All restriction enzymes were obtained from New England BioLabs and primers were obtained from Invitrogen.

2.9 BAC DNA Isolation

Wild type and kaposin-mutant BAC DNA was isolated from 10 mL cultures of GS1783 *E.coli* by standard alkaline lysis using reagents from QIAprep kits (QIAGEN). Briefly, bacteria were pelleted at 4000xg for 15 min at room temperature in a ThermoScientific Sovrall ST40R Centrifuge. QIAprep buffers were then added to the pellet in equal volumes (400 μL); the pellet was resuspended in P1 buffer, lysed for 5 min by adding P2 buffer, and then neutralized by adding N3 buffer. The supernatant containing BAC16-DNA was cleared by centrifugation at 15000 xg for 10 min at room temperature. DNA was precipitated by addition of 800 μL of 100% isopropanol to 1200 μL of supernatant; the resultant pellet was washed with 1 mL of 70% ethanol and left to air dry. The DNA pellet was resuspended in 50 μL of nuclease-free water and stored at -20°C.

2.10 Restriction Digest of KSHV-BAC DNA

In order to verify the absence of large-genome rearrangements, each BACmid clone was subjected to overnight single-enzyme restriction digestion, once each using NheI- (which does not cut within the KSHV terminal repeats) and NotI- high-fidelity restriction enzymes (New England Biolabs) at 37°C. Digested DNA fragments were subjected to 1% agarose pulsed-field gel electrophoresis (PFGE) (Bio-Rad) using 0.5% Tris/Borate/EDTA (TBE) buffer and the following conditions: 6 V/cm, 120° field angle, and switch time linearly ramped from 1 s to 5 s over 14-15 h (CHEF DR III, Bio-Rad). DNA bands were visualized by staining the gel with a solution of 0.5 µg/mL ethidium bromide; excess stain was washed away with deionized water and the gel was imaged on a ChemiDoc Touch Imaging System (Bio-Rad).

2.11 Next-Generation Sequencing of KSHV-BACs

To analyze the integrity of the complete viral genome, viral DNA isolated from GS1783 *E.coli* for wild-type and kaposin-deletion KSHV-BACs was submitted to Dr. Andre Comeau, manager of the Integrated Microbiome Resource at the Centre for Comparative Genomics and Evolutionary Bioinformatics at Dalhousie University, for next-generation sequencing. DNA was fragmented and tagged with sequencing adapters using Nextera XT DNA Library Prep Kit (Illumina). The PCR-derived DNA library was sequenced by MiSeq (Illumina), which generated 300+300bp paired-end sequences. Paired sequences were analyzed for quality, trimmed, and mapped to the BAC16 genome (Genbank, accession no. GQ994935) by Dr. Bruce Curtis, post-doctoral fellow in the lab of Dr. John Archibald at Dalhousie University. Unpaired, trimmed reads were crudely

mapped to the BAC16 genome using Geneious software to demonstrate depth of coverage and proportion of total reads mapping to the KSHV genome.

2.12 Generation of iSLK-BAC16 Cells and Production of Viral Stocks

HEK 293T cells were seeded in complete DMEM in a 6-well tissue culture plate such that they would be ~70-80% confluent the next day. The cells were washed once with PBS and the medium replaced with serum-free and antibiotic-free medium. A transfection mixture containing 2 µg of KSHV-BAC16 DNA and 6 µL of polyethylenimine (PEI) was prepared in 400 µL Opti-MEM I Reduced Serum Medium (Thermo Fisher Scientific) and added dropwise to the medium. Cells were incubated for 5-6 hours at 37°C at which point the medium was replaced with antibiotic-free DMEM and the cells were further cultured for 72 hours. The cells were trypsinized and seeded into a 10 cm tissue-culture plate with medium containing 50 µg/mL of hygromycin B (Invitrogen) to select for BAC16-containing HEK cells. Medium was replaced every 2-3 days with increasing hygromycin B concentration up to a maximum of 100 µg/mL. Following selection, HEK-BAC16 cells were sub-cultured and mixed at a 1:1 ratio with naïve iSLK cells to a total of 2.5 $x10^5$ cells/well in a 6-well tissue culture plate in complete DMEM. After 24 hours, lytic reactivation was induced in HEK-BAC16 by culturing the cells in the presence of 20 ng/mL 12-O-tetradecanoylphorbol-13-acetate (TPA) and 1mM sodium butyrate (NaB) (Sigma-Aldrich) and in the absence of antibiotic. After 96 hours of lytic induction, cells were trypsinized and seeded into a 10 cm tissue-culture plate with medium containing 250 µg/mL geneticin (G418) (Invitrogen), 1 µg/mL puromycin, and 200 µg/mL hygromycin B.

Medium was replaced every 2-3 days with increasing hygromycin B concentration up to a maximum of 1200 μg/mL.

To produce virus stocks, iSLK-BAC16 cells were seeded at a density of $2.5x10^5$ cells/mL in complete DMEM. After 24 hours, lytic reactivation was induced by replacing the medium with antibiotic-free DMEM containing 1 μg/mL doxycycline (Dox) (Sigma-Aldrich) and 1 mM sodium butyrate (NaB) (Sigma-Aldrich). After 96 hours of lytic induction, virus-containing supernatant was harvested and subjected to centrifugation at 4000xg for 5 mins at room temperature to clear cells and debris. Virus was stored in 1 mL aliquots at -80°C prior to use.

2.13 Infection of HUVECs with iSLK-BAC16-Generated KSHV

HUVECs were passaged and seeded as described for 12-well tissue-culture plates on to coverslips coated with 0.1% gelatin (Sigma-Aldrich) in PBS. The next day, viral aliquots were thawed in a 37°C water bath and subjected to centrifugation at 4000xg for 5 mins at room temperature prior to use to pre-clear cell debris. Virus was diluted in serum-free and antibiotic-free EBM-2 medium in the presence of 8 μg/mL polybrene. Virus-containing medium was added to HUVECs and the cells were spinoculated at 800xg for 1 hour at 30°C. Cells were cultured for 1 hour at 37°C at which time the medium was replaced to antibiotic-free EGM-2 and cells were further cultured at 37°C. After 2 days, the medium was replaced with fresh EGM-2, and at 72 hours post-infection cells were washed once with PBS and fixed onto coverslips with treatment of 4% paraformaldehyde in PBS for 30 mins at 37°C. Fixing reagent was washed away thoroughly and coverslips

were stored in PBS at 4°C until staining for immunofluorescence; maximum time of storage was 1 month.

2.14 Immunofluorescence Microscopy

Cells fixed onto coverslips were permeabilized by treatment with 0.1% Triton X-100 (Sigma-Aldrich) diluted in 1X PBS (137 mM NaCl, 2.7mM KCl, 10 mM Na_2HPO_4, 1.8 mM KH_2PO_4, 1 mM $CaCl_2 \cdot 2H_2O$, 0.5 mM $MgCl_2 \cdot 6H_2O$) for 10 mins at room temperature. Coverslips were washed three times and blocked with 1% human AB serum (Sigma-Aldrich) diluted in PBS for 1 hour at room temperature. Cells were stained using either rabbit anti-LANA (1:1000, a kind gift from Craig McCormick and Don Ganem) to determine KSHV-infected cells or rabbit anti-EDC4 (1:1000, Cell Signaling; #2548) to visualize processing bodies (PBs); antibodies were diluted in blocking buffer and applied to coverslips overnight at 4°C in a humidity chamber. Stained cells were washed with PBS and incubated for 1 hour with Alexa Fluor 488-conjugated chicken anti-rabbit IgG H+L (Thermo Fisher Scientific; #1796684) at room temperature.

Following three washes to remove unbound primary antibody, HUVECs were subsequently stained for cellular F-actin by incubating coverslips in Alexa Fluor 647-conjugated phalloidin (1:100, Thermo Fisher Scientific; #A22287) diluted in PBS. Cells were washed sparingly with PBS prior to being mounted onto glass microscope slides (Electron Microscopy Sciences) using ProLong Gold antifade reagent (Thermo Fisher Scientific; #P36930). HUVECs were visualized and photographed by Gillian Singh on a Zeiss LSM 510 scanning confocal microscope, using argon (488 nm) and neon (548 and 633 nm) lasers and 63X oil immersion objective in the Cellular & Molecular Digital

Imaging Facility at Dalhousie University. Images were collected with similar exposure times and identical gains, except for minor adjustments to gain to visualize phalloidin stain. Images were processed using Image J software.

iSLK cells were washed three times after primary staining and incubated for 10 mins at room temperature in 100 ng/mL of 4',6-diamidino-2-phenylindole, dihydrochloride (DAPI) (Thermo Fisher Scientific; #D1306) diluted in PBS to stain cell nuclei. Cells were washed three times with PBS prior to being mounted onto glass microscope slides using ProLong Gold antifade reagent. iSLK cells were visualized and photographed on a Zeiss Axioplan 2 motarized microscope using 40X oil immersion objective. Image J software was used for image processing and to quantify the number of nuclei and LANA dots for 5 fields of view per condition.

2.15 Flow Cytometry of KSHV-Infected iSLK Cells

Naïve iSLK cells were seeded at a density of $2.5x10^5$ cells/well of a 12-well tissue culture plate in complete medium. The next day, cells were spinoculated with KSHV as described for HUVECs with the following modifications: cells were spinoculated for 2 hours in serum-free and antibiotic-free DMEM containing polybrene, and medium was replaced with fresh complete medium immediately after spinoculation. Cells were trypsinized 24 hours post-infection, washed once with 1X PBS, and fixed by treatment with 2% paraformaldehyde for 20 mins at room temperature with constant inversion. Cells were pelleted by centrifugation at 500xg for 5 mins at room temperature, washed with 1X PBS, and re-suspended in 1 mL PBS. Cells were counted using a BD Biosciences FACS Canto II flow cytometer; 100,000 events were counted for each condition using the PE-channel

(488 nm laser with 564-606 nm filter settings). Cells were first gated for live cells using forward (FSC) and side scatter (SSC) measurements, and subsequently gated for RFP-positivity by setting the minimum detection limit for PE-area to 1% for mock-infected cells using Flowing Software 2 (Turku Centre for Biotechnology).

2.16 Immunoblotting

BCBL-1 suspension cells were first harvested by centrifugation at 300xg for 5min. All cells were washed once with 1X PBS (Thermo Fisher Scientific) and lysed in 200 µL of 2X Laemmli buffer (120 mM Tris-HCl, pH 6.8, 4% sodium dodecyl sulfate [SDS], 20% glycerol) and stored at -20°C. Cell lysates were thawed on ice and passed through a 21-gauge needle to shear DNA and reduce viscosity. Protein concentration was quantified by the DC Protein Assay (Bio-Rad). Lysates were mixed with 9 µL of 300 mM 1,4-dithiothreitol (DTT) (Sigma-Aldrich) and 3 µL of 0.1% bromophenol blue (Sigma-Aldrich) and heated at 95°C for 5 minutes. Protein samples (10-20 µg) were separated by SDS-polyacrylamide gel electrophoresis (SDS-PAGE) and transferred to ImmunoBlot polyvinylidene fluoride (PVDF) membranes (Bio-Rad) using a Trans-Blot Turbo transfer system (Bio-Rad). Membranes were blocked in 5% skim milk powder diluted in Tris-buffered saline (50 mM Tris-HCl, pH 7.5, 150 mM NaCl) supplemented with 0.1% Tween 20 (Sigma-Aldrich) (TBS-T) for 1 hour at room temperature. Target proteins were probed with primary antibodies diluted in either 2.5% bovine serum albumin (BioShop) or 2.5% skim-milk diluted in TBS-T overnight at 4°C rocking. Excess and unbound antibody was removed from the membrane by three washes of TBS-T prior to incubation for 1 hour at room temperature with secondary IgG antibodies conjugated to horseradish peroxidase

(HRP) diluted in 2.5% BSA or skim milk. Membranes were washed with TBS-T and exposed to Clarity or Clarity-Max western ECL blotting substrate (Bio-Rad); chemiluminescence was visualized on a ChemiDoc Touch Imaging System (Bio-Rad). Antibodies and their dilutions used in this study were: rabbit polyclonal KapB (1:1000 in skim milk, a kind gift from Craig McCormick and Don Ganem); mouse monoclonal ORF45 (1:1000, Thermo Fisher Scientific; #MA5-14769); mouse monoclonal ORF65 (1:500, a kind gift from Craig McCormick and Shou-Jiang Gao); rabbit monoclonal LANA (1:1000, a kind gift from Craig McCormick and Don Ganem); RTA (1:1000, a kind gift from Craig McCormick and David Lukac); mouse monoclonal ORF57 (1:1000, Santa Cruz; sc-135746); rabbit β-actin HRP-conjugate (1:2000, Cell Signaling; #5125); anti-mouse IgG HRP-linked (1:2000, Cell Signaling; #7076); anti-rabbit IgG HRP-linked (1:2000, Cell Signaling; #7074).

2.17 Statistical Analysis

Experimental data was analyzed using GraphPad Prism 6.0 software using the recommended statistical tests. Data containing multiple grouped sample means were analyzed using two-way repeated measures analysis of variance (ANOVA) with a post-hoc Dunnett's multiple comparisons test. Data in which samples were normalized and reported as mean fold change relative to another sample mean were analyzed using a two-tailed one-sample Student's t-test for significant differences from a hypothetical value of 1. Statistical significance was determined as having a $p < 0.05$.

CHAPTER 3: RESULTS

3.1 Knockdown of the Kaposin Transcript Does Not Impair Lytic Reactivation in KSHV-Infected B-Lymphocytes

To investigate whether the kaposin proteins play an essential role in the lytic life cycle of KSHV, I used the inducible, stable-infected PEL cell line, TREx BCBL-1 (Nakamura et al., 2003). Two lentiviral vectors encoding short hairpin RNAs (shRNA) were used to knockdown the kaposin transcript (shKap1, shKap2). These hairpins targeted sequences downstream of the K12 start codon (Appendix, Figure A.1); shRNA-mediated knockdown of the kaposin transcript is expected to result in decreased levels of all three proteins, KapA, KapB, and KapC, since they are all translated from the same transcript in both latent and lytic virus life cycles (Figure 3.1). BCBL-1 cells were transduced with either shKap1- and shKap2-expressing lentiviruses or a non-targeting hairpin control (NS) for 24 hours. Cells that had been successfully transduced were subsequently selected by culturing the cells in the presence of puromycin for 48 hours. Selected cells were allowed to recover in fresh media for a 24-hour period prior to being seeded for lytic reactivation study. Cells were either treated with doxycycline (Dox) to induce the expression of ORF50, thus activating the virus lytic cycle, or left untreated, thus maintaining the virus in a latent state. As a control, one well of the Dox-treated cells was also treated with phosphonoacetic acid (PAA), known to selectively inhibit herpesvirus DNA polymerases (Overby et al., 1977). Because herpesviruses exhibit precise temporal control of gene expression, PAA-treatment was used as a negative control for genome replication and late gene expression, both of which are reliant on viral polymerase activity. Protein lysates, intracellular DNA extractions, and supernatant were each collected at 12, 24, and 48 hours post-lytic induction (hpi).

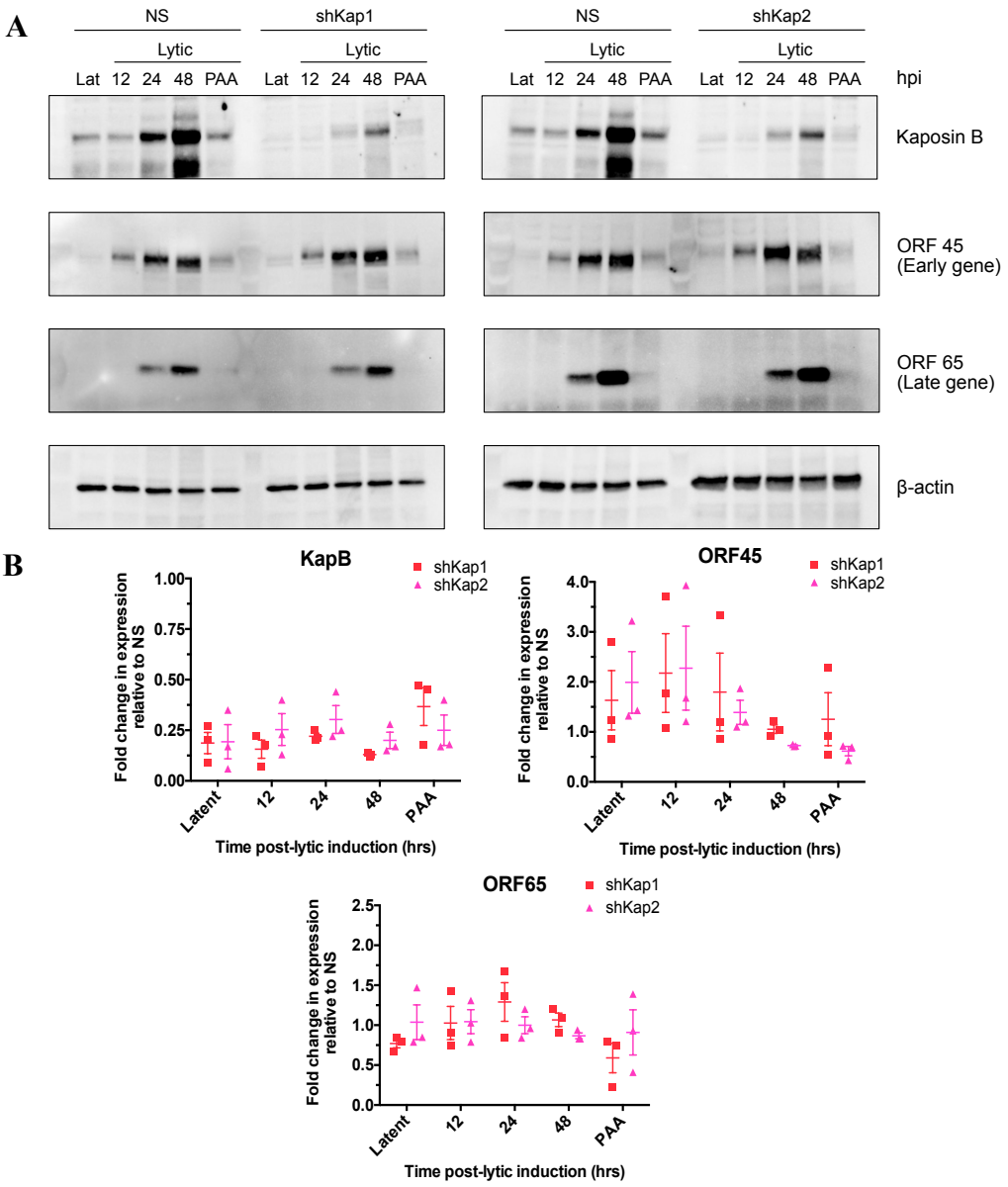

Figure 3.1: Knockdown of the kaposin transcipt does not impair lytic viral gene expression. (A-B) TREx BCBL-1 cells were transduced with recombinant lentiviruses that express short hairpin RNAs (shRNAs) targeted against two different regions of the K12 ORF of the kaposin transcript (shKap1, shKap2) or a non-specific (NS) shRNA control. Cells positive for successful transduction were selected by puromycin treatment. After recovery for 24 hours in complete media, selected cells were seeded and the following day were either induced toward lytic reactivation by culturing in doxycycline or were left untreated (latent, Lat). Lytic cells cultured in both doxycycline and phosphonoacetic acid (PAA) were used as a control for inhibition of genome replication. Lysates were harvested at 12, 24, and 48 hours post induction (hpi) and immunoblotted. Representative immunoblots from one experiment are shown in panel A. Protein band intensity was normalized to β-actin using Bio-Rad Image Lab software and is expressed in panel B as the mean fold change compared to the NS control ± SEM. Data are representative of three independent experiments.

Viral gene expression was analyzed by immunoblotting cell lysates against the viral proteins Kaposin B (latent and lytic), ORF45 (early lytic), and ORF65 (late lytic). Steady state protein levels were determined at each time post lytic induction and then normalized to a protein loading control, β-actin, using BioRad ImageLab software. In control cells transduced to express the NS shRNA control, Kaposin B expression increased throughout the time-course of lytic reactivation; however, protein expression was significantly attenuated whenever cells were transduced with either of the shRNAs targeted against the kaposin transcript (Figure 3.1A). An average kaposin knockdown efficiency between 64 to 87%, as normalized to β-actin, was achieved for each hairpin compared to the NS control and was maintained throughout the time course (Figure 3.1B). The loss of kaposin translation products did not result in significant differences in protein levels for ORF45 nor ORF65 throughout the time-course; however, there was a large variability in the quantitation of protein expression between experiments (Figure 3.1). Notably, ORF45 protein levels were slightly increased compared to the NS control during kaposin knockdown, especially at early time points 12 and 24 hpi during lytic reactivation (Figure 3.1). This suggests that knockdown of the kaposin transcript may result in accelerated viral gene expression during lytic reactivation.

Cellular DNA and associated-viral DNA genomes were extracted during the lytic time course to assay the progression of viral genome replication in the context of kaposin knockdown. The number of intracellular viral genomes was determined by qPCR using primers designed to amplify the viral gene, ORF26; these values were normalized according to a cellular housekeeping gene, β-actin. Since PAA is known to selectively

time-dependent increase in the quantity of intracellular ORF26-DNA in response to lytic inhibit herpesvirus DNA polymerases, cells treated with PAA for 48 hours were used as a negative control for genome replication. All cells transduced to express shRNAs showed a reactivation by doxycycline; this effect was abolished when cells were treated with PAA, indicative of accurate quantitation of viral genome replication using this method (Figure 3.2A). Cells transduced to express shKap1 or shKap2 recapitulated genome replication equal to the NS control (Figure 3.2A), suggesting that knockdown of kaposin transcripts does not affect viral genome replication.

Extracellular virus production was determined by collecting the supernatant from TREx BCBL cells throughout the lytic reactivation time course. Since a plaque assay has yet to be developed for quantifying infectious KSHV particles in the supernatant, an alternative DNase-protection assay was used. Briefly, a sample of supernatant was treated with DNase in order to eliminate DNA not protected by an envelope and protein capsid-coat. The envelope and protein capsid were subsequently lysed to extract virion DNA. Due to the low quantity of DNA contained within virions, salmon sperm DNA was added to the supernatant as a carrier to prevent loss of the viral DNA during extraction (White and Campbell, 2000). Additionally, 1 ng of luciferase plasmid DNA (pLuc2) was added to each sample and was used as a housekeeping gene to normalize the quantity of ORF26-viral DNA as determined by qPCR. The number of DNase-protected genomes in the supernatant steadily increased throughout the time-course of lytic reactivation for all TREx BCBL-1 cells, beginning at 24 hpi (Figure 3.2B), which was the first time-point at which viral DNA was detectable. Additionally, the number of extracellular viral genomes detected for shKap1 kaposin-knockdown cells was not significantly different compared to the NS

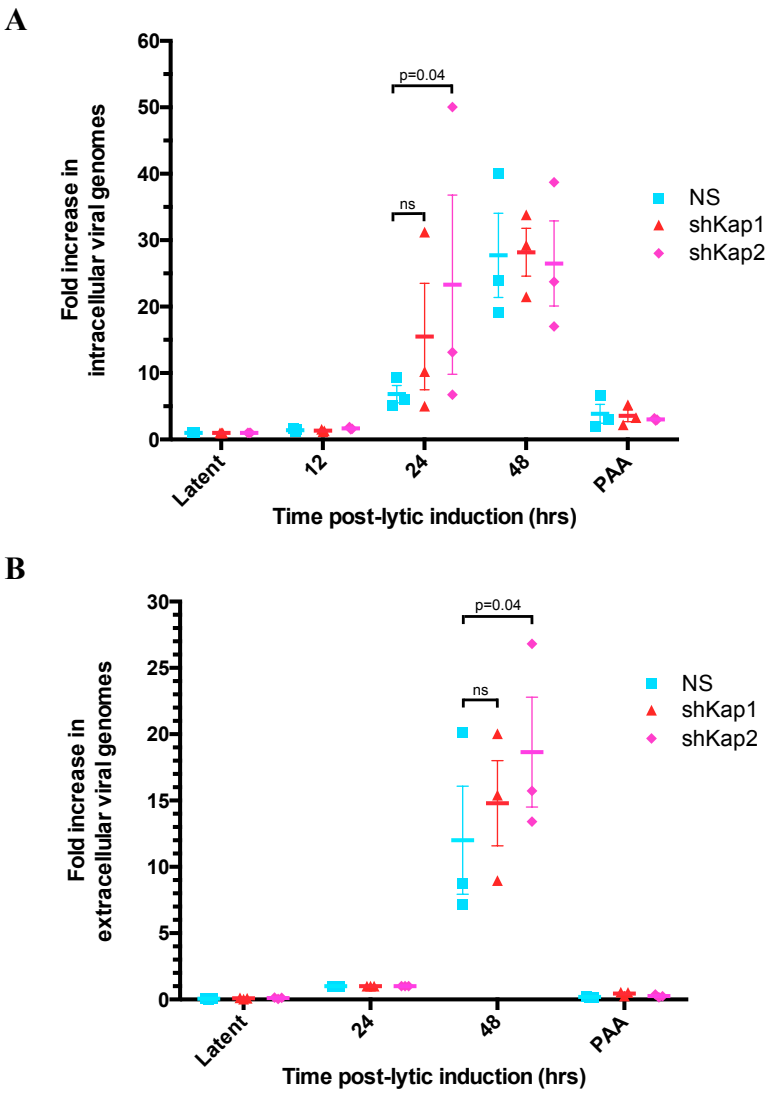

Figure 3.2: Kaposin knockdown does not impair viral genome replication or extracellular virus release. (A-B) TREx BCBL-1 cells transduced with shRNA-expressing lentiviruses targeted against the K12 ORF of the kaposin transcript (shKap1, shKap2) or a non-specific shRNA control (NS) were either left untreated (Latent) or induced toward lytic reactivation by treatment with doxycycline. Cells were also treated with a viral polymerase inhibitor, PAA. A) DNA was extracted from cells at 24 and 48 hours post induction (hpi) and quantified by qPCR using primers against the viral gene, ORF26. Quantification of the number of intracellular viral genomes was normalized to cellular β-actin and reported as the fold increase relative to latent cells using the ΔΔCt method. (B) Supernatants collected from lytic TREx BCBL-1 cells over the course of reactivation were DNase-treated; capsid-protected DNA that was resistant to DNase treatment was extracted and analyzed by qPCR as in A). The number of extracellular viral genomes was normalized to a known amount of luciferase plasmid added during the extraction and reported as the fold increase relative to the first sample with detectable viral genomes, 24 hpi. Data are representative of three independent experiments. Statistical significance was determined by two-way repeated measures ANOVA with Dunnett's multiple comparison test.

control; however, shKap2-expressing cells had a slightly increased number of genomes at 48 hpi compared to the NS control (Figure 3.2B). This effect was consistent with increased intracellular genome replication at 24 hpi (Figure 3.2A) and the observed increase in ORF45 protein expression levels at 12 and 24 hpi. In summary, kaposin knockdown does not impair KSHV lytic gene expression, genome replication, or production of virus particles in KSHV-infected B-lymphocytic cell lines. Moreover, my data suggest that a reduced amount of the kaposin transcript may promote a faster rate of progression through the lytic cycle.

While these assays have shown that the number of capsid-protected genomes released into the supernatant by lytic BCBL-1 cells is not impaired as a result of kaposin knockdown, it does not provide any information regarding the infectious nature of these virions. In order to assess the production of infectious KSHV particles after kaposin knockdown, supernatant was harvested from shRNA-expressing and reactivated BCBL-1 cells, as previously described. The undiluted virus-containing supernatant was used to infect naïve SLK cells, which were subsequently fixed with paraformaldehyde at 24hpi, blocked with human AB serum, and stained for immunofluorescence using primary antibody against LANA, the latent viral protein known to tether the KSHV episome to host chromatin (Cotter and Robertson, 1999). LANA is abundantly expressed following KSHV entry and aggregates to tether viral episomal DNA to host chromatin; therefore, LANA, which characteristically stains as a dot-like pattern in the nucleus, is an ideal marker for latently infected-cells (Ballestas et al., 1999). Virus harvested from lytic, NS shRNA-transduced BCBL-1 cells were positive for LANA dots, at a proportion of approximately 66% of the cell population positively-stained for at least one LANA dot (Figure 3.3). Virus

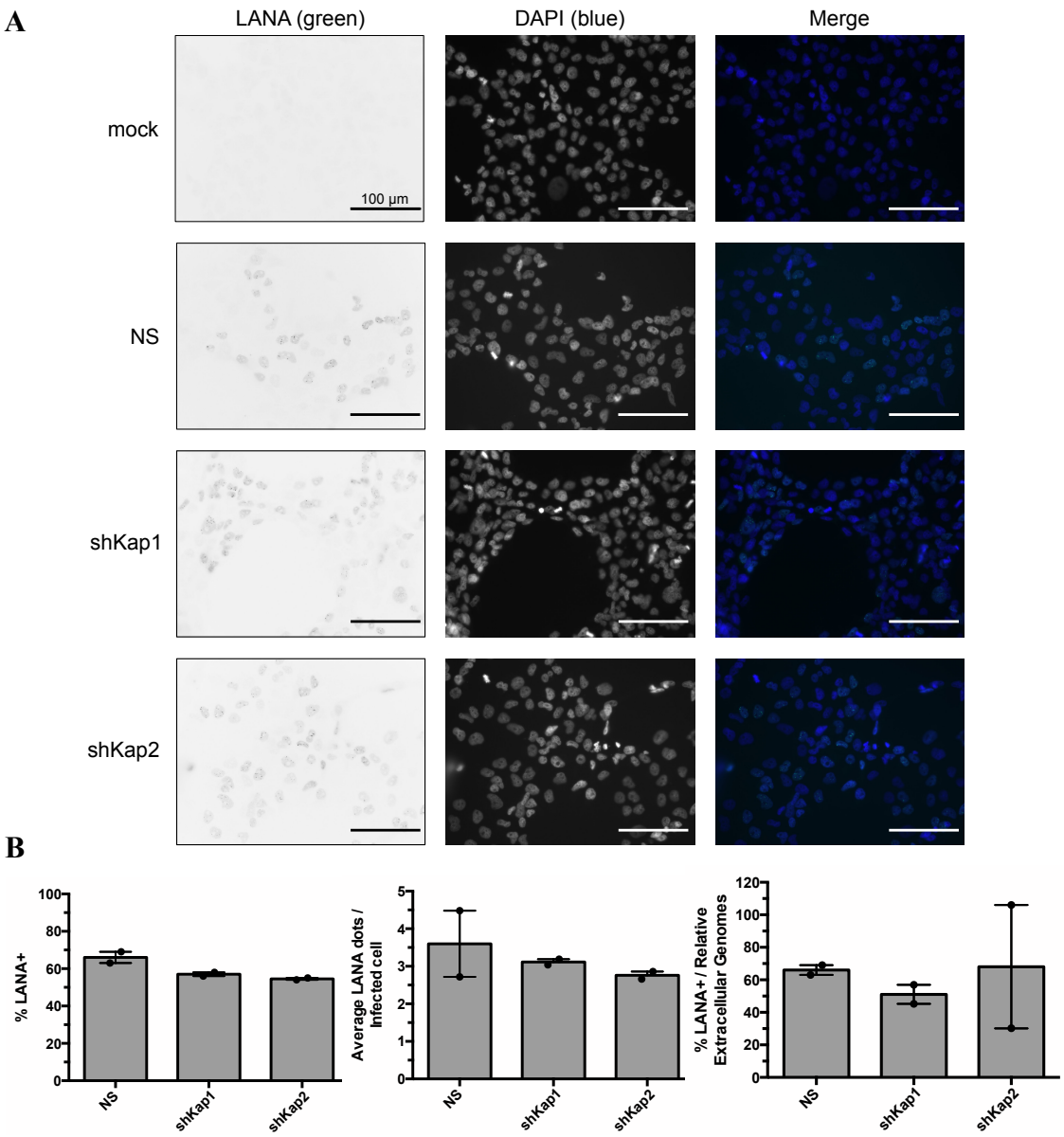

Figure 3.3: The production of infectious KSHV virions is not impaired by kaposin knockdown during lytic reactivation. (A-B) Cell supernatant was harvested 48 hours post-reactivation from lytic TREx BCBL-1 cells that had been transduced to express shRNAs against the kaposin transcript (shKap1, shKap2) or a non-specific shRNA (NS), and were used to infect naïve SLK cells. SLK cells were fixed 24 hours post-infection, stained for immunofluorescence with primary antibody against LANA, and imaged on a Zeiss Axioplan II Microscope. To quantify the proportion of infected-cells, the average number of LANA-positive cells and number of LANA dots were determined using ImageJ software for five fields of field (~300 cells) per each condition and were normalized to the average number of DAPI-nuclei. The proportion of infectious virions in each sample was determined by normalizing the number of LANA-positive cells to the number of DNase-protected viral genomes in the supernatant, as quantified by qPCR described in Figure 3.2. Representative images (panel A) and summary of quantification (panel B) are shown for two independent experiments.

obtained from lytic cells transduced with either shKap1 or shKap2 was capable of producing LANA dots at similar rates compared to the NS shRNA, with an average of 57% and 54.5% of SLK cell populations being LANA-positive, respectively (Figure 3.3). Furthermore, virus obtained from kaposin-knockdown cells was, on average, able to result in similar number of LANA dots per infected SLK cell compared to the NS-shRNA control (Figure 3.3B). The proportion of LANA-positive cells was normalized to the number of extracellular genomes detected by qPCR to account for varying numbers of particles in the supernatants and to gain a clearer perspective of virion infectivity. Similarly, there were no impairments in viruses obtained from kaposin-knockdown cells compared to the NS shRNA control; virions obtained from kaposin-knockdown had on average between 50-68% RFP per extracellular genome compared to 66% for wild-type virions (Figure 3.3B). Consequently, this suggests that kaposin knockdown does not impair the infectivity of virus particles released during lytic reactivation of KSHV in infected B-lymphocytes. More experiments will need to be conducted to establish this conclusion with significant statistical power.

3.2 Construction of a Kaposin-Deletion KSHV BAC library

Although significant kaposin knockdown does not result in drastic impacts to lytic reactivation of KSHV-infected B-lymphocytes, it is possible that the low levels of kaposin proteins that persist after shRNA-mediated knockdown were able to effectively maintain proper function during latency and lytic reactivation, thus masking any phenotypic differences associated with reduced protein expression. Additionally, the experiments in section 3.1 target the kaposin RNA transcript, thus reducing the expression of all three

kaposin proteins, KapA, B, and C; this made it difficult to assign any phenotypic relevance to the individual kaposin proteins via shRNA-knockdown alone.

To address the outstanding question of whether each individual kaposin protein had an effect on KSHV lytic life cycle, I generated recombinant viral genomes that either fail to code for only one particular kaposin protein or a combination of multiple kaposin proteins. I used the well-established KSHV genome-containing bacterial artificial chromosome (BAC), BAC16, as template for generating recombinant kaposin mutant viruses by Lambda Red homologous recombination (Brulois et al., 2012; Tischer et al., 2010). This strategy takes advantage of the *E. coli* strain, GS1783, which contains Lambda Red recombination genes, Exo, Beta, and Gam, under control of a temperature-sensitive promoter (Tischer et al., 2010). Bacteria were induced to express the recombination genes by culturing at 42℃ and subsequently electroporated to uptake a DNA construct designed to have terminal homology ends corresponding to regions that flank the gene of interest: in this case, flanking the direct repeats, DR2 and DR1, of the kaposin locus (Figure 3.4A). This DNA construct was composed of the mutated sequence that was to be introduced into the direct repeats of the kaposin locus. Additional elements were provided to facilitate selection of bacterial colonies that underwent two rounds of successful recombination; this included a kanamycin resistance gene (KanR), for positive selection of the first recombination event, along with a *Bacillus subtilis* levansucrase (SacB) gene, for negative selection of the second recombination event. While KanR confers the ability for bacteria to grow in selection media containing the antibiotic, SacB results in sensitivity to sucrose due to the enzymatic activity of levansucrase to convert sucrose to toxic levans (Gay et al., 1985). Upon identification of recombinant BAC-genomes that had successfully integrated

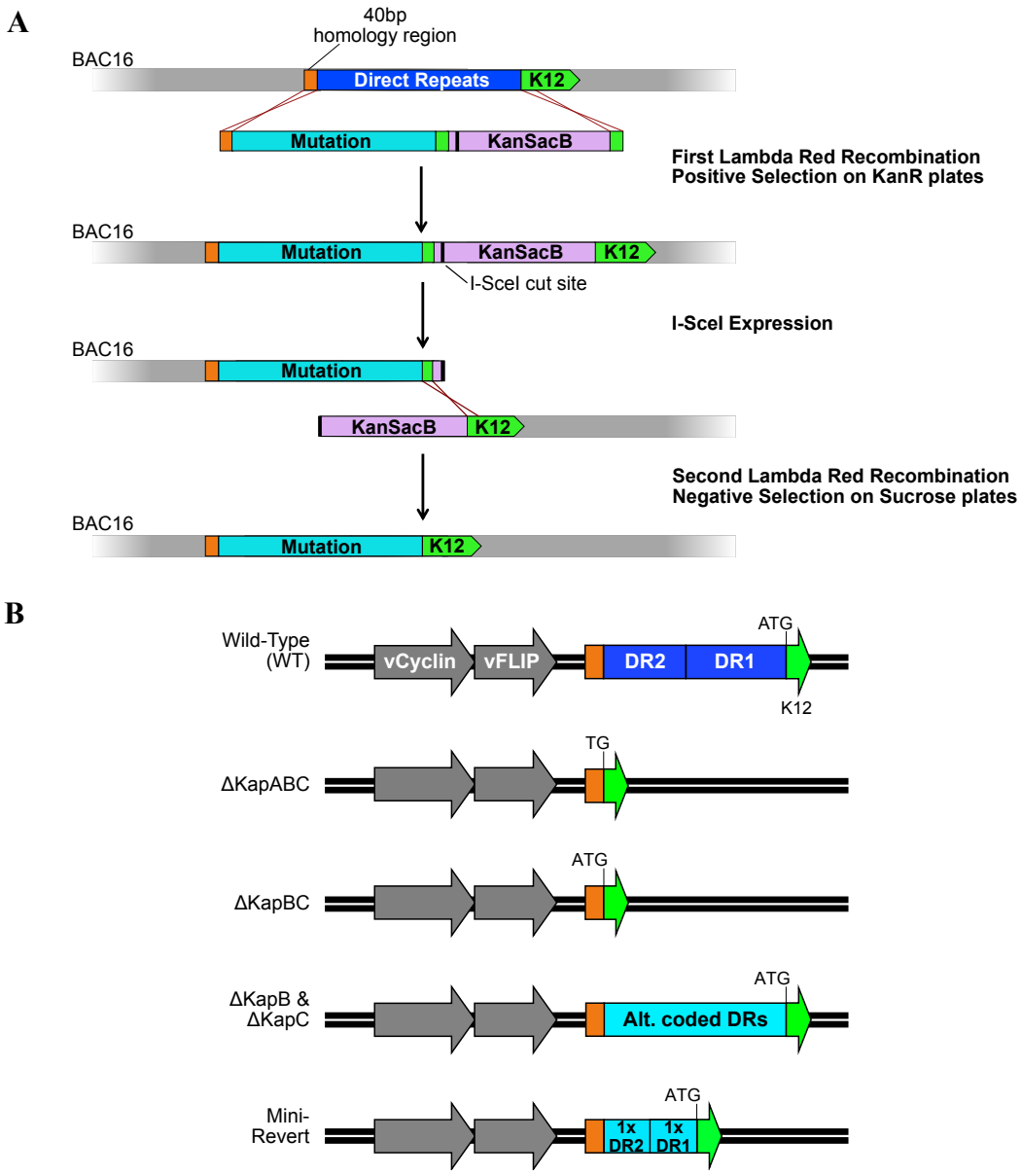

Figure 3.4: Lamda Red recombination strategy was used to generate kaposin-deletion KSHV-BAC mutants. (A) A DNA construct containing terminal 40-bp homology ends to the regions flanking the kaposin locus was introduced into KSHV-BAC16 by two-step Lambda Red recombination carried out in *E.coli*. The construct contained the desired mutation to be inserted into the direct repeats (DR2, DR1) along with selection marker genes for kanamycin resistance (KanR) and Levansucrase metabolic activity (SacB) for positive and negative bacterial selection respectively. (B) Wild-type KSHV-BAC16 was used as a template for the removal of the direct repeats and the K12 AUG start codon to generate a triple mutant (ΔKapABC). The ΔKapABC KSHV-BAC was used as template for future mutants including the replacement of the K12 AUG (ΔKapBC), the introduction of alternatively coded direct repeats (ΔKapB and ΔKapC), or the introduction of one copy each of the DR2 and DR1 repeats to generate a mini-revertant (MiniRevert).

the DNA construct by a first recombination event, the bacteria were induced to express the Lambda Red recombination genes along with an endonuclease, I-SceI, which cleaved within the DNA construct and facilitated a second recombination event. The intended effect would be the removal of the above-mentioned selection markers, thus producing a scarless mutation within the kaposin locus and allow growth of bacterial colonies on sucrose plates (Figure 3.4A).

This method was previously used by a research assistant in the Corcoran lab, Julie Ryu, to generate bacteria harboring KSHV-BACs with a mutation in the kaposin locus that removed the direct repeats and the AUG start codon of the K12 ORF, creating a triple kaposin mutant (ΔKapABC; Figure 3.4B). She subsequently used this recombinant ΔKapABC KSHV-BAC as a template to re-introduce the K12 AUG start codon by Lambda Red recombination, creating a double kaposin mutant that fails to encode KapB or KapC (ΔKapBC; Figure 3.4B).

My objective was to create KSHV-BACs that had removed the coding capacity of either KapB or KapC, but not both. While both proteins rely on the direct repeats that comprise the majority of their primary amino acid sequence, the ORFs are in different reading frames to one another. Therefore, using the BAC16 genome as a template, I designed two gene blocks for synthesis comprised of the nucleotide sequence of the direct repeats; the first DNA construct was composed of alternative codons that disrupted the protein coding capacity of the KapB ORF, due to nonsynonymous or nonsense mutations in the direct repeats, but the KapC ORF contained synonymous nucleotide changes that did not disrupt its amino acid sequence (ΔKapB; Figure 3.4B). The second gene block coded for the inverse mutant; the direct repeats were re-coded such that the KapC ORF contained

nonsynonymous or nonsense mutations, while the KapB ORF contained synonymous mutations that did not disrupt its primary sequence (ΔKapC; Figure 3.4B). Some key differences that were achieved from recoding the direct repeats were: 1) a decrease in the GC-content by 18.4% and 14.7% for ΔKapB and ΔKapC, respectively, 2) a disruption in the repetitiveness of the nucleotide sequence (Figure 3.5), and 3) a change in the predicted RNA structure of the transcript, as determined by RNAfold software (Appendix A, Figure A.2) (Gruber et al., 2008). While the first two characteristics were intentionally incorporated into the design of the gene blocks to facilitate more efficient homologous recombination into the KSHV-BAC16 genome, the resultant change in RNA structure may have caused unanticipated post-transcriptional changes to the kaposin transcript with unknown consequences.

In addition to the above-mentioned KSHV-BAC16 kaposin mutants, it was essential to generate a revertant in which the wild-type direct repeats could be replaced in the kaposin-deletion mutant to verify that off-target mutations did not occur during recombination events. The revertant should reverse any phenotypic differences observed in the mutant viruses. My attempts to replace the entire direct repeat regions with either wild-type BAC16 sequences, or a smaller version of the repeats corresponding to sequences from a KS lung isolate, were not successfully achieved; recombination with such GC-rich, repetitive nucleotide constructs led to partial or incomplete recombination products (see Appendix A, Figure A.3). As a compromise to generating the full revertant, a miniprotein construct of the direct repeats, which coded for one copy each of the DR2 and DR1 amino acid repeats (McCormick and Ganem, 2006), was synthesized to facilitate more efficient recombination (Figure 3.4B, Figure 3.5). The miniprotein has been shown

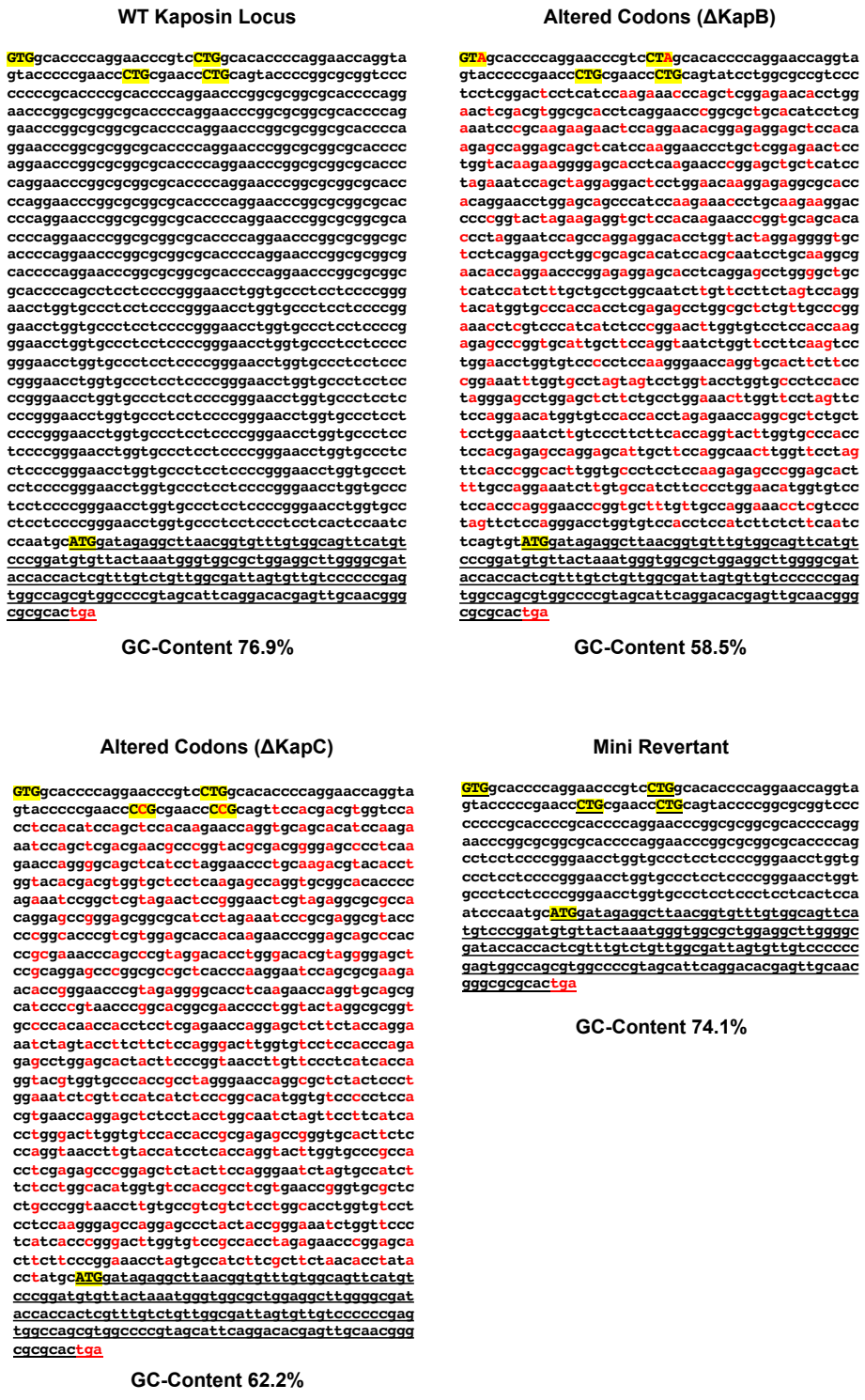

Figure 3.5: GC-content and repetitiveness of the kaposin direct repeats is reduced in alternatively coded gene blocks. The wild-type (WT) direct repeats of the BAC16 kaposin locus were alternatively coded to introduce nonsynonymous and nonsense mutations (red) into either the KapB (ΔKapB) or KapC (ΔKapC) ORF without disrupting the overlapping ORF. The potential translation start codons for the KapB and KapC ORFs (yellow) were also mutated in the corresponding reading frame. The K12 ORF is underlined for reference.

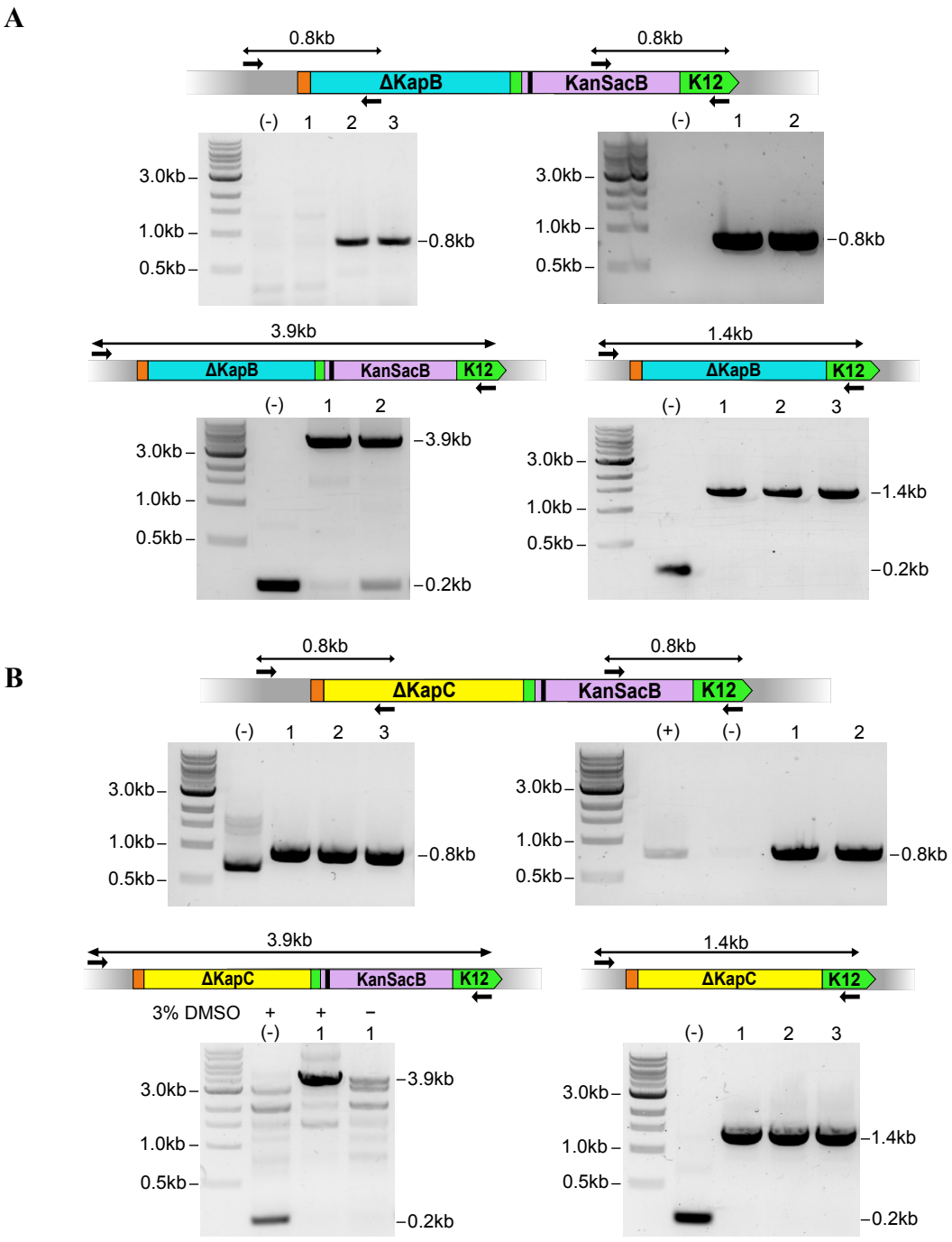

Figure 3.6: Lambda Red recombination of alternatively coded DRs in KSHV-BAC16 was confirmed by colony PCR. (A-B) Colony PCR was conducted on antibiotic-resistant bacterial clones following Lambda Red recombination to introduce alternatively coded direct repeats into the KSHV BAC16 genome. Primers were designed to either amplify regions spanning each of the ends used for recombination to verify correct insert orientation (top) or amplify the entire insert to verify correct size (bottom), in kilobases (kb). Insert size was analyzed both before (bottom, left) and after (bottom, right) the removal of the selection markers, KanSacB. PCR products are shown for ΔKapB (panel A) and ΔKapC (panel B); all PCR products were confirmed by Sanger Sequencing.

to maintain binding of KapB's interaction partner, MK2, albeit at attenuated levels, compared to the full-length protein (McCormick & Ganem, 2006).

All gene blocks were inserted into the ΔKapABC recombinant KSHV-BAC16 using Lambda Red homologous recombination. In addition to inserting the gene blocks, the AUG translation start codon for the K12 ORF was also re-introduced into the ΔKapABC KSHV-BAC16 to restore KapA protein expression. Resultant colonies from recombination events were analyzed by colony PCR using specifically-designed primers to amplify regions spanning the homology ends of both the ΔKapB and ΔKapC alternatively coded direct repeats (Figure 3.6) as well as the mini-revertant direct repeats (Appendix A, Figure A.4). Primer pairs were used in two different combinations; primers that bound regions internal and external to the insert were used to analyze insert orientation, while primers that bound only external regions to the insert were used to analyze insert length (Figure 3.6). Analysis of the ΔKapB mutant did not yield any unexpected PCR products for any of the reactions, indicative that the primers were specific for amplifying the desired regions of the BAC16 genome (Figure 3.6). In generating the ΔKapC mutant, many nonspecific PCR products for the full-length insert were observed after the first recombination event that were similarly observed in the negative control lane (WT BAC16); however, following the addition of DMSO and a second round of recombination, these bands were either minimized or no longer present (Figure 3.6). Amplified PCR products were confirmed by Sanger sequencing (GENEWIZ®) using the primers specified above to confirm successful recombination events.

While the sequencing results of the final PCR products provided assurance that recombination within the kaposin locus had yielded the desired mutations, it was possible

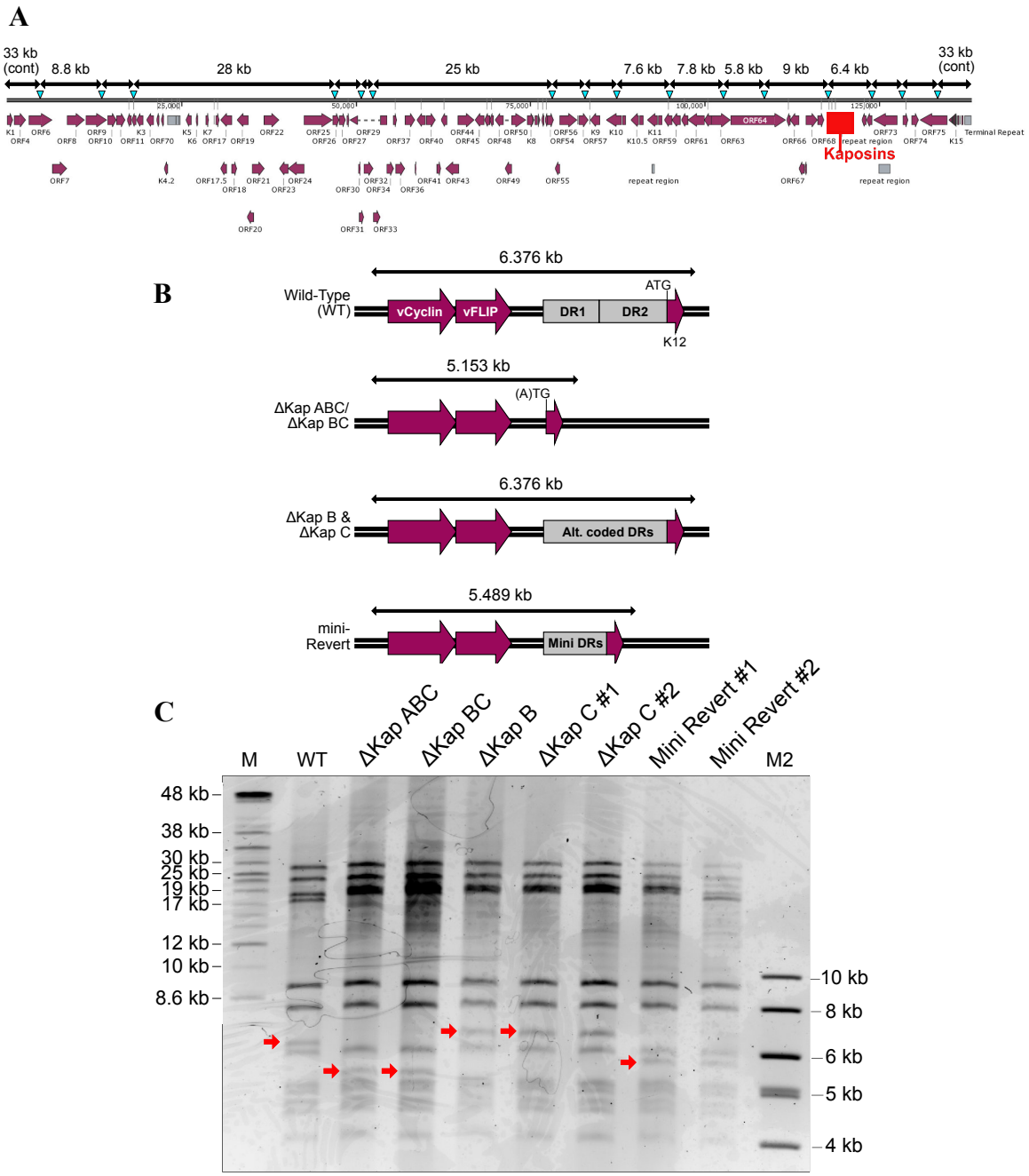

Figure 3.7: Kaposin locus fragment sizes for wild-type and kaposin-deletion mutant KSHV-BACs differ slightly in size from those expected from published sequence. (A) *In silico* NheI-restriction digest map (NheI-cut sites depicted in blue) of the GenBank published KSHV-BAC16 genome (accession no. GQ994935) and associated fragment lengths, in kilobases (kb). Image and fragment sizes were obtained using SnapGene software. (B) Kaposin locus fragments from NheI-digestion of GenBank sequence and expected fragment length differences between wild-type and kaposin-deletion mutants. ORFs (purple arrows) and repeat regions (grey boxes) are indicated. (C) NheI-digested KSHV-BAC16 DNA was analyzed by pulsed-field gel electrophoresis (PFGE) for wild-type (WT) and kaposin-deletion mutants. Kaposin-locus fragments (red arrows) are indicated. DNA molecular weight standards, M (BioRad, CHEF DNA size 8-48-kb) and M2 (New England Biolabs, 1-kb ladder) were used as reference.

that unanticipated off-target recombination events occurred elsewhere in the KSHV-BAC16 genome during the process. Areas that are most susceptible to recombination are repeat regions, such as the 801-bp terminal repeats (TRs) that bind LANA and are essential for episome maintenance (Dheekollu et al., 2013). In order to assess whether major genomic rearrangements had occurred, the DNA of KSHV-BAC16 and kaposin-deletion mutants were isolated from bacteria using an alkaline-lysis, isopropanol-precipitation method. NheI-restriction enzyme digestion, which does not cut within the TR sequence, and analysis by pulsed-field gel electrophoresis (PFGE) yielded DNA fragment-maps for the kaposin-deletion mutants that were compared to the wild-type KSHV-BAC16 (Figure 3.7). Digested fragments from wild-type KSHV-BAC16 DNA migrated to positions that indicated sizes different from those anticipated from the *in silico* digest of the genome conducted using SnapGene software and the GenBank genome of BAC16 (accession no. GQ994935; Figure 3.7). Notably, the 33-kb fragment is absent; based on the position of the other bands, it is believed that this fragment may have been shifted to a smaller 18-kb fragment size (Figure 3.7). This could be a result of a rearrangement within the TR sequences of the WT BACmid that resulted in a smaller fragment size. Additionally, co-migrating with this 18-kb fragment is a fourth large fragment not included in the Genbank sequence; this fragment is believed to correspond to the BAC vector sequences, pBelo45 and Tn1000, inserted during generation of the BAC16 (Brulois et al., 2012).

A decrease of approximately 1000-bp was observed for the kaposin locus fragment for ΔKapABC and ΔKapBC mutants compared to wild-type; this difference was slightly lower than the expected 1200-bp that would correspond to the removal of the DRs and K12 AUG start site (Figure 3.7). The approximately 200-bp that were not accounted for in the

kaposin locus fragment, the size of which was confirmed using Image Lab software (Bio-Rad), is likely indicative of a smaller DR region in the wild-type genome compared to the GenBank published sequence. A difference of 200-bp would correspond to approximately 9 copies of the 23-bp repeats that were missing in the wild-type genome. This speculation was further evidenced by the size of the kaposin locus fragment in the ΔKapB and ΔKapC mutants. If the wild-type genome was identical to the GenBank published sequence, insertion of the alternatively coded repeats back into the ΔKapABC mutant should have resulted in a kaposin locus fragment that matched wild-type in size. However, insertion of the alternatively-coded DRs for the ΔKapB and ΔKapC mutants resulted in a kaposin locus fragment approximately 200-bp larger than that of wild-type, suggesting that the original wild-type sequence differed from the GenBank published sequence.

To confirm the differences in banding pattern between wild-type KSHV-BAC16 and kaposin-deletion mutants, DNA from each KSHV-BAC was subjected to NotI-restriction digest and analyzed by PFGE. Similarly, no differences between the kaposin-deletion mutant banding patterns and that of the wild-type were observed other than the kaposin locus fragment (Figure 3.8). Similar differences in size between the different KSHV-BACs were produced from NotI-digestion compared to NheI-digestion, including the unaccounted 200-bp sequence from the wild-type KSHV-BAC (Figure 3.8). Since this deviation could be reproduced by digesting the DNA with different restriction enzymes, it suggests that the wild-type BACmid does indeed have a deletion in the DRs resulting in a smaller kaposin locus fragment compared to the GenBank published sequence. Recombination of tandem repeat regions that result in a rearrangement, insertion, or deletion is not uncommon and is known to occur in *E.coli* (Bzymek & Lovett, 2001).

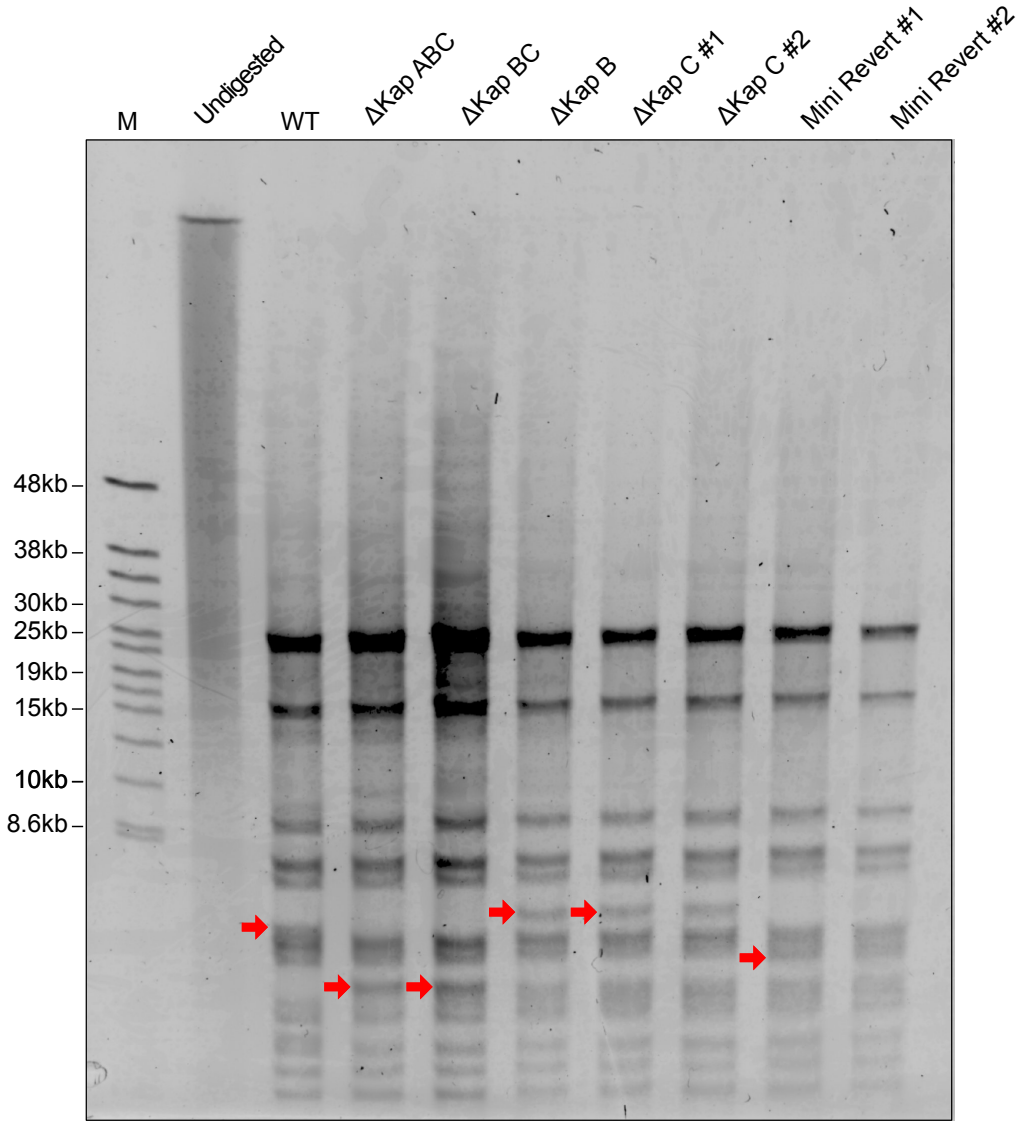

Figure 3.8: Differences in size for the kaposin locus fragment of wild-type and kaposin-deletion mutant KSHV-BAC16 are consistent for different restriction enzyme digestions. NotI-digested KSHV-BAC16 DNA was analyzed by pulsed-field gel electrophoresis (PFGE) for wild-type (WT) and kaposin-deletion mutants. Kaposin-locus fragments (red arrows) are indicated. DNA molecular weight standard, M (BioRad, CHEF DNA size 8-48-kb) was used as reference.

Moreover, recombination of tandem repeats in herpesvirus genomes has been thought to contribute to virus DNA replication and maintain genetic diversity (Reuven et al., 2003; Dheekollu et al., 2013). Therefore, the differences in the wild-type KSHV-BAC16 genome compared to the published GenBank sequence likely arose due to recombination within the DRs prior to kaposin mutagenesis. Since the kaposin-deletion mutant genomes showed the expected size changes to the kaposin locus fragment that are consistent with the removal of the DRs and replacement with alternatively coded gene blocks relative to wild-type, it was believed that the PFGE-analysis confirmed that the KSHV-BAC16 genome remained intact following mutagenesis.

In addition to restriction digest, the DNA of KSHV-BAC16 and kaposin-deletion mutants was analyzed by next-generation sequencing to confirm, at a single-nucleotide level, that no additional mutations were created from Lambda Red recombination. DNA was submitted for 300+300-bp paired-end sequencing on the Illumina MiSeq platform at the Integrated Microbiome Resource (IMR) at the Centre for Comparative Genomics and Evolutionary Bioinformatics (CGEB) at Dalhousie University. Sequencing data was kindly analyzed by Dr. Bruce Curtis, a post-doctoral fellow in the lab of Dr. John Archibald at Dalhousie University. DNA sequences were analyzed for quality, trimmed accordingly, and assembled by creating contigs, which were subsequently mapped back to the GenBank BAC16 genome. A significant proportion of the resulting DNA contigs did not map to the KSHV genome, but rather mapped to the bacterial *E.coli* genome. Although only a small proportion of the reads matched the GenBank BAC16 sequence (Appendix A, Table A.1), when assembled, the contigs did span most of the KSHV genome (Appendix A, Figure A.5). However, the depth of coverage was not sufficient to generate a single complete

contig, thus resulting in many gaps in the sequence (Appendix A, Figure A.5). This data was therefore inconclusive as to whether the DNA of the kaposin-deletion mutant BAC16s differed from wild-type at the single-nucleotide level. However, the sequencing data did confirm that most of the KSHV genome remained intact after mutagenesis and that mutations within the kaposin locus were consistent with the Sanger sequencing data (data not shown).

3.3 Generation of KSHV-BAC Infected iSLK Cells with Kaposin-Deletions

Since the integrity of the KSHV-BACs appear to be intact, it is assumed that all recombinant viral constructs should be capable of establishing an infection in human cells. Having already employed a method for obtaining viral DNA for wild-type and kaposin deletion KSHV-BAC16, my intention was to generate viral stocks from each that could be used to investigate the role of individual kaposin proteins in both the latent and lytic KSHV life cycle. In order to produce viral stocks, I sought to generate stable-infected cell lines from which I could robustly induce lytic reactivation of virus; I therefore used the renal-epithelial cell line, iSLK, which has been previously established as an efficient KSHV-producing cell line (Myoung & Ganem, 2011a; Stürzl et al., 2013). Similar to TREx BCBL-1, iSLK cells have been transduced to express a doxycycline-inducible RTA, allowing for lytic reactivation to be tightly controlled; this system is maintained by culturing the cells in media containing geneticin and puromycin, which selects for the rtTA (Tet-On) -inducible expression system and RTA-transduction, respectively (Myoung & Ganem, 2011a). Successful introduction of the KSHV-BAC16 episome was then determined by red-fluorescent protein (RFP)-expression, a reporter gene which is constitutively expressed

during latency from an active EF1α-promoter in BAC16 and maintained by selection with hygromycin (Brulois et al., 2012).

Despite some research groups reporting that SLK cells can be directly transfected with FUGENE HD to introduce KSHV-BAC16 DNA (Full et al., 2014; Liang et al., 2016), I was unsuccessful in this strategy; no cells were RFP-positive following the suggested protocol. However, other groups have reported using the easily transfectable HEK 293 cell line as a transfer cell line from which iSLK cells can be infected (Bergson, et al., 2014; Jain et al. 2016). HEK 293T cells were transfected with a mixture of wild-type or kaposin-deletion KSHV-BAC16 DNA using PEI. HEK cells that were RFP-positive and survived hygromycin-selection were subsequently used to establish a co-culture system, using a method previously established (Bergson et al., 2014; Jain et al., 2016) in which HEK-BAC16 cells and iSLK cells were seeded in the same well of a tissue culture plate in a 1:1 ratio. The KSHV-infected HEK cells were induced to undergo lytic reactivation by culturing the cells in media containing 12-O-tetradecanoylphorbol-13-acetate (TPA) and sodium butyrate (NaB). TPA and other phorbol esters, which are known activators of protein kinase C (PKC), and histone deacetylase (HDAC) inhibitors, such as NaB, have been shown to activate the KSHV lytic program (Renne et al., 1996; Miller et al., 1997). The co-culture method is believed to facilitate more efficient infection of iSLK cells by cell-cell spread of the virus being produced from lytic HEK-BAC16 cells (Myoung & Ganem, 2011b). After 4 days of lytic induction, the cells were sub-cultured into a 10 cm tissue culture plate and cultured in media containing geneticin, puromycin, and hygromycin, which selected for the rtTA-induction expression system, RTA- transduction, and BAC16 episome, respectively (Figure 3.9). Since 293T cells did not contain these

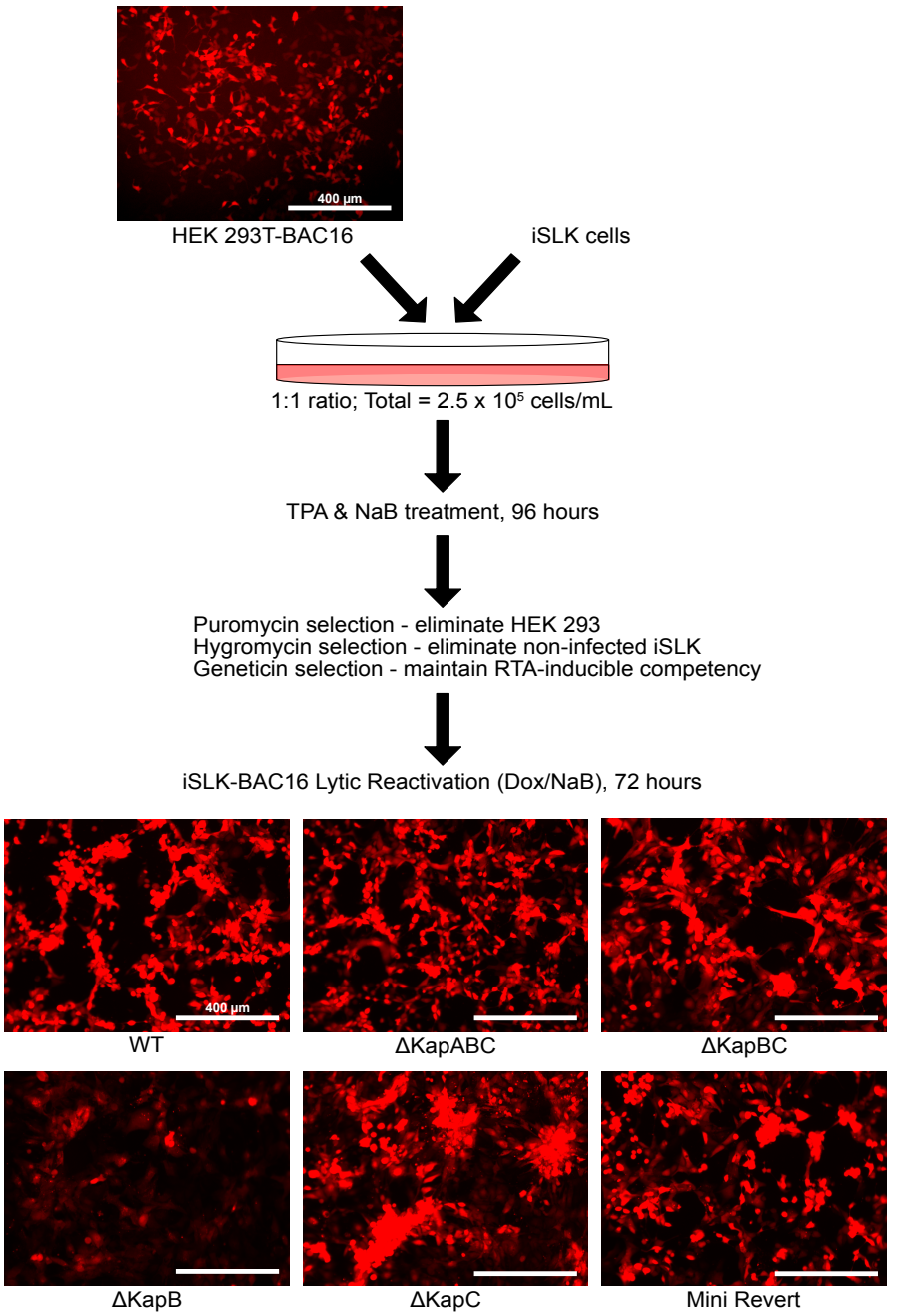

Figure 3.9: iSLK-BAC16 cells were generated from co-culture with HEK-BAC16s. HEK 293T cells were transfected with wild-type (WT) and kaposin-deletion KSHV-BAC16 DNA harvested from GS1783 *E.coli.* RFP-expressing cells were selected by hygromycin treatment, seeded 1:1 in co-culture with iSLK cells, and lytic reactivated for 96 hours with terephthalic acid (TPA) and sodium butyrate (NaB). iSLK-BAC16 cells were selected by culturing in media containing puromycin, geneticin, and hygromycin. Resultant iSLK-BAC16 cells were lytic reactivated by culturing in media containing doxycycline (Dox) and NaB for 72 hours. Images were taken using RFP-filters on an EVOS FL Cell Imaging System with 10X objective (ThermoFisher Scientific). Scale bar = 400 µm.

selection markers, the only remaining RFP-positive cells following this selection step were iSLKs containing a BAC16 episome. The co-culture protocol demonstrated that all KSHV-BAC16 genomes, including kaposin-deletion mutants, were capable of lytic reactivation and production of virions in HEK 293T cells, and that those virions were competent in establishing an infection in neighboring naïve iSLK cells, as confirmed by RFP-expression in wild-type and kaposin-deletion iSLK-BAC16 cells after selection (Figure 3.9). The capacity for iSLK-BAC16 cells to be antibiotic-resistant to puromycin, geneticin, and hygromycin suggested that these cells could also be competent for lytic reactivation and could thus be used to generate virus stocks.

3.4 ΔKapB Mutant iSLK-BAC16 Cells Have a Lower Episome Copy Number

Having generated iSLK cells harboring KSHV-BAC16 episomes for wild-type and kaposin-deletion mutants, these cells were intended to be used for generating virus stocks and assessing any changes in virus life cycle as a result of mutagenesis. Due to the nature of the virus lytic cycle, successful generation of virus progeny and production of high titer stocks can only occur if all stages of the virus life cycle remain intact. Therefore, the production of virus stocks is conditional on the fact that no essential processes were impaired from kaposin mutagenesis. In my assessment of virus production, I therefore simultaneously gathered information regarding both the latent and lytic life cycles of the virus. To assess latency, RFP-expression in the absence of lytic-inducing reagents was determined along with quantitation of intracellular viral genome number. To assess lytic reactivation, RFP and viral protein expression was determined post-induction along with quantitation of DNase-protected extracellular viral genomes.

As a measure of viral gene expression from wild-type and kaposin-deletion mutant iSLK-BAC16 cells, RFP expression was monitored during latency (untreated) and lytic reactivation. Cells were seeded in 6-well tissue-culture plates and either left untreated to assess latency (0 hpi) or cultured in media containing doxycycline, which induces the expression of RTA, and sodium butyrate, which acts as an HDAC inhibitor, to assess lytic reactivation. Cells were imaged with a fluorescent microscope for RFP-expression every 24 hours post-induction (hpi) up to 96 hpi using an EVOS FL Imaging System (Thermo Fisher Scientific). Intensity of RFP-expression was quantified from the images using ImageJ software; an increase in RFP expression over time post-induction was used as an indicator for progression of the lytic cycle which involves upregulated viral gene expression and genome replication. All iSLK-BAC16 cells were competent to express virally encoded genes during latency as evidenced by RFP expression at 0 hpi for wild-type and kaposin-deletion mutants (Figure 3.10, 3.11A). While RFP-expression was approximately equal between wild-type and kaposin-deletion mutants during latency, ΔKapB iSLK-BAC16 cells had significantly lower RFP-expression throughout the lytic reactivation time-course compared to wild-type and all of the other kaposin-deletion mutants (Figure 3.10, 3.11A). This lower level of RFP expression was also comparably less than that of wild-type cells inhibited by PAA-treatment, which blocked viral genome replication; RFP intensity for the ΔKapB mutant was comparable to uninduced wild-type iSLK-BAC16 cells (Figure 3.10, 3.11A). This suggests that the ΔKapB mutant has a defect following lytic induction, but not during latency; however, the stage at which this occurs during the lytic cycle remains unclear.

Since RFP intensity for the ΔKapB mutant iSLK-BAC16 cells was attenuated compared to wild-type during lytic reactivation and not during latency, I decided to investigate the different stages of the virus lytic cycle to determine a possible cause for the phenotypic defect. One component of the lytic cycle that is necessary for increases in viral gene expression, and by extension RFP expression, is viral genome replication. Therefore, in order to identify whether genome replication was impaired in the ΔKapB mutant cells, the number of intracellular viral genomes was quantified by qPCR. DNA was extracted from untreated (latent) and lytic iSLK-BAC16 cells that had been induced for 72 hours with Dox and NaB; intracellular DNA was quantified by qPCR using primers against ORF26 and a housekeeping gene, β-actin. Notably, the ΔKapB mutant iSLK-BAC16 cells had markedly less intracellular genomes compared to wild-type and other kaposin-deletion mutants during latency; the discrepancy between ΔKapB mutant cells and wild-type was further accentuated from 7-fold to 47-fold less genomes after genome replication had occurred, as measured at 72 hpi (Figure 3.11). To this end, it is likely that the defect in RFP expression during lytic reactivation for the ΔKapB mutant was due to a deficiency in viral genome copy number in the cells when the experiment was initiated.

As a consequence of having a deficiency in viral genome copy number, I predicted that the ΔKapB mutant iSLK-BAC16 cells would also show impairments in other viral genes in the temporal cascade of lytic gene expression. To determine if this was the case, iSLK-BAC16 cells were induced to lytic reactivation with Dox and NaB for 72 hours and cell lysates were immunoblotted for latent (KapB and LANA) and immediate early (RTA) proteins, all of which accumulate during lytic reactivation, but are predominantly associated with early lytic gene expression. The KapB polyclonal antibody, kindly

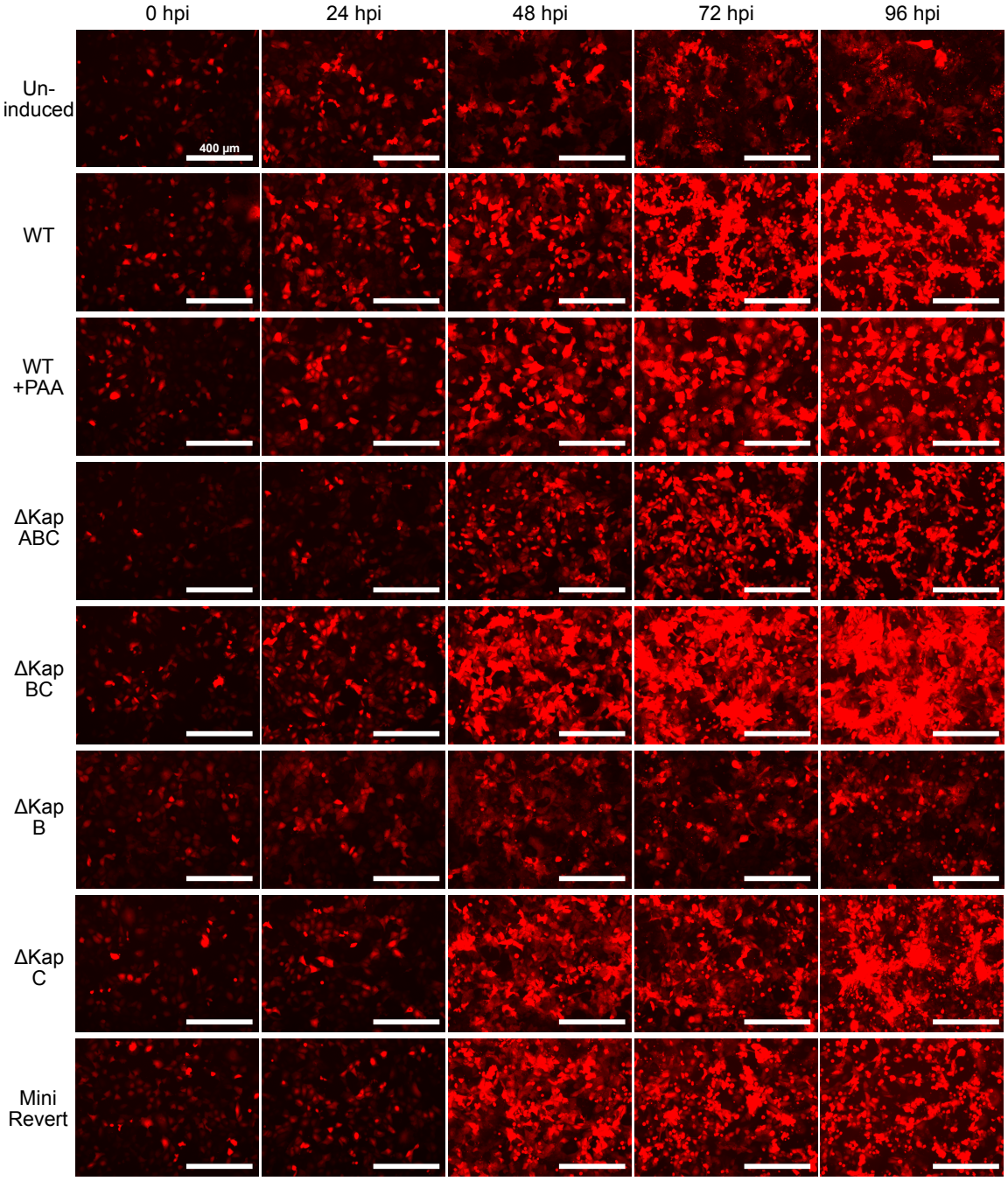

Figure 3.10: KapB mutant iSLK-BAC16 cells have reduced RFP-expression during lytic reactivation. Wild-type (WT) and kaposin-deletion mutant iSLK-BAC16 cells were either left untreated or induced to lytic reactivation by culturing in media containing doxycycline (Dox) and sodium butyrate (NaB). Phosphonoacetic acid (PAA) was added to the media as an inhibitor of the viral DNA polymerase. Images were taken at 0, 24, 48, 72, and 96 hours post-induction (hpi) using RFP-filters on an EVOS FL Imaging System at 10X objective (Thermo Fisher Scientific). Scale bar = 400 µm.

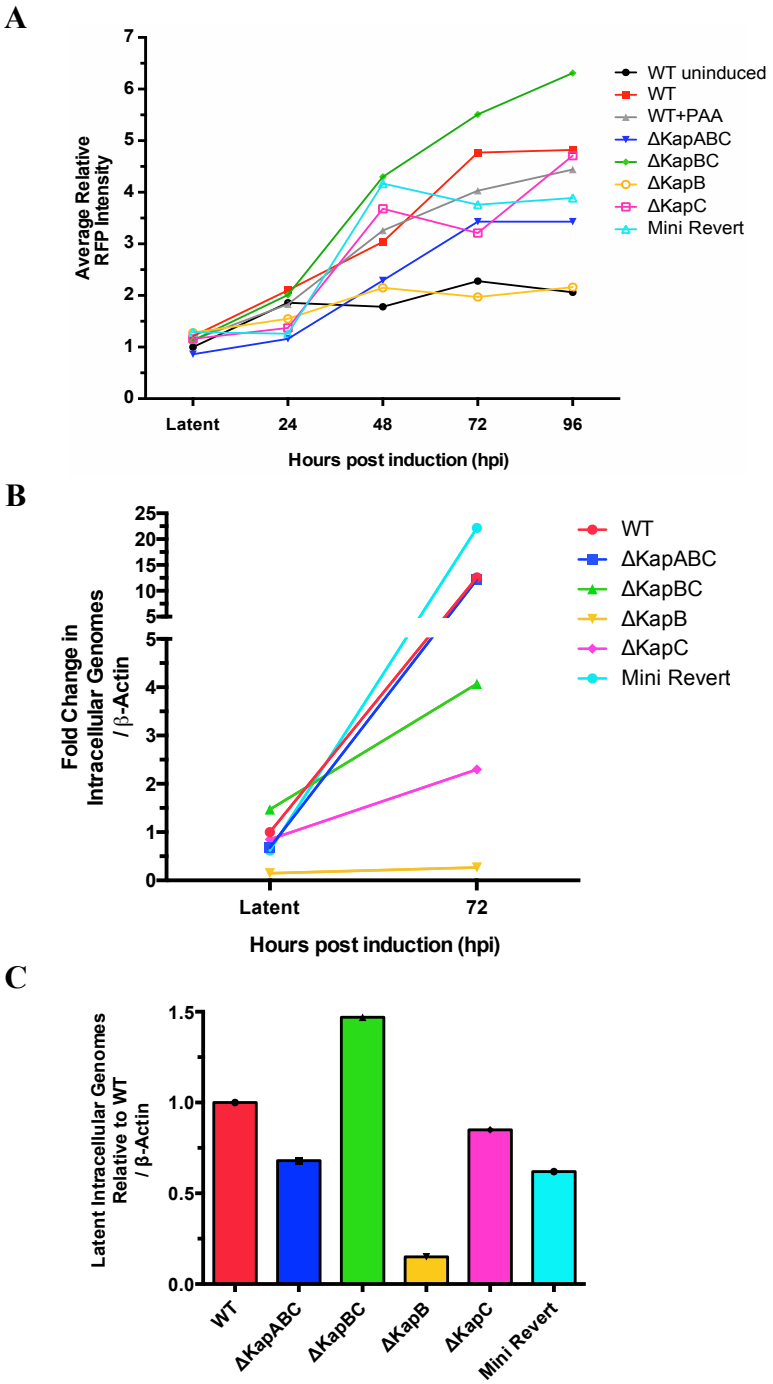

Figure 3.11: RFP expression and viral episome number do not increase following lytic induction in ΔKapB mutant iSLK-BAC16 cells. (A) Average RFP intensity was determined for images of latent and lytic iSLK-BAC16 cells depicted in Fig.3.10. Average integrated density (RFP fluorescence) was determined using ImageJ software and normalized to the intensity for latent uninduced wild-type (WT) cells. (B-C) DNA from uninduced and lytic iSLK-BAC16 was harvested at 72 hours post-inductioin (hpi) and the number of intracellular viral genomes was quantified by qPCR using primers against ORF26. Number of genomes is represented as fold-change compared to uninduced WT and was normalized to β-actin.

provided by Drs. Craig McCormick & Don Ganem, recognizes the DR2 regions of both KapB and KapC; immunoblotting for these proteins also served to confirm that the kaposin mutagenesis was successful. Unfortunately, due to the small size of KapA and inconsistent detection of K12 ORF-containing proteins using the available antibody, I could not confirm KapA protein expression by immunoblot in this study.

Consistent with data suggesting decreased episomes in ΔKapB cells, RTA and LANA expression were markedly reduced in these cells compared to wild-type and other kaposin-deletion mutants (Figure 3.12). KapB expression levels were detected in both wild-type and ΔKapC mutant iSLK-BAC16 cells; the shift in molecular weight between the two bands is consistent with the 200-bp additional DRs for the ΔKapC mutant compared to wild-type, as noted in PFGE analysis (Figure 3.12). KapC expression was also detected at low levels in wild-type cells, however there was no corresponding band detected in the ΔKapB mutant which was expected at approximately 46 kDa, shifted by approximately 7 kDa compared to wild-type due to differences in DRs noted above (Figure 3.12). This deficiency in KapC expression for the ΔKapB mutant was consistent with reduced levels of both LANA and RTA proteins, both of which were markedly less expressed than in wild-type and other kaposin-mutants (Figure 3.12). ΔKapABC and ΔKapBC mutants were negative for both KapB- and KapC-expression, as anticipated due to their lack of DRs (Figure 3.12). The mini-revertant was also negative for KapB & KapC expression (Figure 3.12); this may be because the protein product (approximately 7 kDa in size) was too small to visualize on the same blot. Alternatively, since the antibody used to detect KapB recognizes the DR2 amino acid repeats, there may have been too few repeats in the mini-revertant peptide, which only has one DR2 repeat, to be recognized as an

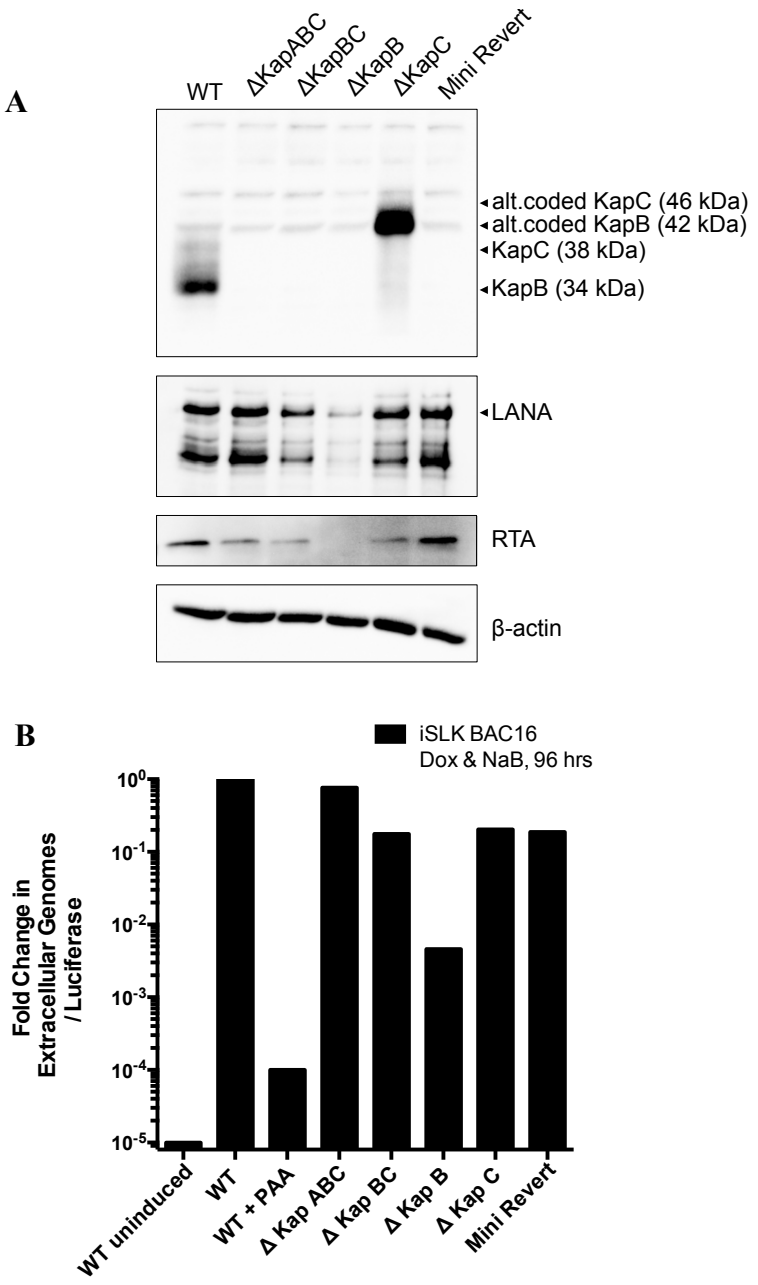

Figure 3.12: ΔKapB mutant iSLK-BAC16 cells display reduced viral gene expression and attenuated virus production consistent with lower number of viral episomes during latency. (A) Wild-type and kaposin-deletion iSLK-BAC16 cells were induced to lytic reactivation with Dox and NaB and cell lysates were harvested at 72 hours post-induction (hpi) for immunoblotting of viral genes using primary antibodies against the DR2 repeat of KapB & KapC, LANA (latent), and RTA (immediate early lytic). (B) Supernatant from lytic iSLK-BAC16 cells was harvested at 96 hpi, treated with DNase, and the amount of DNase-protected extracellular viral DNA was quantified by qPCR using primers designed to amplify ORF26. Number of genomes is represented as fold-change compared to WT and was normalized to a luciferase plasmid spike. PAA treatment was used as an inhibitor of the viral DNA polymerase.

epitope. Altogether, these results suggest that a defect exists for the ΔKapB mutant. The markedly reduced levels of LANA, RTA, and alternatively coded KapC protein, all of which should be expressed at high levels early during lytic reactivation, corroborates the data that a deficiency in KSHV episomes in the ΔKapB cells may be the likely cause for impaired lytic viral gene expression.

Despite there being significant deficiencies in RFP intensity, intracellular genome copies, and viral gene expression for the ΔKapB mutant iSLK-BAC16 cells, it is possible that these cells were still capable of producing progeny virus. To verify this, iSLK-BAC16 cells were induced to lytic reactivation and the supernatant was harvested at 96 hpi and subsequently assayed for DNase-protected viral genomes by qPCR, using the luciferase plasmid spike as a normalization factor. While some kaposin-deletion mutants (ΔKapBC, ΔKapC, and mini Revert) had approximately 5-fold less DNase-protected extracellular genomes released into the supernatant compared to wild-type, the KapB-deletion mutant had a greater than 200-fold reduction (Figure 3.12). However, the ΔKapB mutant had greater number of DNase-protected genomes in the supernatant than both uninduced and PAA-inhibited wild-type cells, indicative that while virus production may be limited in ΔKapB iSLK-BAC16 cells, it is not completely abolished. It is likely that the defect in virus production for the ΔKapB mutant is due to the deficiency in viral genome copy number in the cells when the experiment was initiated; this inequity appears to not only impact viral gene expression, but also virion production. I therefore concluded that comparisons of lytic reactivation profiles between wild-type and kaposin-deletion mutant iSLK-BAC16s should be reserved for when viral genome copy number can be more closely equalized across the different mutants. Additionally, equal genome copy number would

ideally result in more productive lytic cycles for all iSLK-BAC16s and be more suitable for generating virus stocks for phenotypic study.

3.5 Kaposin-Deletion Virions Can Infect Cells Equally Compared to Wild-Type

Possible explanations as to why fewer ΔKapB mutant viral episomes were present in latent iSLK-BAC16 cells compared to wild-type are: 1) the virions produced during co-culture with 293T HEK-BAC16 cells were fewer in number, resulting in decreased virions capable of establishing infection in iSLK cells, or 2) the virions had impaired ability to enter iSLK cells and establish a latent infection in these naïve cells. In order to address questions regarding production of infectious virions, it was necessary to attempt to equalize latent episome numbers such that more virus could to be generated from lytic ΔKapB mutant iSLK-BAC16 cells, since the production status of these cells was insufficient to conduct such studies.

3.5.1 Generation of iSLK-BAC16 Cells With Increased Episomes Through Virus-Passaging

In an attempt to achieve greater production of extracellular virus from all kaposin-deletion mutant iSLK-BAC16 cells, the virus was passaged in naïve iSLK cells. This method was used in an attempt to create populations of each mutant that have equalized number of intracellular viral genomes in the latent population of cells such that it would translate to equivalent number of virions produced during lytic reactivation. The method I used was as follows. Virus-containing supernatant was harvested from lytic iSLK-BAC16 cells induced to reactivate with Dox and NaB for 96 hours and used to infect naïve iSLK cells by spinoculation. For each mutant, different dilutions of inoculating virus-containing

supernatant were used in an attempt to generate approximately the same proportion of RFP-positive iSLK cells following spinoculation. After selecting populations that met this first criterion, infected and replication-competent cells were selected by culturing the cells in media containing puromycin, geneticin, and hygromycin. The resultant virus-passaged (P1) cells were analyzed for the number of intracellular viral genomes during latency by qPCR. All P1-iSLK-BAC16 cells had detectable levels of viral genomes; furthermore, all kaposin-deletion mutant cells had intracellular viral genome numbers that were within a 2-3-fold change relative to wild-type, including the ΔKapB mutant (Figure 3.13). Since this difference in episome number was closer to being equal across the different mutants, these populations of cells were carried forward for future experiments.

After equalizing viral episomes, I sought to compare viral protein levels of KapB across the mutants. P1-iSLK-BAC16 were induced to lytic reactivation for 72 hours and cell lysates were probed with KapB primary antibody for immunoblot. As observed previously, both WT and the ΔKapC mutant were positive for a protein band corresponding to KapB; the difference in molecular weight between the wild-type KapB and that of the kaposin-mutant was consistent with previous results (Figure 3.12, Figure 3.13). Both wild-type and the ΔKapB mutant were positive for a band consistent with KapC protein; this band had approximately the same shift in molecular weight consistent with a loss of 9 copies of DRs in the wild-type genome (Figure 3.13) which agrees with the differences observed by PFGE analysis of the WT BAC DNA. ΔKapABC, ΔKapBC, and the mini revertant were all negative for their respective kaposin proteins as a result of missing DRs, in the case of the ΔKapABC, ΔKapBC mutants, or too few DRs to be probed by immunoblot, as for the mini revertant (Figure 3.13). Despite being unable to perfectly

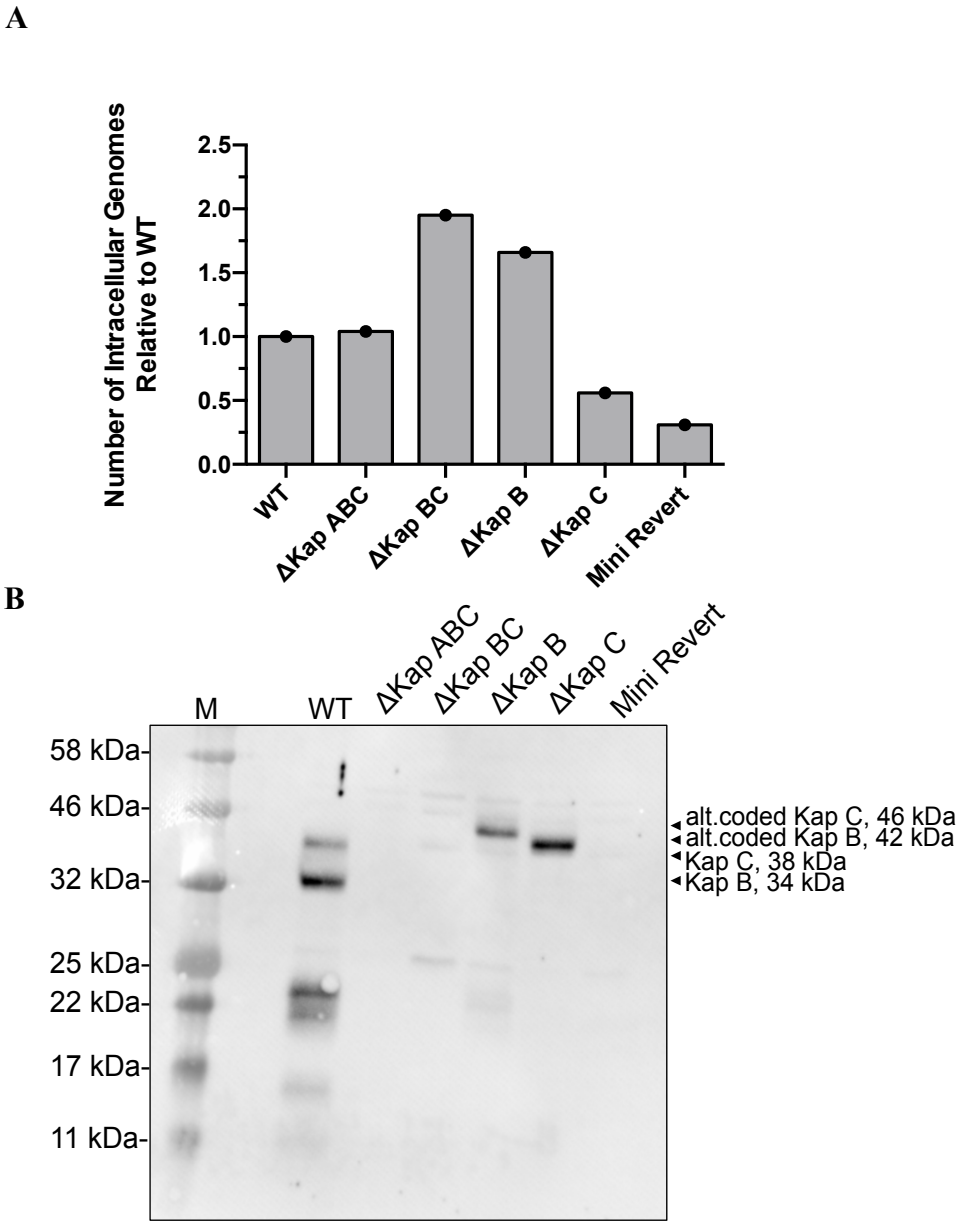

Figure 3.13: Passaging of virus in iSLKs resulted in equalization of viral episome number and greater kaposin protein expression for the ΔKapB mutant. (A) Wild-type (WT) and kaposin-deletion mutant KSHV was harvested from lytic iSLK-BAC16 cells at 96 hours post-induction (hpi) and used to *de novo* infect iSLK cells (P1-iSLK-BAC16). DNA from latently-infected cells was harvested and analyzed for intracellular viral genomes by qPCR. Quantity of viral genomes was normalized to β-actin and is represented as the fold change relative to WT. (B) Cell lysates harvested from lytic P1-iSLK-BAC16 cells at 72 hpi were immunoblotted for KapB & KapC protein expression using a primary antibody against the DR2 repeats. Colour Protein Standard, Broad Range (New England Biolabs) was used as a molecular weight reference (M).

equalize viral episome numbers in latent cells, these results suggest that the strategy to passage the virus in iSLK cells shows potential, as for the first time I was able to observe patterns of expression for the kaposin gene products as would be expected from this mutant library. These results provide some validity to the idea that the defect in viral gene expression from previous experiments was likely due to low genome copy numbers.

3.5.2 ΔKapB Mutant Virions Can Competently Enter and Express Viral Genes During *de novo* Infection

By equalizing the number of genomes, I hypothesized that virion production would be restored to all kaposin-deletion mutants that had previously had deficiencies compared to wild-type, namely the ΔKapB mutant. P1-iSLK-BAC16 cells were used to generate virus stocks through induced lytic reactivation for 96 hours, as previously described. These virus stocks were used to address two questions: 1) whether virion production was equal across the different kaposin-deletion mutants compared to wild-type, and 2) if those virions were capable of establishing an infection in naïve iSLK cells. To determine the number of virions produced from each population of cells, the number of DNase-protected extracellular genomes was quantified by qPCR as previously described. Notably, there were three kaposin-mutants that had significantly lower production of DNase-protected genomes than wild-type; ΔKapBC, ΔKapB, and ΔKapC mutants had on average 6-fold, 33-fold, and 5-fold less genomes, respectively (Figure 3.14A). Both the ΔKapABC mutant and mini Revertant did not release significantly different amounts of DNase-protected genomes into the supernatant compared to wild-type (Figure 3.14A). These results highlight that despite the P1-iSLK-BAC16 cells having approximately equal number of viral episomes, there is still a defect in lytic reactivation for some of the kaposin-deletion mutants.

In order to fully characterize whether infectious virions are being released from kaposin-deletion mutant cells, the virus stocks harvested from P1-iSLK-BAC16 cells were used to *de novo* infect iSLK cells by spinoculation. At 24 hours post-infection (hpi), infected iSLK cells were fixed and analyzed by flow cytometry for RFP-expression to determine the proportion of infected cells. Though RFP expression does not indicate that the virus has undergone a full replication cycle, it is a phenotype that demonstrates that the virion successfully entered and delivered the KSHV genome to the nucleus, and that a virally-encoded gene can be expressed. The proportion of RFP-expressing cells was determined by gating such that 1% of mock-infected cells were RFP-positive. Following infection with wild-type KSHV-BAC16, an average of approximately 60% of cells were RFP-positive (Figure 3.14). While some of the kaposin-deletion mutants, such as the ΔKapABC and miniRevert had comparable ratios of RFP-expressing cells, others, such as the ΔKapBC, ΔKapB, and ΔKapC mutants, had markedly less (Figure 3.14). This data was consistent with the virion production data that showed significantly less virions in ΔKapBC, ΔKapB, and ΔKapC mutant virus stocks. To more clearly show this correlative relationship, the proportion of RFP-expressing cells was normalized to the number of extracellular viral genomes. This analysis showed that despite some kaposin-deletion mutant virus preparations having lower concentration of DNase-protected genomes, the virions in the preparation had equal, if not greater, ability to enter cells, deliver their genomes to the nucleus and express viral genes compared to wild-type (Figure 3.14). This data supports my working model that an impairment exists in the lytic production of progeny virus in cells infected with ΔKapBC, ΔKapB, and ΔKapC mutant viruses; however, the viral entry process is not impaired by the mutations they encode.

Figure 3.14: Kaposin-deletion mutant virions enter, uncoat and express a viral-encoded gene in naïve iSLK cells. (A) The number of DNase-protected extracellular genomes in the supernatant of lytic wild-type (WT) and kaposin-deletion mutant P1-iSLK-BAC16 cells at 96 hours post-induction was quantified by qPCR as previously described in Fig 3.2. Number of genomes is represented as fold-change compared to WT and was normalized to a luciferase plasmid spike, as described in Fig.3.2. ns, not statistically significant, *P<0.05, **P<0.005, ***P<0.0005 for two-tailed one-sample Student's t-test. (B) Virus-containing supernatant was used to infect naïve iSLK cells. Cells were fixed 24 hours post-infection and the proportion of RFP-expressing cells determined by flow cytometry on a FACSCanto II (BD Biosciences). Data was analyzed using Flowing Software 2 (Turku Centre for Biotechnology) with the RFP+ gate set to 1% of cells for mock-infection. (C) RFP+ cells were quantified and normalized to the number of DNase-protected genomes as a measure of virion ability to enter and uncoat in iSLK cells. Bars indicate averages ± SEM; data are representative of three independent experiments.

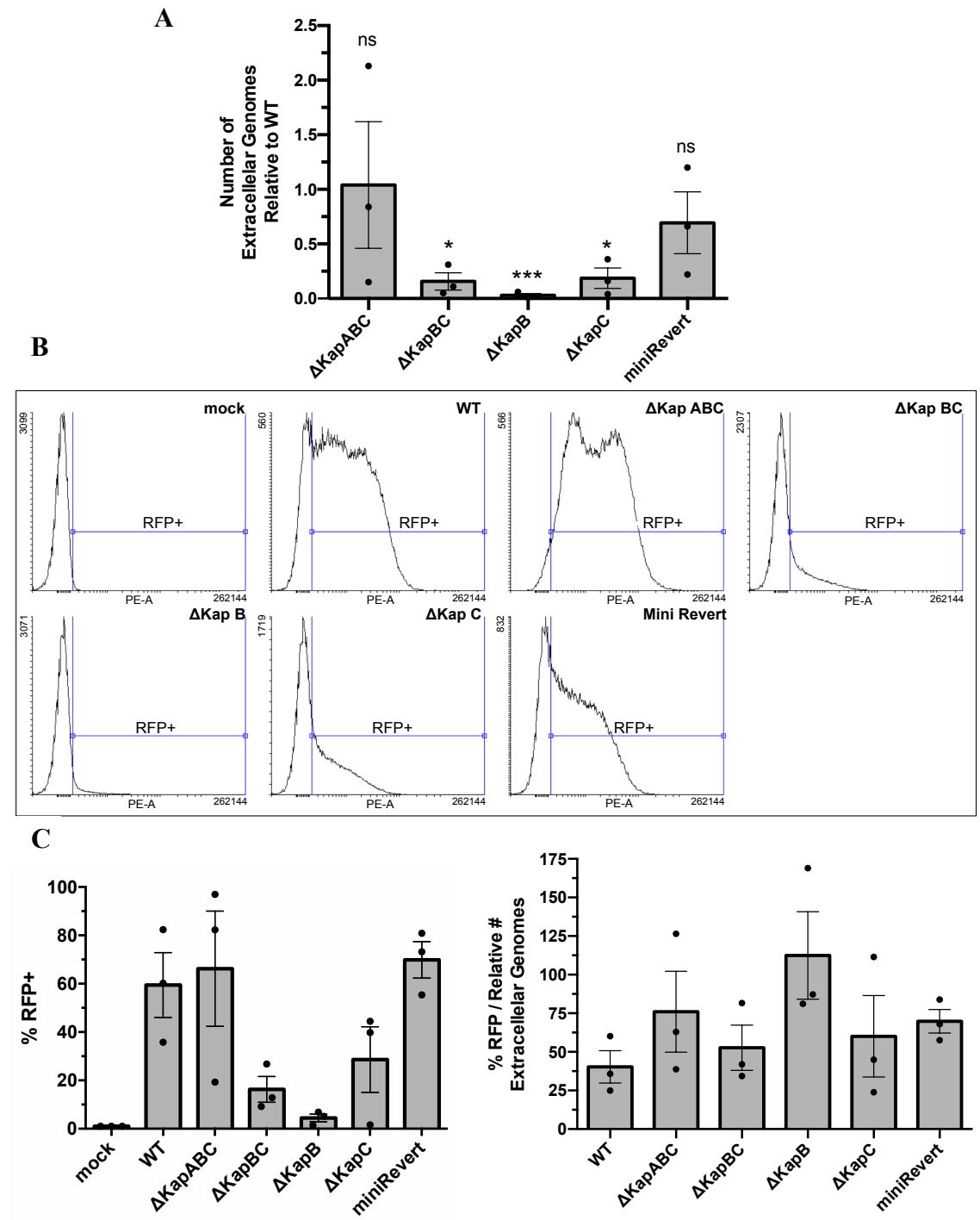

Figure 3.14: Kaposin-deletion mutant virions enter, uncoat and express a viral-encoded gene in naïve iSLK cells.

3.6 ΔKapB Virions Fail to Cause Elongated Cell Morphology Upon Infection of Primary Endothelial Cells

In order to confirm that kaposin-deletion mutant viruses were able to establish a latent infection similar to wild-type, I used virus obtained from lytic-induced P1-iSLK-BAC16 cells to infect primary human umbilical vein endothelial cells (HUVECs). The assumption was such that if infectivity was unaffected by kaposin-deletion, the virus should be able to: 1) maintain viral episomes tethered to human chromatin by LANA expression, and 2) elongate cellular morphology to a 'spindled' phenotype, both evidenced in latent KSHV-infected endothelial cells (Ciufo et al., 2001). HUVECs were seeded onto gelatin-coated coverslips and the next day spinoculated with P1-iSLK-BAC16 virus and cultured for 72 hours post-infection. Cells were subsequently stained for immunofluorescence using a primary antibody against LANA and Alexa Fluor-Phalloidin (Thermo Fisher Scientific), a conjugate stain for filamentous actin.

Virus stocks from wild-type and kaposin-deletion mutant P1-iSLK-BAC16 cells were capable of infecting primary HUVECs as evidenced by RFP-expressing cells, which were not observed in mock-infected cells (Figure 3.15). All virus-infected cells also stained positive for LANA dots, an indicator that viral genomes are capable of expressing LANA to tether viral genomes to host chromatin, and a hallmark of latent-infected cells (Figure 3.15). Spindling of endothelial cells is another hallmark of latent infection and is evidenced by an elongation of infected cells compared to their normal round morphology; wild-type KSHV-infected cells clearly showed this phenotype in comparison to mock-infected cells (Figure 3.15). Furthermore, all kaposin-mutant KSHV-infected cells were capable of eliciting this phenotype, except for ΔKapB mutant virus infections (Figure 3.15). While all

Figure 3.15: ΔKapB mutant KSHV fails to cause spindling in infected primary endothelial cells. HUVECs were infected with virus stocks harvested at 96 hours post-induction from lytic wild type (WT) and kaposin-deletion mutant P1-iSLK-BAC16 cells. At 72 hours post-infection, cells were fixed, permeabilized, and stained using primary antibody against LANA with secondary detection by anti-rabbit Alexa Fluor 488 antibody (green) and fluorescent dye for filamentous actin, Alexa Fluor 647 Phalloidin (white). RFP expression is indicative of virus-infected cells. Images were taken by Gillian Singh on a Zeiss 510 Meta Laser Scanning Confocal Microscope using 63X oil immersion objective and processed using ImageJ software. Images are representative of three independent experiments.

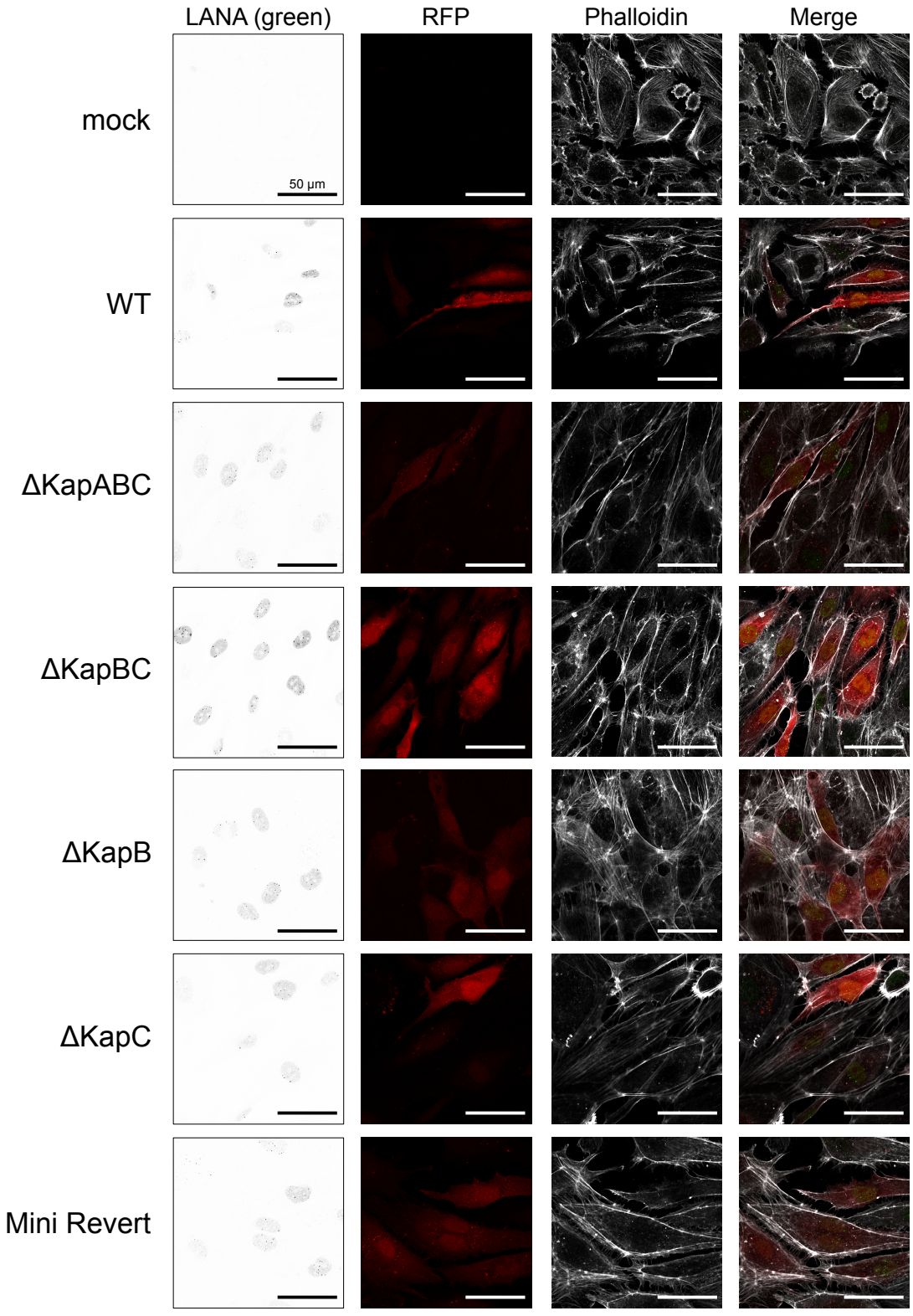

Figure 3.15: ΔKapB mutant KSHV fails to cause spindling in infected primary endothelial cells.

other viruses resulted in elongation and parallel alignment of infected cells relative to one another, I failed to find any ΔKapB mutant KSHV-infected cells with these characteristic phenotypes (Figure 3.15). These results suggest that while ΔKapB mutant virions were capable of entering, uncoating, and expressing viral genes, they were defective in reprogramming cells to elicit changes in cell morphology consistent with latent infection phenotypes. As a result of defective latent programming, it is possible that cells infected with ΔKapB mutant viruses are limited in their ability to express lytic viral genes to produce progeny virions as equally as wild-type KSHV.

3.7 Viral Gene Expression During Lytic Reactivation is Attenuated in ΔKapB Mutant iSLK-BAC16 Cells

Having determined that kaposin-mutant viruses are capable of entering, uncoating, and expressing virally-encoded genes, such as LANA and RFP, equally compared to wild-type, I still had outstanding questions regarding the attenuated production of virions from lytic reactivated ΔKapBC, ΔKapB, and ΔKapC iSLK-BAC16 cells. While most of the kaposin-mutant viruses appear to elicit latent morphological changes in infected primary endothelial cells, the limited ability for ΔKapB mutant viruses to induce spindling raises the question as to whether this phenotype is the cause of deficient virus production in ΔKapB mutant iSLK-BAC16 cells.

To investigate which stage of the virus life cycle, latent or lytic, is being most disrupted by kaposin-mutagenesis, I sought to conduct a time-course of lytic reactivation during which latent, early, and late lytic viral gene expression was analyzed. P1-iSLK-BAC16 cells were induced to reactivate by culturing in medium containing Dox and NaB and cell lysates were harvested at 0, 24, 48, and 72 hours post-induction (hpi). Lysates were

immunoblotted using primary antibodies against KapB & KapC (latent/early lytic), LANA (latent), ORF57 (early lytic), and ORF65 (late lytic). PAA was added to the culture medium as an inhibitor of the viral DNA polymerase and was used as a negative control for gene expression that occurs following viral genome replication.

LANA protein was consistently detected in all cell lysates at all time points throughout the lytic reactivation time course (Figure 3.16). LANA protein levels appeared to slightly increase throughout the lytic time course, with only minor decreases in expression levels for the ΔKapC mutant (Figure 3.16). KapB & KapC proteins were detected in lytic wild-type cells at 12 hpi and steadily increased in expression up to 72 hpi, consistent with early lytic gene expression (Figure 3.16). As expected, ΔKapABC and ΔKapBC mutants were negative for kaposin expression, while the mini-revertant iSLK cells were also negative for kaposin expression, likely due to a lack of DR epitopes for antibody binding (Figure 3.16). Alternatively-coded KapB protein was detected at an expected molecular weight of 42 kDa for ΔKapC mutant iSLKs (Figure 3.16), approximately 7 kDa larger than that of wild-type due to the difference in DRs noted from PFGE-analysis (Figure 3.7). Alternatively-coded KapC was only faintly detected at 72 hpi for the ΔKapB mutant at a molecular weight of approximately 46 kDa; the expression level of KapC was markedly less than that of wild-type (Figure 3.16). ORF57, which were used as a marker of early gene expression, protein levels were slightly decreased in ΔKapBC, ΔKapB, and ΔKapC mutants compared to wild-type; this trend was more pronounced for ORF65, a marker for late gene expression, protein levels which were diminished in ΔKapBC and ΔKapC mutants and not detected in ΔKapB mutant cells (Figure 3.16). Taken together, these results confirm that the likely reason for decreased virion production from

Figure 3.16: ΔKapB mutant iSLK-BAC16 cells have decreased late gene expression during lytic reactivation compared to wild-type. Wild-type (WT) and kaposin-deletion mutant P1-iSLK-BAC16 cells were either induced to lytic reactivation with Dox and NaB and cell lysates harvested at 24, 48, and 72 hours post-induction (hpi) or left untreated and harvested 24 hours later (latent, Lat). PAA treatment, which inhibits the viral DNA polymerase, was used as a negative control for viral genome replication. Lysates were immunoblotted for viral protein expression using primary antibodies against KapB & KapC (latent/early lytic), LANA (latent), ORF57 (early lytic), and ORF65 (late lytic). β-actin was used as a protein loading control. Molecular weights, in kDa, are shown for Colour Protein Standard, Broad Range (New England Biolabs).

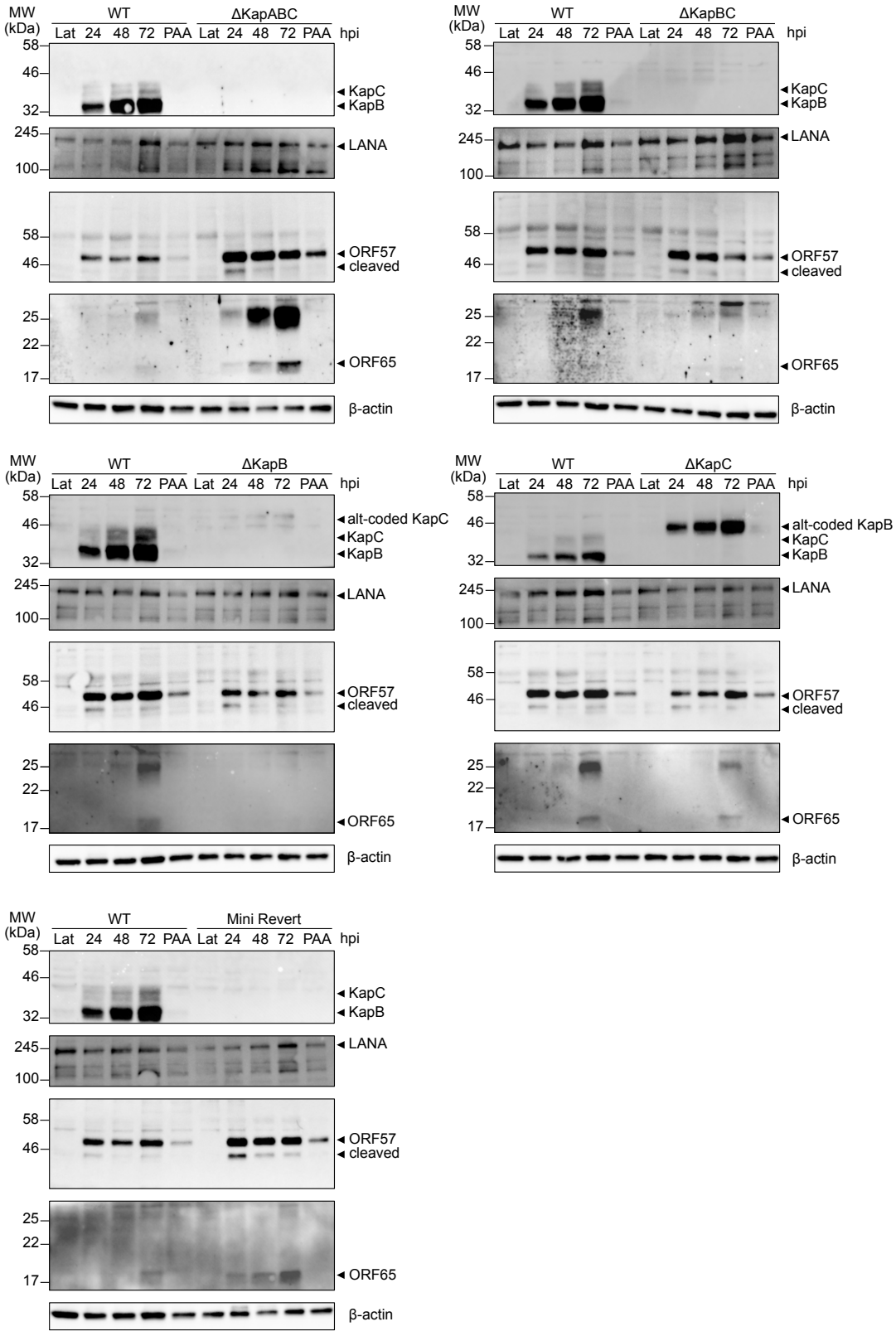

Figure 3.16: ΔKapB mutant iSLK-BAC16 cells have decreased late gene expression during lytic reactivation compared to wild-type.

ΔKapBC, ΔKapB, and ΔKapC mutant iSLK-BAC16 cells is due to a lack of expression of lytic viral genes during reactivation. While differences in protein levels of early lytic genes, such as ORF57 and KapC proteins, in these kaposin-mutant cells was not markedly different than wild-type, the difference in expression of late lytic genes was much greater. These slight differences in early lytic protein levels likely contribute to the larger discrepancies in late lytic proteins due to the temporal cascade of gene expression; differences in gene expression accumulate as the cycle progresses through genome replication and late gene expression. The initial cause of such decreases in early gene expression for ΔKapB mutant cells could be attributed to a failure of infected cells to recapitulate latent phenotypes, as observed in infected HUVECs that lacked a spindled morphology; however, future experiments to confirm this relationship would need to be conducted.

Contrary to the above-noted deficiencies in ORF57 and ORF65 expression for some kaposin-mutants, the ΔKapABC and mini-revertant iSLK-BAC16 cells showed increased levels of ORF57 and ORF65 compared to wild-type (Figure 3.16). Furthermore, ORF65 protein began to accumulate at earlier time points in these mutants compared to wild-type; ORF65 could be detected at 24 and 48 hpi for ΔKapABC and mini-revertant iSLK cells compared to the 72 hpi detected ORF65 band in wild-type (Figure 3.16). This suggests that these kaposin-mutant iSLK-BAC16 cells have an accelerated progression of lytic reactivation compared to wild-type cells.

To gain insight in to whether the deficiency in late viral gene expression is due to a lack of the KapB protein, a *trans*-complementation assay was conducted. iSLK-BAC16 cells were either left untreated or transduced with recombinant lentiviruses designed to

express a 22-kDa construct of KapB or an empty vector. This version of KapB has less copies of each of the DRs compared to the BAC16 genome, resulting in a smaller protein product, but with identical amino acid repeats. Successfully transduced cells were selected by culturing cells in the presence of blasticidin for 96 hours, which were subsequently recovered for 24 hours in complete medium. Selected cells were then either left untreated (latent) or induced to lytic reactivate for 72 hours by culturing the cells in media containing Dox and NaB. Cells lysates were immunoblotted using primary antibodies directed against KapB and ORF65, with β-actin used as a protein loading control. Consistent with previous results, ΔKapB iSLK-BAC16 cells showed reduced ORF65 protein expression compared to WT (Figure 3.17). Transduction with neither KapB nor the empty vector resulted in a change in ORF65 expression compared to un-transduced WT BAC16 cells; notably, *trans*-complemented KapB had significantly lower levels of expression than that of the viral-encoded KapB (Figure 3.17). Similarly, ΔKapB iSLK-BAC16 cells showed no change to late lytic viral gene expression as a result of lentiviral transduction (Figure 3.17). While these results seem to suggest that the defect in lytic gene expression is not due to a lack of KapB protein, such a conclusion should be reserved for when *trans*-complemented protein expression levels more closely match viral-encoded KapB expression.

Collectively, these data suggest that different kaposin products have specific roles that in combination can lead to either reduced or enhanced lytic viral gene expression and influence the successful production of progeny virions during lytic reactivation. Due to the drastic differences in lytic cycle gene expression and kinetics compared to WT, additional experiments are required to identify the exact cause of each phenotypic effect as a result of kaposin mutagenesis.

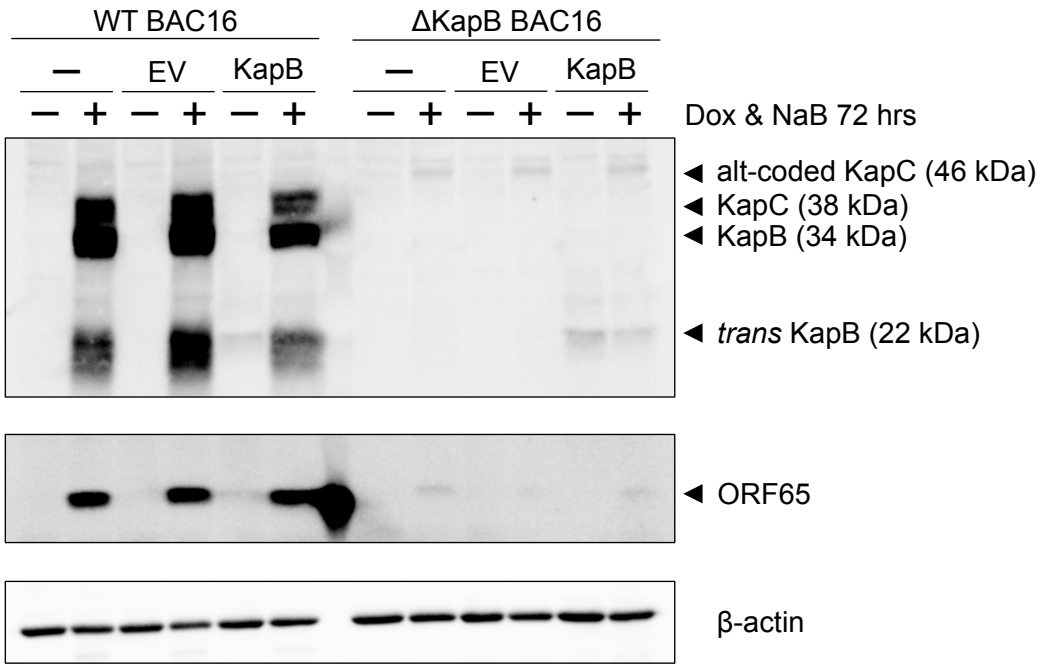

Figure 3.17: Trans-complementation of KapB protein fails to rescue defect in late lytic gene expression in ΔKapB-mutant iSLK-BAC16 cells. Wild-type (WT) and ΔKapB-mutant iSLK-BAC16 cells were either left un-transduced or transduced with recombinant lentiviruses to express a 22-kDa KapB protein or an empty vector (EV). Cells were selected for successful transduction by culturing in the presence of puromycin for 48 hours and either left untreated or induced to lytic reactivate for 72 hours by culturing in doxycycline (Dox) and sodium butyrate (NaB). Cell lysates were harvested and immunoblotted using primary antibodies against KapB/KapC and ORF65; β-actin was used as a protein loading control.

CHAPTER 4: DISCUSSION

4.1 Overview

While herpesviruses demonstrate relatively conserved virion structure, their large dsDNA genomes exhibit an incredible amount of diversity and evolution in terms of gene size and organization (Hayward et al., 1984). Within the gamma-herpesviruses, gene arrangement can be subdivided into distinct classes or gene blocks that vary from conserved 'core' genes to 'virus-specific' genes; comparison of sequences between viruses of different host species has provided valuable information regarding specific gene function (Nicholas, 2000). For example, molecular mimicry of cellular genes by KSHV, such as vCyclin, has provided insight into potential interaction partners and upregulated pathways during virus infection (Russo et al., 1996). However, sequencing data can only provide so much information; herpesvirus genomes are a complex assortment of cis-regulatory sequences and open reading frames (ORFs) that have been optimized for coding capacity and temporal expression according to the different kinetic classes: latent, immediate-early-, early-, and late-lytic genes (Nicholas, 2000). As a result, nucleotide sequences and gene function cannot always be inferred from evolutionary conservation.

The focus of this thesis work, the kaposin locus, epitomizes such complexity. Within this locus resides a GC-rich direct repeat region adjacent to the KapA ORF that shows elaborate translation potential of its own and of which there is no known homology (Sadler et al., 1999). The virus generates an abundance of the kaposin transcript during latency and lytic reactivation from constitutive and RRE-associated promoters, respectively, which implies that this region has significant importance for viral pathogenicity. These GC-rich tandem repeats have also been implicated as having an

essential ori-Lyt function for lytic genome replication, further highlighting their multifaceted role (Wang et al., 2006). However, except for knowledge gained by the ectopic expression of individual kaposin ORFs, very little is known about this region of the KSHV genome. Furthermore, the role of each protein during the KSHV life cycle is unclear.

With this thesis work, I sought to fill this knowledge gap by characterizing the role of individual kaposin proteins in KSHV-infected cells, particularly during the lytic life cycle. My initial experiments involving knockdown of the kaposin transcript in B-cells were unable to identify effects that were specific to individual proteins; this is because KapA, B, and C expression originate from the same transcript. I therefore generated a (novel) library of recombinant viruses in which the coding capacity of specific kaposin proteins was mutagenized. Despite characterization of these viruses presenting its own set of difficulties, I was able to identify deficiencies in both the latent and lytic life cycle for a subset of these kaposin-mutant viruses. This allowed us, for the first time, to propose new roles for the kaposin transcript and proteins in the lytic replication cycle.

4.2 Knockdown of the Kaposin Transcript Does Not Reveal a Role for Kaposin mRNA or Protein Products During the Lytic Life Cycle.

My initial experiments to characterize kaposin function during the lytic cycle involved shRNA-mediated knockdown of the entire transcript in TREx BCBL-1 cells. Assessment of lytic infection was conducted by measuring each step of the progressive cycle; in brief these included lytic viral gene expression by immunoblot, genome replication by qPCR of intracellular DNA, assembly and egress by qPCR of DNase-protected viral genomes, and ability of virions to infect naïve cells by immunofluorescence.

This work showed that despite consistent knockdown of the kaposin transcript, there were no impairments in viral gene expression (Figure 3.1), genome replication and egress (Figure 3.2), or ability of produced virions to establish infection in naïve cells (Figure 3.3). Significant differences were observed in the rate of genome replication between the kaposin-knockdown cells and the non-specific hairpin control; surprisingly, cells deficient in kaposin transcripts were found, on average, to replicate faster (Figure 3.3). This was seen as an increase in ORF45 viral gene expression (Figure 3.1) and increased intracellular and extracellular viral genomes at 24 hours post-induction (hpi) and 48 hpi, respectively, (Figure 3.2) for both shKap-transduced cells compared to the NS-control.

A significant limitation to this set of experiments is the inability to distinguish between an effect caused by reduced RNA transcript levels or protein. There have been a number of implications for an RNA-mediated effect for the K12-associated transcript. Firstly, the miRNAs encoded in the K12 ORF have been demonstrated to cause significant changes to host gene expression at the RNA level; this level of regulation is thought to reprogram the cellular environment in such a manner that favours KSHV-induced oncogenesis (Forte et al., 2015). Furthermore, the K12 transcript generated from an RRE in the ori-Lyt[R] has been implicated as having functional activity in the process of lytic genome replication (Wang et al., 2006).

The identification of a causal relationship is further complicated because the levels of expression of all three kaposin proteins are being altered in addition to RNA transcripts when shRNA-knockdown is conducted (Sadler et al., 1999). Interestingly, despite targeting the kaposin mRNA, KapB protein levels were greater in shKap-transduced cells at 48 hours post-lytic induction than in latent NS-control cells (Figure 3.1). The effect of this relative

increase in kaposin proteins compared to latency could have any number of effects related to host RNA stability and gene expression. Firstly, both KapA and KapB have been shown to alter host viral gene expression directly through recruitment of transcription factors such as AP-1 and c-myc, respectively (Xie et al., 2005; Chang et al., 2016). Additional mechanisms include KapB's activation of signaling pathways that alter ARE-mRNA transcript levels leading to upregulated expression of pro-inflammatory cytokines, such as IL-6 (McCormick & Ganem, 2005).

Due to the convoluted nature of activity that could be arising from the kaposin transcript or its encoded proteins, the slight differences noted in lytic viral gene expression and rate of production of intracellular and extracellular viral genomes were difficult to interpret. It is possible that only slight differences were observed in shKap-transduced cells compared to NS-control cells because RNA-interference is not 100% effective; shRNA-mediated knockdown of KapB expression averaged between 64-80% efficiency (Figure 3.1). Alternatively, mixed results may be a hybrid of both transcript- and protein-related phenotypes, in which case, it would be impossible to distinguish them through interpretation of these experiments alone. It was therefore necessary to complement this work with site-specific mutagenesis studies.

4.3 BAC-Mutagenesis of the Kaposin Locus Generated a Novel Library of Recombinant Viruses and Revealed the Propensity for Loss of GC-rich Repeat Regions

The creation of herpesvirus BACs has allowed for an expansion of virus research; BACs are an ideal tool as they can accommodate the large DNA genomes of herpesviruses and can be stably propagated in *E. coli* (Warden et al., 2011). BACs also present a means

for site-directed mutagenesis by recombineering, a strategy that has been heavily employed in the KSHV field for gene characterization using both published BACs, BAC36 and BAC16 (Zhou et al., 2002; Brulois et al., 2012). To date, there have been no published studies that have characterized kaposin mutant BACs. While Toth et al. (2016) refer to a K12 knockout BAC16 virus with a deletion of the DRs and K12, they fail to report any analyses related to this mutant. Gallo et al. (2017) similarly refer to the generation of a K12 mutant in which a kanamycin cassette disrupts the K12 ORF, but report limited phenotypic analysis related to this virus. A study conducted by Campbell et al. (2018) investigated the role of the RRE promoter in the kaposin locus, and in so doing created a K12 RRE-mutant; however, this study focused more on RTA-recruitment and genomic architecture rather than kaposin gene function.

In this study, I used the BAC16 genome as a template for generating mutations within the kaposin locus that would allow for clearer interpretation of individual gene function. Recombineering was carried out in *E.coli* using the temperature-sensitive Lambda Red recombination and positive and negative selection cassette, KanSacB, for 'scarless' mutagenesis (Tischer et al., 2006). Specific mutations were introduced into the kaposin proteins by homologous recombination (Figure 3.4); mutations were achieved by either removing the DRs only (ΔKapBC) or in combination with the K12 AUG start codon (ΔKapABC), or by replacing the DRs with alternatively coded nucleotide sequences (ΔKapB, ΔKapC, mini Revert) (Figure 3.5). The effects of alternative coding of the DR sequences were two-fold: 1) the translation potential of either KapB or KapC was eliminated with multiple termination codons, while the other protein's expression was maintained with alternative codons, and 2) the repeat structure of the DRs and the naturally

high GC-content were disrupted and lowered, respectively (Figure 3.5). In all of the recombinant kaposin-mutant BACs, the regulatory sequences for transcriptional promoters and miRNA processing were left intact.

The resultant recombinant BACs were verified using various different methods. Preliminary verification was conducted by colony PCR using specific primers designed to amplify DNA spanning between the DRs and the beginning of the K12 ORF; amplified DNA matching the expected size was subsequently sequenced. This method proved very effective for screening colonies, as most successful PCR amplifications were positive for the expected mutation with no off-target changes in the kaposin locus. Unfortunately, due to the highly repetitive and GC-rich nature of the wild-type DRs, Sanger sequencing could not produce the full nucleotide sequence of the amplified DNA. This is consistent with recent transcriptome studies that failed to determine the exact nucleotide sequence of the T1.7 transcript from the LT_d promoter due to the high GC-content of the DR2 repeats (Bruce et al., 2017; Rose et al., 2018).

In addition to the above-mentioned mutants, I sought to create a recombinant KSHV BAC16 in which the DRs were restored to wild-type; this mutant was to act as a phenotypic revertant for future kaposin gene characterization. I used this opportunity to address an additional question regarding the kaposin locus, which is the functional relevance of the number of repeats within the DRs. The three different revertants described in this study contained varying numbers of DR repeats; however, only the mini-revertant, composed of one copy each of the DR2 and DR1 repeats, was successfully detected by PCR and sequencing. It is likely that the other two constructs with increased number of DRs and high GC-content were too difficult to introduce by homologous recombination;

the constructs likely experienced intramolecular recombination events (Zhao et al., 2010). It may still be possible to restore the DRs to wild-type with multiple rounds of recombination to slowly expand the number of repeats of the mini-revertant; however, each induction of recombinase genes risks off-target mutations or large-genome rearrangements. Thus, the generation of a mini-revertant in this study presented a suitable compromise, especially since a miniprotein version of KapB has been shown to maintain protein function, albeit at attenuated activity (McCormick & Ganem, 2006).

PFGE-analysis of each recombinant BAC was used to identify whether large-genome rearrangements occurred during the recombineering method. The NheI-restriction digest pattern for the wild-type (WT) BAC16 differed from the anticipated fragment sizes generated using SnapGene software; notably, the largest fragment corresponding to the TR fragment, was smaller than the expected 33-kb size and instead migrated as an 18-kb fragment (Figure 3.7). The lack of this 33-kb fragment was also confirmed by comparing my WT BAC16 restriction digest pattern with those from other BAC16 mutagenesis studies (Lee et al., 2014; Jain et al., 2016). Interestingly, the WT digest pattern matched a sample from a study by Jain et al. (2016) that was reported as having non-intact TRs. It is therefore likely that the TRs in the WT BAC16 experienced some form of rearrangement, resulting in a deletion of approximately 15-kb. The nucleotide sequence of the TRs is prone to experience recombination events due to the high GC-content and repetitiveness of the 801-bp subunits (Russo et al., 1996; Dheekollu et al., 2013). A loss of approximately 15-kb in the TR would be consistent with a deletion of approximately 19 copies of the 801-bp subunits, thus a significant proportion of the sequence. It is unclear what effect this deletion would have on the virus life cycle; previous studies have shown that a plasmid containing

2-4 copies of TRs was sufficient to confer long-term maintenance when in the presence of LANA (Ballestas et al., 1999; Lim et al., 2004; Hu & Renne, 2005). Therefore, while latent episome persistence may not be affected from TR-deletions, it is possible that smaller TR regions, which would impact the total length of the viral genome, may impact proper genome encapsidation. A decrease in the internal pressure from enclosing a smaller genome into a normal-sized capsid could influence the ejection of viral DNA during the entry process, thus making the virus less infectious (Bauer et al., 2013). Therefore, the WT virus should be compared to a virus containing the number of TRs indicated for the GenBank published sequence to verify whether any phenotypic differences resulted from a loss of TRs.

Regardless, the mutants previously generated by Julie Ryu (ΔKapABC and ΔKapBC) and characterized in this study by Sanger sequencing and PFGE were shown to have the same NheI- and NotI-digest pattern compared to WT, except for the kaposin locus fragment, which showed a decrease in size that was consistent with the removal of the DRs (Figure 3.7, Figure 3.8). However, insertion of the alternatively coded DRs (ΔKapB and ΔKapC) resulted in an unanticipated difference in fragment size for the kaposin fragment compared to WT; this fragment was approximately 200bp larger than expected. Since the design of the alternatively coded DRs reflected the published Genbank fragment length, this difference in size must be due to a deviation from the DR consensus sequence in the WT BAC16. Consistent with TR recombination, the high GC-content and repetitive nucleotide sequence makes the DRs a likely region for recombination (Brown, 2014). Unfortunately, these are the same characteristics that make confirmation by sequencing difficult.

Next-generation sequencing by Illumina MiSeq was conducted, in collaboration with Dr. John Archibald's lab, on BAC16 DNA isolated from GS1783 *E. coli* to analyze whether specific mutations had occurred elsewhere in the genome. Through this analysis, a significant proportion of the total sequencing reads mapped not to the KSHV BAC16 genome, but instead to the *E.coli* genome. This is likely a result of poor preparation of BAC DNA, which should have included a large-construct DNA-preparation kit (Qiagen) or Exonuclease V (New England BioLabs) and phenol/chloroform extraction steps, which are recommended for reducing linear genomic DNA and enriching for circular low-copy BAC DNA (Jain et al., 2016). Nevertheless, the sequences that did align to the KSHV genome covered a significant proportion of the unique ~140-kb coding region, despite not generating a single contiguous piece of DNA (Appendix A, Figure A.5). Furthermore, these sequences confirmed the specific mutations within the kaposin locus that were generated by recombineering.

These results, in combination with Sanger sequencing and PFGE-analysis, provided me with a reasonable level of confidence that mutagenesis was successfully carried out for the kaposin proteins, and that minimal to no off-target effects were generated in the process, despite initial differences identified in the TR and DR regions from the Genbank-published WT sequence that occurred prior to recombineering. These results should be confirmed by Illumina sequencing of newly prepared BAC16 DNA with the above-mentioned modifications to the DNA-preparation protocol. In order to confirm the deletion in the TRs, long-read sequencing using a MinION (Oxford Nanopore Technologies) may be required to assemble long enough reads that span the TRs. Ideally, a WT BAC16 clone that matches the GenBank sequence should be used. However, if the

viruses generated using the WT sequence from my study and that of the Genbank consensus sequence show no phenotypic differences, it could be concluded that the initial rearrangements in the TR and DR have little to no significance (to this study).

4.4 Variable Episome Number Between Kaposin-Mutant Virus-Infected Cells Complicated the Analysis of Latent and Lytic Life Cycles

Direct transfection of recombinant BAC16 DNA into mammalian cells is an inefficient process; in addition to my study, this has been reported by others who have attempted to produce virus in iSLK cells (Jain et al., 2016). Co-culture of directly BAC-transfected HEK 293Ts, which have been shown to elicit strong patterns of lytic viral gene expression (Renne et al., 1998), with naïve iSLK cells, a well-established KSHV producer cell line (Myoung & Ganem, 2011), proved to be a much more efficient method. Similar to my study, others have shown that iSLK cells can be infected with higher efficiency by cell-to-cell spread of virions produced from HEK-BAC16 cells induced to undergo lytic reactivation (Figure 3.9) (West et al., 2014; Jain et al., 2016).

The iSLK-BAC16 cells were used to characterize any phenotypic differences in the lytic viral life cycle due to kaposin-mutagenesis. Deficiencies were observed in ΔKapB iSLK-BAC16 lytic viral genome replication (Figure 3.11), viral gene expression (Figure 3.11, Figure 3.12), and virion release (Figure 3.12), which correlated with a reduced number of episomes during latency (Figure 3.11). Episome copy number is an indicator of stable KSHV infection; generally, the loss of KSHV episomes, as has been observed in BAC36 viruses lacking CTCF-binding sites in the latency locus, leads to deregulated latent and lytic gene transcription (Kang et al., 2011). In this study, the ΔKapB iSLK-BAC16 cells had 7-fold fewer episomes than WT, a difference that was further magnified to 47-

fold at 72 hours post-lytic induction (Figure 3.11). Consistent with the reported relationship between episome number and viral gene expression, I similarly observed deficiencies in latent (LANA) and lytic (ORF65) protein expression in ΔKapB cells. There are a few possible reasons as to why there might be different number of episomes in some of the iSLK-BAC16 cell populations.

1) Defective entry and/or latency establishment: One explanation could be that due to kaposin-mutagenesis, specifically KapB, the virions produced from lytic HEK-BAC16 cells are not as efficient at entering naïve iSLK cells during co-culture, and that the first passage of iSLK cells start with markedly lower episomes. In this case, the virions that infected iSLK cells may represent forms of defective virus; this term has been previously used to describe KSHV that, upon entry, is able to maintain efficient latent replication and proliferation, but harbors a lytic replication-defective genome (Deng et al., 2004). Alternatively, perhaps DR mutagenesis resulted in the production of defective virions that cannot successfully enter host cells and/or establish a successful latent gene expression program. This phenomenon would more closely resemble a scenario in which KSHV enters a cell type that is non-susceptible to infection (Bechtel et al., 2003), an event that has not been previously described as a consequence of KSHV-mutagenesis.

2) Defective latency maintenance: Alternatively, differences in episome number may be caused by a failure to efficiently maintain viral genomes during cell division. The maintenance and distribution of KSHV episomes is a complex process; unlike Epstein-Barr virus which equally distributes its viral genomes to daughter cells during cell division, KSHV genomes are believed to cluster into foci that are unevenly distributed into progeny cells (Chiu et al., 2017). It is possible that despite equal infection of iSLK cells, kaposin-

mutant viruses cannot effectively distribute and maintain viral episomes during cell division, thus resulting in a gradual loss of episomes, even under antibiotic selection (Skalsky et al., 2007). In the future, it would be prudent to monitor the number of episomes in BAC-infected cells over time to determine this with certainty.

3) Defective production of infectious virions: One explanation could be that kaposin mutagenesis caused a defect in the lytic cycle, resulting in the decreased production of infectious virions from lytic-induced HEK-BAC16 cells, and causing a reduced number of episomes in iSLK-BAC16 cells after co-culture. This was similarly observed for a study conducted by Peng et al. (2014), where an ORF6 deletion in BAC36 resulted in the virus's inability to produce infectious virions in HEK 293T cells unless they were trans-complemented with the protein by lentiviral transduction during lytic reactivation. Despite approximately equal number of episomes in the ΔKapBC and ΔKapC iSLK-BAC16 cells compared to WT, the impaired ability for these mutants to replicate their genomes following induced-reactivation suggests that a defect during the lytic cycle may be a likely cause.

To address some of these potential theories, I attempted to obtain virus stocks with sufficient titers to conduct experiments; however, virion production is largely dependent on the number of initial viral genomes, thus making it difficult to equalize the titer of virus stocks without first equalizing episome copy number. This effect was mitigated by passaging each recombinant virus to infect a naïve population of iSLK cells, thus generating the iSLK-BAC16-P1 cells. The passaging method involved each virus being serial diluted to achieve approximately equal numbers of RFP-expressing, hygromycin-resistant cells following antibiotic selection. Although this endpoint was largely semi-

quantitative, it provided the best opportunity, given the limitations of a virus that by default establishes latency, to normalize the number of infectious virions encountered by each naïve cell population. While qPCR determination of DNase-protected genomes is an effective method for estimating particle number, it does not provide information on infectious units and was therefore not an applicable value for viral passaging. Until a modified plaque assay is developed for KSHV, which is a difficult task for a virus that predominantly establishes latency following entry and fails to cause cytolytic effect, the best available tool for quantifying the number of infectious particles in a viral stock is measuring constitutive expression of a fluorescent gene in infected cells. Due to markedly unequal titers of virus being produced from each of the original iSLK-BAC16 populations, some viruses needed to be heavily diluted in order to achieve similar quantities of infectious virions. At increased dilutions, the number of virions became more difficult to estimate, possibly due to virus aggregates. In retrospect, these issues may be addressed by sonication of virus preparations instead of centrifugation prior to dilution (Arens et al., 1988).

I chose to passage viral iSLK cell lines under hygromycin selection in order to increase virus production from iSLK-BAC16 cells because I felt this approach was the best option to equalize episome copy number. Indeed, an increase in episome number was observed for ΔKapB virus; however, the opposite effect was observed for ΔKapC and mini-revertant viruses, which had reduced number of episomes compared to WT (Figure 3.13). These results highlighted the fact that before further analysis, I needed to establish whether all BAC16 infectious particles were capable of successfully entering and establishing a latent program before other stages of the virus life cycle could be investigated.

4.5 Kaposin Mutagenesis Does Not Affect Virus Entry, but Likely Impacts Endothelial Cell Reprogramming

Viral entry is defined as the delivery of a replication-competent form of the genome to the correct subcellular compartment; in the case of herpesviruses and KSHV, this involves host cell attachment, capsid uncoating, delivery of the genome to the nucleus, and expression of latent viral genes from a chromatin-tethered, circular episome (Kumar and Chandran, 2016). In this study, virions obtained from kaposin-mutant virus-infected iSLK cells were analyzed for their ability to enter and infect naïve iSLK cells; this was measured by detecting RFP expression from the viral genome by flow cytometry. Since there were fewer particles in the virus-containing supernatants for ΔKapBC, ΔKapB, and ΔKapC samples, it was reasonable to find that these samples resulted in fewer RFP-positive cells following *de novo* infection (Figure 3.14). After normalization of the percentage of RFP-expressing cells to the number of DNase-protected virions in each sample, I found that the proportion of particles that were infectious in each sample was approximately the same for all kaposin-mutant recombinant viruses compared to wild-type (Figure 3.14). This means that kaposin-mutagenesis does not affect the ability of virions to enter, uncoat, and express viral genes in newly infected cells.

RFP-expression was used as a proxy to determine whether the virus successfully entered cells; however, this measurement cannot provide a complete picture regarding latency establishment, which would be better examined through detection of specific viral transcripts or proteins expressed following *de novo* infection. This experiment does provide a better understanding of the role, or lack thereof, for kaposin proteins during attachment, uncoating, and delivery of viral DNA to the nucleus. This result is consistent with the idea that KapB has never been found to be incorporated into virions or extracellular vesicles

released during the lytic cycle, and therefore does not affect virus entry (Bechtel et al., 2005; Gong et al., 2017).

Products of the kaposin locus, particularly KapB, have been proposed to play an important role in the endothelial cell reprogramming that occurs during latency and viral tumourigenesis, in particular, to a spindled morphology and upregulated inflammatory gene expression (Yoo et al, 2010; Corcoran et al, 2015). Because of this, I wanted to assess the ability of each virus to orchestrate and recapitulate latent viral phenotypes by conducting immunofluorescence on *de novo* infected HUVECs. LANA and actin staining revealed that while ΔKapB-infected cells are capable of expressing RFP and the latent viral gene, LANA, they do not display a spindled morphology that is characteristic of KSHV-latency (Figure 3.15). While this experiment does not provide a complete picture as to whether latency has been impacted by kaposin mutagenesis, it does provide preliminary evidence that cooperativity between latent viral genes may be important. This is made evident by the triple (ΔKapABC) and double (ΔKapBC) kaposin mutants, which both appear to induce spindling despite knockout of KapB protein expression.

The idea of kaposin gene cooperativity is a complex issue, especially considering that the virus has been known to undergo abortive lytic phase following *de novo* infection. In such a case, both latent and a limited number of lytic viral genes are co-expressed until a latent program is established; this has been observed in primary human dermal microvascular endothelial cells and foreskin fibroblasts (Krishnan et al., 2004). My assessment of endothelial cell reprogramming was determined by cell spindling and the expression of LANA and RFP; however, many other viral genes involved in either the latent or lytic cycle could have been expressed concurrently and influenced spindling

phenotypes. These include vFLIP and viral G-protein coupled receptor (vGPCR), latent and lytic genes, respectively, that alone are known to induce endothelial cell spindling *in vitro* (Grossmann et al., 2006; Bais et al., 2003). The likelihood that kaposin gene products cooperate with viral and cellular genes toward the establishment of latency is underscored by the ability of KapB to bind multiple cellular proteins, including MK2 and c-myc, to upregulate inflammatory cytokine expression and angiogenic factors, respectively (McCormick & Ganem, 2005; Chang et al., 2016).

The effect of kaposin-mutagenesis on the reprogramming of endothelial cells might be better characterized by looking at specific BEC and LEC markers; this is of particular interest considering KapB's reported role in upregulating LEC-specific markers in an ARE-mRNA-, and PROX1-dependent manner (Yoo et al., 2010). Furthermore, a transcriptomic and proteomic analysis would provide valuable information about additional cellular and viral genes whose expression is modulated during *de novo* infection of endothelial cells as a result of kaposin mutagenesis. Common methods such as high throughput RNA-sequencing and tandem mass spectrometry (MS/MS) have been previously used with BAC16 models to investigate the role of specific viral gene products during latent and lytic viral life cycles (Gong et al., 2014; Anders et al., 2016).

4.6 The Kaposin Locus Has a Significant Role in the Lytic Cycle, but Requires Further Characterization

Reactivation of the herpesvirus lytic cycle can be triggered by various stresses to the host cell; this leads to the upregulated expression of cellular and viral genes whose coordinated activity function to exponentially replicate the viral genome, assemble virus particles, and release progeny virions from the cell surface. This surge of enzymatic activity

is regulated by many *cis*- and *trans*- acting factors that work at both the level of nucleic acid and protein to achieve a temporal cascade of viral gene expression (Sun et al., 1999).

My investigation of the effect on lytic cycle progression due to kaposin-mutagenesis was conducted through an analysis of viral gene expression, genome replication, and the extracellular release of progeny virions; this analysis consistently showed that ΔKapB mutant viruses were deficient in all three categories compared to WT (Figure 3.16, Figure 3.11, Figure 3.14). As previously stated, initial efforts to characterize the stages of the lytic cycle were complicated by the difference in episome number. Since latent genome copy number was never equalized throughout my experiments, it makes it difficult to determine whether differences in lytic cycle progression are a result of varied episome number, kaposin-mutagenesis, or a combination of both. Nevertheless, defects associated with the ΔKapB lytic cycle were not improved in virus-passaged iSLK cells, despite episome copy number in ΔKapB being higher than WT for these experiments (Figure 3.13, Figure 3.16). Similarly, ΔKapBC and ΔKapC mutant viruses showed reduced lytic viral gene expression (Figure 3.16), genome replication (Figure 3.11), and virus production compared to WT (Figure 3.14), both prior to and following virus-passaging in iSLK cells. Taken together, these data support the idea that viruses deficient in KapB and/or KapC expression have a defect in lytic cycle progression, regardless of starting episome copy number.

Interestingly, the ΔKapABC mutant did not show impairments following lytic reactivation; on the contrary, both it and the mini-revertant virus displayed increased rates of viral gene expression compared to WT (Figure 3.16). These results were consistent with those obtained from knockdown of the entire kaposin transcript in BCBL-1 cells (Figure

3.2). Re-introduction of the AUG start codon to the kaposin locus appears to be negatively-correlated with lytic cycle progression, suggestive that translation of a K12-containing protein, either KapA and/or KapC, negatively impacts the lytic cycle. This would be consistent with the idea that some latent gene products play a role in lytic gene silencing, as has been observed for LANA, which inhibits ORF50 transcription (Lu et al., 2006). However, a recent study conducted by Gallo et al. (2017) seems to contradict this notion; disruption of the K12 ORF by insertion of an antibiotic cassette abrogated lytic genome replication.

Upon close inspection of the lytic viral gene expression profile conducted for each recombinant virus, deficiencies in early gene (ORF57) expression for the ΔKapB and ΔKapC viruses were only slight in comparison to the deficit observed in late gene (ORF65) expression, with ΔKapB faring the worst of these two mutants (Figure 3.16). Furthermore, along with ΔKapBC, these three recombinant viruses displayed reduced rates of genome replication (Figure 3.11). Taken together, these results suggest that mutagenesis of the DRs affects ori-Lyt [R] function, thereby impairing lytic genome replication and subsequent late gene expression. These results would be consistent with the study conducted by Lin et al. (2003), where the absence of GC-rich repeats could not support genome replication from the ori-Lyt. However, this mechanism may be dependent on the host cell context; some studies have found that deletion of the ori-Lyt[R] is well tolerated by both KSHV and MHV-68, and that the virus can maintain replication in certain cell types *in vitro* and *in vivo*, respectively (Xu et al., 2006; Sattler et al., 2016). My study supports this notion; I noted that the ΔKapABC virus, which is deficient in the GC-rich repeats, was capable of replicating, perhaps at an increased rate compared to wild-type. However, insertion of

alternatively coded regions that disrupt the repeat structure and GC-content of the DRs appear to abrogate genome replication, thus supporting the idea that the GC-repeats are necessary for replication. Real-time PCR quantitation of the intracellular genomes throughout the lytic cycle should be repeated to confirm this effect on replication.

The deficiency in lytic viral gene expression, as measured by ORF65 protein levels, could not be restored following limited KapB expression provided in *trans* by lentiviral transduction (Figure 3.17). While this experiment suggests that KapB protein does not play a role during the lytic cycle, there are aspects of this *trans*-complementation assay that ideally should be modified prior to making such a conclusion. First, *trans*-complemented KapB protein levels should more closely match those of the viral-encoded KapB; this might be achieved by inclusion of an RRE to the promoter of *trans*-KapB, thus allowing for transcription and translation levels to follow lytic cycle kinetics. Additionally, the size of the protein generated from *trans*-complemented constructs should more closely match that of wild-type KapB to ensure that any differences observed in lytic viral gene expression are not due to a smaller protein. The characteristic of varying numbers of repeats in the DRs as found in different KSHV isolates and its effect on protein function are still unclear and should be investigated independently.

My analysis of viral gene expression was limited to only one gene per kinetic class of the temporal cascade. Future work should focus on obtaining a more comprehensive characterization of the effect of kaposin-mutagenesis on viral gene expression. Due to the limited availability and efficacy of antibodies for KSHV viral proteins, as noted for the KapA protein, this analysis will likely predominantly rely on reverse transcription-PCR (RT-PCR), as is typically done for KSHV BAC16 mutagenesis studies (Lee et al., 2014;

Liang et al., 2015; Bergson et al., 2016; Nishimura et al., 2017). In line with my results, it is believed that other late viral genes, such as K8.1 (glycoprotein) and ORF26 (heterotriplex capsid protein), will likely experience similar deficiencies in expression for the ΔKapBC, ΔKapB, and ΔKapC viruses compared to WT.

While it is likely that defects in late viral gene expression are the cause of impaired virion production in some of the kaposin-mutant viruses, it is possible that stages following genome replication, such as assembly and egress, could also be affected. Since this study only investigated the production of DNase-protected virions in the supernatants of lytic BAC16-infected cells, no specific information on assembly and egress was collected in this study. Transmission electron microscopy is a common method to assess virion morphology and proper assembly of DNA-containing capsids (Nii et al., 1968; Gardner et al., 2018) and could be used to complete my analysis of the lytic cycle. However, while KapA has been shown to be localized to cellular membranes, there has yet to be any evidence to suggest any direct involvement in virion egress (Kliche et al., 2001).

4.7 Potential Roles for Kaposin in the Lytic Virus Life Cycle

Various functions have been attributed to KapA and KapB proteins through ectopic expression and phenotypic analysis; some effects caused by kaposin expression include changes to cell morphology through actin-remodeling, upregulated expression of pro-inflammatory cytokines, and the reprogramming of endothelial cells (Kliche et al., 2001; Xie et al., 2005; McCormick & Ganem, 2005; Corcoran et al., 2015; Yoo et al., 2010). While my kaposin mutagenesis study was unable to address and validate each of these effects in the context of the virus, I did obtain phenotypic evidence to suggest potential

cooperativity between the kaposins and other viral proteins, as well as additional roles for the kaposin transcript (summarized in Figure 4.1).

One important aspect that must be considered is that differences in latent cells may predispose the virus to a defect in the lytic cycle; therefore, my mutagenesis study may affect both latent and lytic viral life cycles. A key aspect of my study was the disruption of the ~1-kb GC-rich nucleotide sequence adjacent to the K12 ORF and a component of the ori-Lyt [R]. The relationship of GC-rich regions and CpG islands with increased transcriptional activity and potential to act as promoter elements, especially in vertebrate genomes, adds an additional level of complexity to the kaposin locus (reviewed in Deaton & Bird, 2011). Research conducted by the Lieberman lab group have found RNA polymerase II-containing complexes in association with the kaposin locus during latency; this recruitment is mediated by CTCF-binding and histone-methylation events on the chromatinized viral genome (Kang et al., 2011; Kang et al., 2013). Recently, the chromatin loops induced by CTCF have not only been shown to play a role in latent genome organization but can also impact RTA-recruitment to RREs during lytic induction, including those associated with PAN and K12 transcripts (Kang et al., 2013; Campbell et al., 2018). Such transcriptional activity could explain the abundance of latent T0.7 transcripts, both in infected endothelial cells and KS lesions; the DRs may present an active chromatin locus for transcription that 'poises' the virus for lytic reactivation (Bruce et al., 2017; Rose et al., 2018; Campbell et al., 2018). By disrupting the DRs through either deletion or alternatively coded nucleotide sequences, as was done for the ΔKapBC, ΔKapB, and ΔKapC viruses in this study, the latent transcriptional activity could have been

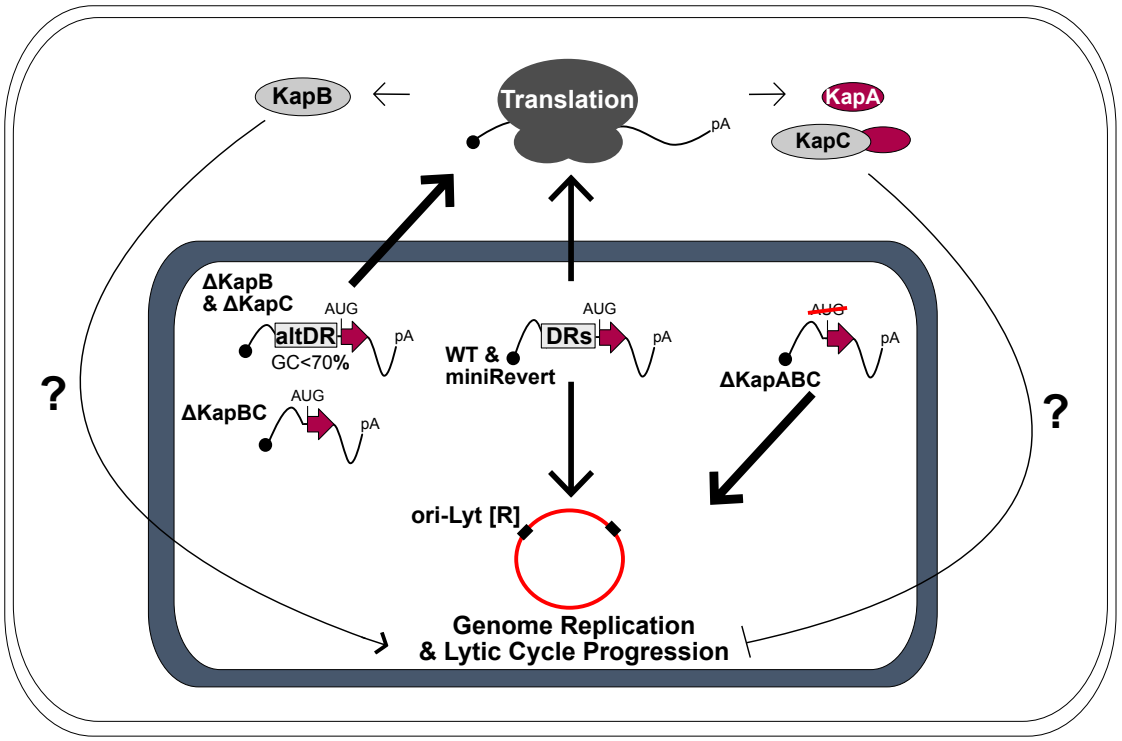

Figure 4.1: Proposed roles for kaposin in the lytic virus life cycle. Diagram depicting the possible roles for kaposin during the lytic virus life cycle, both at the RNA and protein level. This model proposes a role for both the kaposin transcript and translated proteins; while the wild-type (WT) and mini-revertant sequences can provide both RNA and protein functions, mutagenesis of the kaposin locus may alter the translation potential, thus influencing RNA activity. The role of kaposin RNA is hypothesized to act as a scaffold for the recruitment of K-bZIP and core replication machinery to the ori-Lyt for lytic genome replication. While it is still unclear what role each of the kaposin proteins plays in the lytic cycle, my results suggest that K12-containing proteins, KapA and KapC may negatively influence lytic cycle progression, while KapB may act to promote it. This could be mediated by recruitment of cellular transcription factors or activation of signaling cascades, as previously published, or could be mediated by interactions with other viral proteins.

disrupted, thus not only affecting latent phenotypes, but also the progression through the lytic cycle. This theory, however, does not match phenotypes observed for the ΔKapABC mutant, which has no DRs yet appears to proceed through the lytic cycle at an increased rate.

Clearly, consideration of the GC-rich component of the kaposin locus alone does not account for the differences observed for the kaposin mutants. As suggested by Wang et al. (2006), it is possible that generation of a specific transcript originating from the ori-Lyt permits proper replicative function. This is evidenced by recent work conducted with the T1.4 RNA, which originates from ori-Lyt [L] and similarly contains a GC-rich region and a small C-terminal ORF like the kaposin transcript (Wang et al., 2006). T1.4 was found to be essential for ori-Lyt function by forming an RNA-DNA complex that facilitated the binding of K-bZIP to the ori-Lyt DNA (Liu et al., 2018). Studies from EBV have found similar RNA-DNA interactions that may be mediated by GC-rich regions. The EBV BHLF1 RNA, which is similarly transcribed at the ori-Lyt, was found to be required for genome replication, however the AUG start codon for the BHLF1 ORF was dispensable (Rennekamp et al., 2011). This observation appears to match my data; reduction of the DR GC-content for both the ΔKapB and ΔKapC viruses or complete deletion of the DRs for the ΔKapBC virus was correlated with a deficiency in lytic cycle progression. This RNA-DNA interaction at the ori-Lyt could be mediated by RNA structure; the likelihood of higher-order G-quadruplex structures within the GC-rich regions of the transcript could be involved (Madireddy et al., 2016; Liu et al., 2018). Given this information, future work with the BAC16 mutant viruses should investigate the K-bZIP- and DNA-binding affinity of the K12 RNA-transcripts generated during the lytic cycle. Furthermore, the effect of G-

quadruplex stabilizing compounds on these interactions would be a valuable piece of data toward generating a potential mechanism for defects in lytic cycle progression as a result of kaposin mutagenesis (Madireddy et al., 2016).

Interestingly, removal of the DRs in combination with removal of the K12 AUG start codon, as in the ΔKapABC virus, significantly improved lytic cycle outcomes. This observation is difficult to reconcile with the above model, but may be due to an important balance between transcription and translation of the K12 RNA; while the transcript may predominantly function as an RNA during the lytic cycle, altering the translation potential of the transcript may indirectly abolish this effect. The role of RNA function in KSHV infection has been an important area of research; the abundant transcription of PAN RNA, a polyadenylated lncRNA, has been shown to activate KSHV and cellular gene expression, while also acting as a scaffold to retain unspliced viral transcripts in the nucleus (reviewed in Rossetto et al., 2014; Vallery et al., 2018). It is plausible that the kaposin RNA transcript may also have a role in infection; by re-insertion of the AUG translation initiation codon or alteration of the DR-coding content, the nucleotide sequence may have been skewed to promote translation, thus reducing the RNA functional activity. This theory could be addressed by *trans*-complementation assays in which specific plasmids designed to express kaposin transcripts either lacking or containing translation initiation codons are supplemented back into the kaposin-mutant KSHV-infected cells during both latent and lytic life cycles in order to rescue phenotypic deficiencies. Such a rescue would present evidentiary support for the importance of DRs as a *cis*-signal for RNA function. Alternatively, a *trans*-complementation assay in which transcription of a kaposin RNA lacking GC-rich repeat regions yet still maintaining translation competency would be

expected to abrogate lytic cycle progression similar to ΔKapB, ΔKapC, and ΔKapBC viruses due to defective RNA function and upregulated protein translation. However, this result would be conditional on the fact that a *cis*-generated transcript to the ori-Lyt and KSHV genome is not required for proper replicative function, a theory that still remains to be validated for the kaposin locus.

4.8 Concluding Remarks

The complexity of the kaposin locus stems not only from its versatile translation potential but also an assortment of *cis*-regulatory elements that have various roles in both the latent and lytic viral life cycles of KSHV. The coordinated efforts of cellular and viral proteins in both states of infection are necessary for KSHV to subvert its host, reprogram normal cell function, and maintain tumour progression.

In this thesis, I provide the first characterization of kaposin gene function by mutagenesis in the context of KSHV-infected cells. This work involved the construction of a novel library of kaposin deletion-mutant recombinant viruses by recombineering of the BAC16 viral clone. This mutagenesis targeted the translation potential of the kaposin transcript in order to generate viruses that are deficient in individual kaposin proteins. I used a unique recoding strategy to specifically design nucleotide sequences that allowed me to eliminate one protein at a time from a coding region with multiple ORFs. My preliminary analysis of entry and latency establishment showed that while all kaposin-mutant viruses are capable of entering and expressing latent viral genes, some mutations cause the virus to lose its ability to induce endothelial cell spindling, a hallmark of KS lesion cells. Furthermore, deletion of KapB and KapC, but not in combination with KapA

deletion, resulted in impaired lytic viral gene expression, genome replication, and progeny virus production.

This work led me to hypothesize novel roles for the kaposin transcript. Not only can the transcript be used to translate multiple proteins that act in cooperation with cellular and viral genes to elicit phenotypic changes to KSHV-infected cells during latency, but also as an important element for lytic cycle progression. While more research into the details of kaposin protein cooperativity and its function as an RNA that promotes genome replication are necessary, this work identifies the kaposin locus as an important node of control for the virus to regulate both latent and lytic virus life cycles toward the development of cancer.

REFERENCES

Anders, P.M., Zhang, Z., Bhende, P.M., Giffin, L., & Damania, B. (2016). The KSHV K1 protein modulates AMPK function to enhance cell survival. *PLoS Pathog.*, *12*(11), e1005985.

Aneja, K.K. & Yuan, Y. (2017). Reactivation and lytic replication of Kaposi's sarcoma-associated herpesvirus: an update. *Front. Microbiol., 8*, 613. doi: 10.3389/fmicb.2017.00613.

Antman, K. & Chang, Y. (2000). Kaposi's sarcoma. *N.Engl. J. Med., 342*, 1027-1038.

Arens, M., Swierkosz, E., & Dilworth, V. (1988). Effects of sonication and centrifugation of clinical specimens on the recovery of herpes simplex virus. *Diagn. Microbiol. Infect. Dis., 11*(3), 137-143.

Arias, C. Weisburd, B., Stern-Ginossar, N., Mercier, A., Madrid, A.S., Bellare, P., … & Ganem, D. (2014). KSHV 2.0: a comprehensive annotation of the Kaposi's sarcoma-associated herpesvirus genome using next-generation sequencing reveals novel genomic and functional features. *PLoS Pathog., 10*(1), e1003847.

Asahi-Ozaki, Y., Sato, Y., Kanno, T., Sata, T., & Katano, H. (2006). Quantitative analysis of Kaposi's sarcoma-associated herpesvirus (KSHV) in KSHV-associated diseases. *J. Infect. Dis., 193*(6), 773-782.

AuCoin, D.P., Colletti, K.S., Xu, Y., Cei, S.A., & Pari, G.S. (2002). Kaposi's sarcoma-associated herpesvirus (human herpesvirus 8) contains two functional lytic origins of dna replication. *J. Virol.*, *76*(15), 7890–7896.

AuCoin, D.P., Colletti, K.S., Cei, S.A., Papousková, I., Tarrant, M., & Pari, G. S. (2004). Amplification of the Kaposi's sarcoma-associated herpesvirus/human herpesvirus 8 lytic origin of DNA replication is dependent upon a cis-acting AT-rich region and an ORF50 response element and the trans-acting factors ORF50 (K-Rta) and K8 (K-bZIP). *Virology*, *318*(2), 542–555.

Bais, C., Van Geelen, A., Eroles, P., Mutlu, A., Chiozzini, C., Dias, S., … & Mesri, E.A. (2003). Kaposi's sarcoma associated herpesvirus G protein-coupled receptor immortalizes human endothelial cells by activation of the VEGF receptor-2/ KDR. *Cancer Cell, 3*(2), 131-143.

Ballestas, M.E., Chatis, P.A., & Kaye, K.M. (1999). Efficient persistence of extrachromosomal KSHV DNA mediated by latency-associated nuclear antigen. *Science, 284*, 641-644.

Ballestas, M.E. & Kaye, K.M. (2001). Kaposi's sarcoma-associated herpesvirus latency-associated nuclear antigen 1 mediates episome persistence through cis-acting terminal repeat (TR) sequence and specifically binds TR DNA. *J. Virol., 75*(7), 3250-3258.

Ballestas, M.E. & Kaye, K.M. (2011). The latency-associated nuclear antigen, a multifunctional protein central to Kaposi's sarcoma-associated herpesvirus latency. *Future Microbiol.*, *6*(12), 1399-413.

Ballon, G., Chen, K., Perez, R., Tam, W., & Cesarman, E. (2011). Kaposi sarcoma herpesvirus (KSHV) vFLIP oncoprotein induces B cell transdifferentiation and tumorigenesis in mice. *J. Clin. Invest.*, *121*(3), 1141-53.

Ballon, G., Akar, G., & Cesarman, E. (2015). Systemic expression of Kaposi sarcoma herpesvirus (KSHV) Vflip in endothelial cells leads to a profound proinflammatory phenotype and myeloid lineage remodeling in vivo. *PLoS pathogens*, *11*(1), e1004581.

Bartel, D.P. (2004). MicroRNAs: genomics, biogenesis, mechanism, and function. *Cell, 116*(2), 281-297.

Bauer, D.W., Huffman, J.B., Homa, F.L., & Evilevitch, A. (2013). Herpes virus genome, the pressure is on. *J. Am. Chem. Soc.*, *135*(30), 11216-11221.

Bechtel, J.T., Liang, Y., Hvidding, J., & Ganem, D. (2003). Host range of Kaposi's sarcoma-associated herpesvirus in cultured cells. *J. Virol., 77*(11), 6474-6481.

Bechtel, J.T., Winant, R.C., & Ganem, D. (2005). Host and viral proteins in the virion of Kaposi's sarcoma-associated herpesvirus. *J. Virol., 79*(8), 4952-4964.

Beckstead, B.H., Wood, G.S., & Fletcher, V. (1985). Evidence for the origin of Kaposi's sarcoma from lymphatic endothelium. *Am. J. Pathol., 119*(2), 294-300.

Bergson, S., Kalt, I., Itzhak, I., Brulois, K.F., Jung, J.U., & Sarid, R. (2014). Fluorescent tagging and cellular distribution of the Kaposi's sarcoma-associated herpesvirus ORF45 tegument protein. *J. Virol., 88*(21), 12839-12852.

Bergson, S., Itzhak, I., Wasserman, T., Gelgor, A., Kalt, I., & Sarid, R. (2016) The Kaposi's-sarcoma-associated herpesvirus orf35 gene product is required for efficient lytic virus reactivation. *Virology, 499*, 91-98.

Bermek, O., Willcox, S., & Griffith, J.D. (2014). DNA replication catalyzed by herpes simplex virus type 1 proteins reveals trombone loops at the fork. *J. Biol. Chem.*, *290*(5), 2539-45.

Bhutani, M., Polizzotto, M.N., Uldrick, T.S., & Yarchoan, R. (2015). KSHV-associated malignancies: epidemiology, pathogenesis, and advances in treatment. *Semin. Oncol., 42*(2), 223-246.

Brulois, K.F., Chang, H., Lee, A.S., Ensser, A., Wong, L.Y., Toth, Z., … & Jung, J.U. (2012). Construction and manipulation of a new Kaposi's sarcoma-associated herpesvirus bacterial artificial chromosome clone. *J. Virol.*, *86*(18), 9708-9720.

Bzymek, M. & Lovett, S.T. (2001). Instability of repetitive DNA sequences: the role of replication in multiple mechanisms. *Proc. Natl. Acad. Sci. USA, 98*(15), 8319-8325.

Cai, X., Shihua, L., Zhihong, Z., Gonzalez, C.M., Blossom, D., & Cullen, B.R. (2005). Kaposi's sarcoma-associated herpesvirus expresses an array of viral microRNAs in latently infected cells. *Proc. Natl. Acad. Sci. U. S. A.*, *102*(15), 181–216.

Campadelli, G., Brandimarti, R., Lazzaro, C.D., Ward, P.L., Roizman, B., & Torrisi, M.R. (1993). Fragmentation and dispersal of Golgi proteins and redistribution of glycoproteins and glycolipids processed through the Golgi apparatus after infection with herpes simplex virus 1. *Proc. Natl. Acad. Sci. U. S. A.*, *90*(7), 2798-2802.

Campbell, M. & Izumiya, Y. (2012). Post-translational modifications of Kaposi's sarcoma-associated herpesvirus regulatory proteins - SUMO and KSHV. *Front. Microbiol.*, *3*, 31.

Campbell, M., Watanabe, T., Nakano, K., Davis, R.R., Lyu, Y., Tepper, C.G., … & Izumiya, Y. (2018). KSHV episomes reveal dynamic chromatin loop formation with domain-specific gene regulation. *Nat. Commun.*, *9*(1), 49.

Cannon, J.S., Ciufo, D., Hawkins, A.L., Griffin, C.A., Borowitz, M.J., Hayward, G.S., & Ambinder, R. F. (2000). A new primary effusion lymphoma-derived cell line yields a highly infectious Kaposi's sarcoma herpesvirus-containing supernatant. *J. Virol.*, *74*(21), 10187-10193.

Centers for Disease Control. (1981). Kaposi's sarcoma and Pheumocystis pneumonia among homosexual men – New York City and California. *MMWR Morb. Mortal. Wkly Rep., 30*, 305-308.

Cesarman, E., Chang, Y., Moore, P.S., Said, J.W., & Knowles, D.M. (1995). Kaposi's sarcoma-associated herpesvirus-like DNA sequences in AIDS-related body cavity-based lymphomas. *N. Eng. J. Med., 332*, 1186-1191.

Cesarman, E., Moore, P.S., Rao, P., Inghirami, G., Knowles, D.M., & Chang, Y. (1995b). In vitro establishment and characterization of two acquired immunodeficiency syndrome-related lymphoma cell lines (BC-1 and BC-2) containing Kaposi's sarcoma-associated herpesvirus-like (KSHV) DNA sequences. *Blood, 86*(7), 2708-2714.

Cesarman, E. (2014). Gammaherpesviruses and lymphoproliferative disorders. *Annu. Rev. Pathol. 9*, 349–372.

Chandriani, S., & Ganem, D. (2010). Array-based transcript profiling and limiting-dilution reverse transcription-PCR analysis identify additional latent genes in Kaposi's sarcoma-associated herpesvirus. *J. Virol.*, *84*(11), 5565-5573.

Chang, H.C., Hsieh, T.H., Lee, Y.W., Tsai, C.F., Tsai, Y.N., Cheng, C.C., & Wang, H.W. (2016). c-Myc and viral cofactor kaposin B co-operate to elicit angiogenesis through modulating miRNome traits of endothelial cells. *BMC Syst. Biol.*, *10 Suppl 1*(Suppl 1), 1. doi:10.1186/s12918-015-0242-3

Chang, P.J., Shedd, D., Gradoville, L., Cho, M.S., Chen, L.W., Chang, J., & Miller, G. (2002). Open reading frame 50 protein of Kaposi's sarcoma-associated herpesvirus directly activates the viral PAN and K12 genes by binding to related response elements. *J. Virol., 76*(7), 3168-3178.

Chen, C.Y. & Shyu, A.B. (1995). AU-rich elements: characterization and importance in mRNA degradation. *Trends Biochem. Sci., 20*(11), 465-470.

Chen, J., Ueda, K., Sakakibara, S., Okuno, T., Parravicini, C., Corbellino, M., & Yamanishi, K. (2001). Activation of latent Kaposi's sarcoma-associated herpesvirus by demethylation of the promoter of the lytic transactivator. *Proc. Natl. Acad. Sci. USA, 98*(7), 4119-4124.

Chen, D., Sandford, G., & Nicholas, J. (2009). Intracellular signaling mechanisms and activities of human herpesvirus 8 interleukin-6. *J. Virol., 83*(2), 722-733.

Child, E.S. & Mann, D.J. (2001). Novel properties of the cyclin encoded by human herpesvirus 8 that facilitate exit from quiescence. *Oncogene, 20*(26), 3311-3322.

Chiu, Y.F., Sugden, A.U., Fox, K., Hayes, M., & Sugden, B. (2017). Kaposi's sarcoma-associated herpesvirus stably clusters its genomes across generations to maintain itself extrachromosomally. *J. Cell Biol.*, *216*(9), 2745-2758.

Choi, Y.B, & Nicholas, J. (2008). Autocrine and paracrine promotion of cell survival and virus replication by human herpesvirus 8 chemokines. *J. Virol., 82*(13), 6501-6513.

Ciufo, D.M., Cannon, J.S., Poole, L.J., Wu, F.Y., Murray, P., Ambinder, R.F., & Hayward, G.S. (2001). Spindle cell conversion by Kaposi's sarcoma-associated herpesvirus: formation of colonies and plaques with mixed lytic and latent gene expression in infected primary dermal microvascular endothelial cells cultures. *J. Virol., 75*(12), 5614-5626.

Corcoran, J.A., Johnston, B.P., & McCormick, C. (2015). Viral activation of MK2-hsp27-p115RhoGEF-RhoA signaling axis causes cytoskeletal rearrangements, p-body disruption and ARE-mRNA stabilization. *PLoS Pathog.*, *11*(1), e1004597.

Cotter 2nd, M.A. & Robertson, E.S. (1999). The latency-associated nuclear antigen tethers the Kaposi's sarcoma-associated herpesvirus genome to host chromosomes in body cavity-based lymphoma cells. *Virology*, *264*(2), 254-264.

Dai, X. & Zhou, Z.H. (2014). Purification of herpesvirus virions and capsids. *Bio Protoc., 5(*15), e1193.

Dai, X., Gong, D., Lim, H., Jih, J., Wu, T.T., Sun, R., & Zhou, Z.H. (2018). Structure and mutagenesis reveal essential capsid protein interactions for KSHV replication. *Nature*, *553*(7689), 521-525.

Davis, D.A., Naiman, N.E., Wang, V., Shrestha, P., Haque, M., Hu, D., … Yarchoan, R. (2015). Identification of caspase cleavage sites in KSHV latency-associated nuclear antigen and their effects on caspase related host defense responses. *PLoS Pathog., 11*(7), e1005064.

Deaton, A.M., & Bird, A. (2011). CpG islands and the regulation of transcription. *Genes Dev.*, *25*(10), 1010-1022.

Deiss, L.P. & Frenkel, N. (1986). Herpes simplex virus amplicon: cleavage of concatemeric DNA is linked to packaging and involves amplification of terminally reiterated a sequence. *J. Virol., 57*(3), 933-941.

Deng, J.H., Zhang, Y.J., Wang, X.P., & Gao, S.J. (2004). Lytic replication-defective Kaposi's sarcoma-associated herpesvirus: potential role in infection and malignant transformation. *J. Virol.*, *78*(20), 11108-11120.

Deng, B., O'Connor, C. M., Kedes, D. H., & Zhou, Z. H. (2007). Direct visualization of the putative portal in the Kaposi's sarcoma-associated herpesvirus capsid by cryoelectron tomography. *J. Virol.*, *81*(7), 3640–3644.

Dheekollu, J., Chen, H.S., Kaye, K.M., & Lieberman, P.M. (2013). Timeless-dependent DNA replication-coupled recombination promotes Kaposi's sarcoma-associated herpesvirus episome maintenance and terminal repeat stability. *J Virol., 87*(7), 3699-3709.

Dittmer, D., Lagunoff, M., Renne, R., Staskus, K., Haase, A., & Ganem, D. (1998). A cluster of latently expressed genes in Kaposi's sarcoma-associated herpesvirus. *J. Virol*, *72*(10), 8309–8315.

Dong S., Forrest J.C., Liang X. (2017) Murine gammaherpesvirus 68: a small animal model for gammaherpesvirus-associated diseases. In Q.Cai, Z. Yuan, & K. Lan (Eds), *Infectious Agents Associated Cancers: Epidemiology and Molecular Biology.* Advances in Experimental Medicine and Biology, vol 1018. Springer, Singapore. https://doi.org/10.1007/978-981-10-5765-6_14

Douglas, J.L., Gustin, J.K., Moses, A.V., Dezube, B.J., & Pantanowitz, L. (2010). Kaposi Sarcoma Pathogenesis: A Triad of Viral Infection, Oncogenesis and Chronic Inflammation. *Transl. Biomed.*, *1*(2), 172.

Du, M.Q., Liu, H., Diss, T.C, Ye, H., Hamoudi, R.A., Dupin, N., … & Isaacson, P.G. (2001). Kaposi sarcoma-associated herpesvirus infects monotypic (IgM lambda) but polyclonal naïve B cells in Castleman disease and associated lymphoproliferative disorders. *Blood, 97*(7), 2130-2136.

Duprez, R., Lacoste, V., Brière, J., Couppié, P., Frances, C., Sainte-Marie, D., … & Gessain, A. (2007). Evidence for a multiclonal origin of multicentric advanced lesions of Kaposi sarcoma. *J. Natl. Cancer Inst., 99*(14), 1086-1094.

Ensoli, B. & Stürzl, M. (1998). Kaposi's sarcoma: a result of the interplay among inflammatory cytokines, angiogenic factors and viral agents. *Cytokine Growth Factor Rev., 9*(1), 63–83.

Fay, N. & Panté, N. (2015). Nuclear entry of DNA viruses. *Front. Microbiol., 6*, 467.

Field, N., Low, W., Daniels, M., Howell, S., Daviet, L., Boshoff, C., & Collins, M. (2003). KSHV vFLIP binds to IKK-gamma to activate IKK. *J. Cell Sci., 116*(pt18), 3721-3728.

Forte, E., Raja, A.N., Shamulailatpam, P., Manzano, M., Schipma, M.J., Casey, J.L., & Gottwen, E. (2015). MicroRNA-mediated transformation by the Kaposi's sarcoma-associated herpesvirus kaposin locus. *J. Virol., 89*(4), 2333-2341.

Friborg, J., Kong, W.P., Flowers, C.C., Flowers, S.L., Sun, Y., Foreman, K.E., … & Nabel, G.J. (1998). Distinct biology of Kaposi's sarcoma-associated herpesvirus from primary lesions and body cavity lymphomas. *J. Virol., 72*(12), 10073-10082.

Friedman-Kien, A.E. (1981). Disseminated Kaposi's sarcoma syndrome in young homosexual men. *J. Am. Acad. Dermatol., 5*(4), 468-471.

Full, F., Jungnickl, D., Reuter, N., Bogner, E., Brulois, K., Scholz, B., … Ensser, A. (2014). Kaposi's sarcoma associated herpesvirus tegument protein ORF75 is essential for viral lytic replication and plays a critical role in the antagonization of ND10-instituted intrinsic immunity. *PLoS Pathog.*, *10*(1), e1003863.

Gandy, S.Z., Liinnstaedt, S.D., Muralidhar, S., Cashman, K.A., Rosenthal, L.J., & Casey, J.L. (2007). RNA editing of the human herpesvirus 8 kaposin transcript eliminates its transforming activity and is induced during lytic replication. *J. Virol., 81*(24), 13544-13551.

Gallo, A., Lampe, M., Günther, T., & Brune, W. (2017). The viral Bcl-2 homologs of Kaposi's sarcoma-associated herpesvirus and rhesus rhadinovirus share an essential role for viral replication. *J. Virol., 91*(6), e01875-16.

Ganem, D. (2010). KSHV and the pathogenesis of Kaposi sarcoma: listening to human biology and medicine. *J. Clin. Invest., 120*(4), 939–949.

Gao, Y., Smith, P.R., Karran, L., Lu, Q.L., & Griffin, B.E. (1997). Induction of an exceptionally high-level, nontranslated, Epstein-Barr virus-encoded polyadenylated transcript in the Burkitt's lymphoma line Daudi. *J. Virol.*, *71*(1), 84-94.

Gao, X., Ikuta, K., Tajima, M., & Sairenj, T. (2001). 12-*O*-tetradecanoylphorbol-13-acetate induces Epstein–Barr virus reactivation via NF-κB and AP-1 as regulated by protein kinase C and mitogen-activated protein kinase. *Virology, 286*(1), 91-99.

Gardner, M.R., & Glaunsinger, B.A. (2018). Kaposi's sarcoma-associate herpesvirus orf68 is a DNA binding protein required for viral genome cleavage and packaging. *J. Virol., 92*(16), e00840-18.

Gay, P., Lecoq, D., Steinmetz, M., Berkelman, T., & Kado, C.I. (1985). Positive selection procedure for entrapment of insertion sequence elements in gram-negative bacteria. *J. Bacteriol., 164*(2), 918-921.

Giffin, L., & Damania, B. (2014). KSHV: pathways to tumorigenesis and persistent infection. *Adv. Virus Res., 88*, 111-159.

Gong, D., Wu, N.C., Xie, Y., Feng, J., Tong, L., Brulois, K.F., … & Wu, T.-T. (2014). Kaposi's sarcoma-associated herpesvirus ORF18 and ORF30 are essential for late gene expression during lytic replication. *J. Virol., 88*(19), 11369-11382.

Grinde, B. (2013). Herpesviruses: latency and reactivation – viral strategies and host response. *J. Oral Microbiol.*, *5*, 10.3402/jom.v5i0.22766. http://doi.org/10.3402/jom.v5i0.22766

Grossmann, C., Poodgrabinska, S., Skobe, M., & Ganem, D. (2006). Activation of NF-kappaB by the latent vFLIP gene of Kaposi's sarcoma-associated herpesvirus is required for the spindle shape of virus-infected endothelial cells and contributes to their proinflammatory phenotype. *J. Virol.*, *80*(14), 7179-85.

Grundhoff, A., & Ganem, D. (2003). The latency-associated nuclear antigen of Kaposi's sarcoma-associated herpesvirus permits replication of terminal repeat-containing plasmids. *J. Virol., 77*(4), 2779–2783.

Grundhoff, A., Sullivan, C.S., & Ganem, D. (2006). A combined computational and microarray-based approach identifies novel microRNAs encoded by human gamma-herpesviruses. *RNA*, *12*(5), 733–750.

Günther T. & Grundhoff A. (2010). The epigenetic landscape of latent Kaposi sarcoma-associated herpesvirus genomes. *PLoS Pathog., 6*(6), e1000935.

Guo, H., Shen, S., Wang, L., & Deng, H. (2010). Role of tegument proteins in herpesvirus assembly and egress. *Protein Cell*, 1(11): 987-998.

Han, Z. & Swaminathan, S. (2006). Kaposi's sarcoma-associated herpesvirus lytic gene ORF57 is essential for infectious virion production. *J. Virol., 80*(11),5251–5260.

Heldwein, E.E. & Krummenacher, C. (2008). Entry of herpesviruses into mammalian cells. *Cell. Mol. Life Sci., 65*, 1653-1668.

Herndier, B. & Ganem, D. (2001). The biology of Kaposi's sarcoma. *Cancer Treat Res.*, *104*, 89–126.

Homa, F.L. & Brown, J.C. (1997). Capsid assembly and DNA packaging in herpes simplex virus. *Rev. Med. Virol*., *7(2)*, 107-122.

Honess, R.W. & Roizman, B. (1974). Regulation of herpesvirus macromolecular synthesis I. Cascade regulation of the synthesis of three groups of viral proteins. *J. Virol., 14*(1)**,** 8-19.

Hong, Y.K., Harvey, N., Noh, Y.H., Schacht, V., Hirakawa, S., Detmar, M., & Oliver, G. (2002). Prox1 is a master control gene in the program specifying lymphatic endothelial cell fate. *Dev. Dyn., 225*(3), 351-357.

Hong, Y.K., Foreman, K., Shin, J.W., Hirakawa, S., Curry, C.L., Sage, D.R., … & Detmar, M. (2004). Lymphatic reprogramming of blood vascular endothelium by Kaposi sarcom-associated herpesvirus. *Nat. Genet., 36*(7), 683-685.

Hu, J., Garber, A.C., & Renne, R. (2002). The latency-associated nuclear antigen of Kaposi's sarcoma-associated herpesvirus supports latent DNA replication in dividin cells. *J. Virol., 76*(22), 11677-11687.

Hu, J., & Renne, R. (2005). Characterization of the minimal replicator of Kaposi's sarcoma-associated herpesvirus latent origin. *J. Virol.*, *79*(4), 2637-2642.

Jain, V., Plaisance-Bonstaff, K., Sangani, R., Lanier, C., Dolce, A., Hu, J., … Krueger, B. (2016). A toolbox for herpesvirus miRNA research: construction of a complete set of KSHV miRNA deletion mutants. *Viruses*, *8*(2), 54.

Järviluoma, A., Child, E.S., Sarek, G., Sirimongkolkasem, P., Peters, G., Ojala, P.M., & Mann, D. J. (2006). Phosphorylation of the cyclin-dependent kinase inhibitor p21Cip1 on serine 130 is essential for viral cyclin-mediated bypass of a p21Cip1-imposed G1 arrest. *Mol. Cell. Biol.*, *26*(6), 2430-40.

Jenner, R.G., Maillard, K., Cattini, N., Weiss, R.A., Boshoff, C., Wooster, R., & Kellam, P. (2003). Kaposi's sarcoma-associated herpesvirus-infected primary effusion lymphoma has a plasma cell gene expression profile. *Proc. Natl. Acad. Sci. USA, 100*, 10399–10404.

Johnson, D.C. & Baines, J.D. (2011). Herpesviruses remodel host membrane for virus egress. *Nat. Rev. Microbiol., 9*(5), 382-394.

Jones, T., Ramos da Silva, S., Bedolla, R., Ye, F., Zhou, F., & Gao, S.J. (2014). Viral cyclin promotes KSHV-induced cellular transformation and tumorigenesis by overriding contact inhibition. *Cell Cycle*, *13*(5), 845-58.

Kaaya, E.E., Parravicini, C., Ordonez, C., Gendelman, R., Berti, E., Gallo, R.C., & Biberfeld, P. (1995). Heterogeneity of spindle cells in Kaposi's sarcoma: comparison of cells in lesions and in culture. *J. Acquir. Immune Defic. Syndr. Hum. Retrovirol., 10*(3), 295–305.

Kaminer, B. & Murray, J.F. (1950). Sarcoma idiopathicum multiplex haemorrhagicum of Kaposi, with special reference to its incidence in the South African Negro, and two case reports. *S. Afr. J. Clin. Sci., 1*(1), 1-25.

Kang, H., Wiedmer, A., Yuan, Y., Robertson, E., & Lieberman, P.M. (2011). Coordination of KSHV latent and lytic gene control by CTCF-cohesin mediated chromosome conformation. *PLoS Pathog.*, *7*(8), e1002140.

Kang, H., Cho, H., Sung, G.H., & Lieberman, P.M. (2013). CTCF regulates Kaposi's sarcoma-associated herpesvirus latency transcription by nucleosome displacement and RNA polymerase programming. *J. Virol.*, *87*(3), 1789-1799.

Kaposi, M. (1872) Idiopathisches multiples Pigmentsarkom der Haut. *Arch Dermatol Syphilol, 4*, 265-273.

Kempkes, B., Pich, D., Zeidler, R., & Hammerschmidt, W. Immortalization of human primary B lymphocytes in vitro with DNA. *Proc. Natl. Acad. Sci. USA*, 92(13), 5875-5879.

King C. A. (2013). Kaposi's sarcoma-associated herpesvirus kaposin B induces unique monophosphorylation of STAT3 at serine 727 and MK2-mediated inactivation of the STAT3 transcriptional repressor TRIM28. *J. Virol.*, *87*(15), 8779-8791.

Klepp, O., Dahl, O., & Stenwig, J.T. (1978). Association of Kaposi's sarcoma and prior immunosuppressive therapy: a 5-year material of Kaposi's sarcoma in Norway. *Cancer, 42*(6), 2626-2630.

Kliche, S., Nagel, W., Kremmer, E., Atzler, C., Ege, A., Knorr, T., … & Hass, T. (2001). Signaling by human herpesvirus 8 kaposin A through direct membrane recruitment of cytohesin-1. *Mol. Cell., 7*(4), 833-843.

Krishnan, H.H., Naranatt, P.P., Smith, M.S., Zeng, L., Bloomer, C., & Chandran, B. (2004). Concurrent expression of latent and a limited number of lytic genes with immune modulation and antiapoptotic function by Kaposi's sarcoma-associated herpesvirus early during infection of primary endothelial and fibroblast cells and subsequent decline of lytic gene expression. *J. Virol.*, *78*(7), 3601-3620.

Kumar, B., & Chandran, B. (2016). KSHV entry and trafficking in target cells-hijacking of cell signal pathways, actin and membrane dynamics. *Viruses*, *8*(11), 305.

Labo N., Miley W., Benson C.A., Campbell T.B., & Whitby D. (2015). Epidemiology of Kaposi's sarcoma-associated herpesvirus in HIV-1-infected US persons in the era of combination antiretroviral therapy. *AIDS*, *29*, 1217–1225.

Lee, E.C., Yu, D., Martinez de Velasco, J., Tessarollo, L., Swing, D.A., Court, D.L., … & Copeland, N.G. (2001). A highly efficient Escherichia coli-based chromosome engineering system adapted for recombinogenic targeting and subcloning of BAC DNA. *Genomics, 73*(1), 56-65.

Lee, H. R., Doğanay, S., Chung, B., Toth, Z., Brulois, K., Lee, S., …& Jung, J.U. (2014). Kaposi's sarcoma-associated herpesvirus viral interferon regulatory factor 4 (vIRF4) targets expression of cellular IRF4 and the Myc gene to facilitate lytic replication. *J. Virol.*, *88*(4), 2183-2194.

Lefort, S., & Flamand, L. (2009). Kaposi's sarcoma-associated herpesvirus K-bZIP protein is necessary for lytic viral gene expression, DNA replication, and virion production in primary effusion lymphoma cell lines. *J. Virol.*, *83*(11), 5869-80.

Li, H., Komatsu, T., Dezube B.J., & Kaye, K.M. (2002). The Kaposi's sarcoma-associate herpesvirus K12 transcript from a primary effusion lymphoma contains complex repeat elements, is spliced, and initiates from a novel promoter. *J. Virol., 76*(23), 11880-11888.

Li, Q., Zhou, F., Ye, F., & Gao, S.J. (2008). Genetic disruption of KSHV major latent nuclear antigen LANA enhances viral lytic transcriptional program. *Virology, 379*(2), 234-244.

Liang, Y., Chang, J., Lynch, S.J., Lukac, D.M., & Ganem, D. (2002). The lytic switch protein of KSHV activates gene expression via functional interaction with RBP-Jkappa (CSL), the target of the Notch signaling pathway. *Genes Dev.*, *16*(15), 1977-1989.

Liang, Q., Chang, B., Lee, P., Brulois, K.F., Ge, J., Shi, M., … & Jung, J.U. (2015). Identification of the essential role of viral Bcl-2 for Kaposi's sarcoma-associated herpesvirus lytic replication. *J. Virol.*, *89*(10), 5308-5317.

Liang, Q., Wei, D., Chung, B., Brulois, K.F., Guo, C., Dong, S., … Jung, J.U. (2018). Novel role of vBcl2 in the virion assembly of Kaposi's sarcoma-associated herpesvirus. *J. Virol., 92*, e00914-17.

Lim, C., Seo, T., Jung, J., & Choe, J. Identification of a virus trans-acting regulatory element on the latent DNA replication of Kaposi's sarcoma-associated herpesvirus. *J. Gen. Virol., 85*(Pt 4), 843-855.

Livak, K.J. & Schmittgen, T.D. (2001). Analysis of relative gene expression data using real-time quantitative PCR and the $2^{-\Delta\Delta CT}$ method. *Methods, 25*(4), 402-408.

Liu, D., Wang, Y., & Yuan, Y. (2018). Kaposi's sarcoma-associated herpesvirus K8 is an RNA binding protein that regulates viral DNA replication in coordination with a noncoding RNA. *J. Virol., 92*(7), e02177-17.

Lu, F., Zhou, J., Wiedmer, A., Madden, K., Yuan, Y., & Lieberman, P.M. (2003). Chromatin remodeling of the Kaposi's sarcoma-associated herpesvirus ORF50 promoter correlates with reactivation from latency. *J. Virol., 77*(21), 11425-11435.

Madireddy, A., Purushothaman, P., Loosbroock, C.P., Robertson, E.S., Schildkraut, C.L., & Verma, S.C. (2016). G-quadruplex-interacting compounds alter latent DNA replication and episomal persistence of KSHV. *Nucleic Acids Res., 44*(8), 3675-3694.

Majerciak, V., Pripuzova, N., McCoy, J.P., Gao, S.J., & Zheng, Z.M. (2006). Targeted disruption of Kaposi's sarcoma-associated herpesvirus ORF57 in the viral genome is detrimental for the expression of ORF59, K8alpha, and K8.1 and the production of infectious virus. *J. Virol.*, *81*(3), 1062-71.

McCormick, C. & Ganem, D. (2005). The kaposin B protein of KSHV activates the p38/MK2 pathway and stabilize cytokoine mRNAs. *Science, 307*(5710), 739-741.

McCormick, C. & Ganem, D. (2006). Phosphorylation and function of the kaposin B direct repeats of Kaposi's sarcoma-associated herpesvirus. *J. Virol., 80*(12), 6165-6170.

McGregor A. (2003). Transposon and transposome mutagenesis of plasmids, cosmids, and BACs. In N. Casali & A. Preston (Eds), *E. coli Plasmid Vectors.* Methods in Molecular Biology, vol 235. Humana Press. https://doi.org/10.1385/1-59259-409-3:233

McHugh, D., Carduff, N., Barros, M.H.M, Rämer, P.C., Raykova, A., Murer, A., …& Münz, C. (2017). Persistent KSHV infection increases EBV-associated tumor formation in vivo via enhanced EBV lytic gene expression. *Cell Host Microbe, 22*(1), 61-73.

McKeehan, W. & Hardesty, B. (1969). The mechanism of cycloheximide inhibition of protein synthesis in rabbit reticulocytes. *Biochem. Biophys. Res. Commun., 36*(4), 625-630.

Miller, G., Heston, L., Grogan, E., Gradoville, L., Rigsby, M., Sun, R., … & Chang, Y. (1997). Selective switch between latency and lytic replication of Kaposi's sarcoma herpesvirus and Epstein-Barr virus in dually infected body cavity lymphoma cells. *J. Virol.*, *71*(1), 314-24.

Miranda-Saksena, M., Denes, C.E., Diefenbach, R.J., & Cunningham, A.L. (2018). Infection and transport of herpes simplex virus type 1 in neurons: role of the cytoskeleton. *Viruses, 10*(2), 92.

Mochizuki, H., Schwartz, J.P., Tanaka, K., Brady, R.O., & Reiser, J. (1998). High-titer human immunodeficiency virus type-1 based vector systems for gene delivery into nondividing cells. *J. Virol., 72*(11), 8873-8883.

Montaner, S., Sodhi, A., Molinolo, A., Bugge, T.H., Sawai, E.T., He, Y., … & Gutkindn, J.S. (2003). Endothelial infection with KSHV genes in vivo reveals that vGPCR initiates Kaposi's sarcomagenesis and can promote the tumorigenic potential of viral latent genes. *Cancer Cell., 3*(1), 23-26.

Muralidhar, S., Pumfery, A.M., Hassani, M., Sadaie, M.R., Kishishita, M., Brady, J.N., … & Rosenthal, L.J. (1998). Identification of kaposin (open reading frame K12) as a human herpesvirus 8 (Kaposi's sarcoma-associated herpesvirus) transforming gene. *J. Virol.*, *72*(6), 4980-4988.

Mutlu, A.D., Cavallin, L.E., Vincent, L., Chiozzini, C., Eroles, P., Duran, E.M., … Mesri, E.A. (2007). In vivo-restricted and reversible malignancy induced by human herpesvirus-8 KSHV: a cell and animal model of virally induced Kaposi's sarcoma. *Cancer Cell*, *11*(3), 245-258.

Myoung, J. & Ganem, D. (2011a). Generation of a doxycycline-inducible KSHV producer cell line of endothelial origin: maintenance of tight latency with efficient reactivation upon induction. *J. Virol. Methods*, *174*(1-2), 12-21.

Myoung, J. & Ganem, D. (2011b). Infection of lymphoblastoid cell lines by KSHV: critical role of cell-associated virus. *J. Virol., 85*(19), 9767-9777.

Nador, R.G., Cesarman, E., Chadburn, A., Dawson, D.B., Ansari, M.Q., Sald, J., & Knowles, D.M. (1996). Primary effusion lymphoma: a distinct clinicopathologic entity associated with the Kaposi's sarcoma-associated herpes virus. *Blood, 88*(2), 645-656.

Nakamura, H., Lu, M., Gwack, Y., Souvlis, J., Zeichner, S.L., & Jung, J.U. (2003). Global changes in Kaposi's sarcoma-associated virus gene expression patterns following expression of a tetracycline-inducible Rta transactivator. *J. Virol.*, *77*(7), 4205-4220.

Narkhede, M., Arora, S., & Ujjani, C. (2018). Primary effusion lymphoma: current perspectives. *Onco Targets Ther., 11*, 3747-3754.

Naranatt, P.P., Krishnan, H.H., Smith, M.S., & Chandran, B. (2005). Kaposi's sarcoma-associated herpesvirus modulates microtubule dynamics via RhoA-GTP-diaphanous 2 signaling and utilizes the dynein motors to deliver its DNA to the nucleus. *J. Virol.*, *79*, 1191–1206.

Nealon, K., Newcomb, W.W., Pray, T.R., Craik, C.S., Brown, J.C., & Kedes, D.H. (2001). Lytic replication of Kaposi's sarcoma-associated herpesvirus results in the formation of multiple capsid species: Isolation and molecular characterization of A, B, and C capsids from a gammaherpesvirus. *J. Virol.*, *75*(6), 2866–2878.

Newcomb, W.W. & Brown, J.C. (1991). Structure of the herpes simplex virus capsid: effects of extraction with guanidine hydrochloride and partial reconstitution of extracted capsids. *J. Virol., 65*(2), 613-620.

Newcomb, W.W., Homa, F.L., Thomsen, D.R., Booy, F.P., Trus, B.L., Steven, A.C., … Brown, J.C. (1996). Assembly of the herpes simplex virus capsid: Characterization of intermediates observed during cell-free capsid formation. *J. Mol. Biol.*, *263*(3), 432–446.

Newcomb, W.W., Thomsen, D.R., Homa, F.L., & Brown J.C. (2003). Assembly of the herpes simplex virus capsid: identification of soluble scaffold-portal complexes and their role in formation of portal-containing capsids. *J. Virol., 77*(18), 9862–9871.

Nickoloff, B.J., & Griffiths, C.E. (1989). The spindle-shaped cells in cutaneous Kaposi's sarcoma. Histologic simulators include factor XIIIa dermal dendrocytes. *Am. J. Pathol., 135*(5), 793-800.

Nii, S., Morgan, C., & Rose, H.M. (1968). Electron microscopy of herpes simplex virus. II. Sequence of development. *J. Virol., 2*(10), 517-536.

Nishimura, M., Watanabe, T., Yagi, S., Yamanaka, T., & Fujimuro, M. (2017). Kaposi's sarcoma-associated herpesvirus ORF34 is essential for late gene expression and virus production. *Sci. Rep., 7*(1), 329.

Nishizaka, Y. (1992). Intracellular signaling by hydrolysis of phospholipids and activation of protein kinase C. *Science, 258*(5082), 607-614.

Oksenhendler, E., Boutboul, D., Fajgenbaum, D., Mirouse, A., Fieschi, C., Malphettes, M., …& Galicier, L. (2018). The full spectrum of Castleman disease: 273 patients studied over 20 years. *Br. J. Haematol. 180*(2), 206–216.

Oksenhendler, E., Carcelain, G., Aoki, Y., Boulanger, E., Maillard, A., Clauvel, J.P., & Agbalika, F. (2000). High levels of human herpesvirus 8 viral load, human interleukin-6, interleukin-10, and C reactive protein correlate with exacerbation of multicentric castleman disease in HIV-infected patients. *Blood, 96*(6), 2069-2073.

Overby, L.R., Duff, R.G. & Mao, J.C. (1977). Antiviral potential of phosphonoacetic acid. *Ann. N.Y. Acad. Sci.*, *284*, 310-320.

Parravicini, C., Chandran, B., Corbellino, M., Berti, E., Paulli, M., Moore, P.S., & Chang, Y. (2000). Differential viral protein expression in Kaposi's sarcoma associated herpesvirus-infected diseases: Kaposi's sarcoma, primary effusion lymphoma, and multicentric Castleman's disease. Am. J. Pathol., 156(3), 743-749.

Pearce, M., Matsumura, S., & Wilson, A.C. (2005). Transcripts encoding K12, v-FLIP, v-Cyclin, and the microRNA cluster of Kaposi's sarcoma-associated herpesvirus originate from a common promoter. *J. Virol.,* 14457-14464.

Pellet, P.E. & Roizman, B. (2013). Herpesviridae. In B. Fields, D.M. Knipe, & P.M. Howley (Eds.), *Fields virology* (6th ed.). Philadelphia: Wolters Kluwer Health/Lippincott Williams & Wilkins.

Peng, C., Chen, J., Tang, W., Liu, C., & Chen, X. (2014). Kaposi's sarcoma-associated herpesvirus ORF6 gene is essential in viral lytic replication. *PloS One*, *9*(6), e99542.

Perkins, E.M., Anacker, D., Davis, A., Sankar, V., Ambinder, R.F., & Desai, P. (2008). Small capsid protein pORF65 is essential for assembly of Kaposi's sarcoma-associated herpesvirus capsids. *J. Virol., 82*(14), 7201-7211.

Pfeffer, S., Sewer, A., Lagos-Quintana, M., Sheridan, R., Sander, C., Grässer, F.A., … Tuschl, T. (2005). Identification of microRNAs of the herpesvirus family. *Nature Methods*, *2*(4), 269–276.

Picchio, G.R., Sabbe, R.E., Gulizia, R.J., McGrath, M., Herndier, B.G., & Mosier, D.E. (1997). The KSHV/HHV8-infected BCBL-1 lymphoma line causes tumors in SCID mice but fails to transmit virus to a human peripheral blood mononuclear cell graft. *Virology, 238*(1), 22-29.

Poffenberger, K.L., & Roizman, B. (1985). A noninverting genome of a viable herpes simplex virus 1: presence of head-to-tail linkages in packaged genomes and requirements for circularization after infection. *J. Virol.*, *53*(2), 587-95.

Poudyal, R., Renne, R., & Kladde, M.P. (2017). Epigenetic regulation of gammaherpesviruses: a focus on Kaposi's sarcoma-associated herpesvirus (KSHV/HHV-8). In W. Doerfler & J. Casadesús (Eds.), *Epigenetics of Infectious Diseases*. Epigenetics and Human Health. Springer, Cham. https://doi.org/10.1007/978-3-319-55021-3_2

Purdue, M.L., Cohen, J.C., Kemp, M.C., Randall, C.C., O'Callaghan, D.J. (1975). Characterization of three species of nucleocapsids of equine herpesvirus type-1 (EHV-1). *Virology, 64*(1), 187-204.

Purushothaman, P., Uppal, T., & Verma, S.C. (2015). Molecular biology of KSHV lytic reactivation. *Viruses, 7*(1), 116-153.

Purushothaman, P., Dabral, P., Gupta, N., Sarkar, R., & Verma, S. C. (2016). KSHV genome replication and maintenance. *Front. Microbiol.*, *7*(54), 1–14.

Rainbow, L., Platt, G.M., Simpson, G.R., Sarid, R., Gao, S.J., Stoiber, H., Herrington, C.S., Moore, P.S., … & Schulz, T.F. (1997). The 222- to 234-kilodalton latent nuclear protein (LNA) of Kaposi's sarcoma-associated herpesvirus (human herpesvirus 8) is encoded by orf73 and is a component of the latency-associated nuclear antigen. *J. Virol.*, *71*(8), 5915-5921.

Regezi, J.A., MacPhail, L.A., Daniels, T.E., Greenspan, J.S., Greenspan, D., Dodd, C.L., … & Hansen, L.S. (1993). Oral Kaposi's sarcoma: a 10-year retrospective histopathologic study. *J. Oral Pathol. Med., 22*(7): 292-297.

Renne, R., Zhong, W., Herndier, B., McGrath, M., Abbey, N., Kedes, D., & Ganem, D. (1996). Lytic growth of Kaposi's sarcoma-associated herpesvirus (human herpesvirus 8) in culture. *Nat. Med.*, *2*(3), 342–346.

Renne, R., Lagunoff, M., Zhong, W., & Ganem, D. (1996b). The size and conformation of Kaposi's sarcoma-associated herpesvirus (human herpesvirus 8) DNA in infected cells and virions. *J. Virol., 70*(11), 8151-8154.

Renne, R., Blackbourn, D., Whitby, D., Levy, J., & Ganem, D. (1998). Limited transmission of Kaposi's sarcoma-associated herpesvirus in cultured cells. *J. Virol.*, *72*(6), 5182-5188.

Renne, R., Barry, C., Dittmer, D., Compitello, N., Brown, P.O., & Ganem, D. (2001). Modulation of cellular and viral gene expression by the latency-associated nuclear antigen of Kaposi's sarcoma-associated herpesvirus. *J. Virol., 75*(1), 458-468.

Rennekamp, A.J., & Lieberman, P.M. (2010). Initiation of Epstein-Barr virus lytic replication requires transcription and the formation of a stable RNA-DNA hybrid molecule at OriLyt. *J. Virol.*, *85*(6), 2837-50.

Reuven, N.B., Staire, A.E., Myers, R.S., & Weller, S.K. (2003). The herpes simplex virus type 1 alkaline nuclease and single-stranded DNA binding protein mediate strand exchange in vitro. *J. Virol., 77*(13), 7425-7433.

Roizman, B., Knipe, D.M., & Whitley, R.J. (2013). Herpes simplex viruses. In B. Fields, D.M. Knipe, & P.M. Howley (Eds.), *Fields virology* (6th ed.). Philadelphia: Wolters Kluwer Health/Lippincott Williams & Wilkins.

Roller, R.J. & Baines, J.D. (2017). Herpesvirus nuclear egress. In K. Osterrieder (Ed), *Cell biology of herpes viruses*. Advances in anatomy, embryology and cell biology, vol 223. Springer, Cham.

Rossetto, C.C. & Pari, G.S. (2014). PAN's labyrinth: molecular biology of Kaposi's sarcoma-associated herpesvirus (KSHV) PAN RNA, a multifunctional long noncoding RNA. *Viruses, 6*(11), 4212-4226.

Russo, J.J., Bohenzky, R.A., Chien, M.C., Chen, J., Yan, M., Maddalena, D., … & Moore, P.S. (1996). Nucleotide sequence of the Kaposi sarcoma-associated herpesvirus (HHV8). *Proc. Natl. Acad. Sci. USA, 93*(25), 14862-14867.

Sadler, R., Wu, L., Forghani, B., Renne, R., Zhong, W., Herndier, B., & Ganem, D. (1999). A complex translational program generates multiple novel proteins from the latently expressed kaposin (K12) locus of Kaposi's sarcoma-associated herpesvirus. *J. Virol.*, *73*(7), 5722–5730.

Sakakibara, S., Ueda, K., Nishimura, K., Do, E., Ohsaki, E., Okuno, T., & Yamanishi, K. (2004). Accumulation of heterochromatin components on the terminal repeat sequence of Kaposi's sarcoma-associated herpesvirus mediated by the latency-assoociated nuclear antigen. *J. Virol., 78*(14), 7299-7310.

Samaniego, F., Markham, P.D., Gendelman, R., Gallo, R.C., & Ensoli, B. (1997). Inflammatory cytokines induce endothelial cells to produce and release basic fibroblast growth factor and to promote Kaposi's sarcoma-like lesions in nude mice. *J. Immunol., 158*(4), 1887-1894.

Sathish, N., Zhu, F.X., & Yuan, Y. (2009). Kaposi's sarcoma-associated herpesvirus ORF45 interacts with kinesin-2 transporting viral capsid-tegument complexes along microtubules. *PLoS Pathog., 5*(3), e1000332.

Sattler, C., Steer, B., & Adler, H. (2016). Multiple lytic origins of replication are required for optimal gammaherpesvirus fitness in vitro and in vivo. *PLoS Pathog.*, *12*(3), e1005510.

Schulz, T.F. & Chang, Y. (2007). KSHV gene expression and regulation. In A. Arvin, G. Campadelli-Fiume, E.Mocarski, et al. (Eds.), *Human herpesviruses: biology, therapy, and immunoprophylaxis*. Cambridge: Cambridge University Press.

Schwam, D.R., Luciano, R.L., Mahajan, S.S., Wong, L., & Wilson, A.C. (2000). Carboxy terminus of human herpesvirus 8 latency-associated nuclear antigen mediates dimerization, transcriptional repression, and targeting to nuclear bodies. *J. Virol.*, *74*(18), 8532-40.

Sharan, S.K., Thomason, L.C., Kuznetsov, S.G., & Court, D.L. (2009). Recombineering: a homologous recombination-based method of genetic engineering. *Nat. Protoc.*, *4*(2), 206-23.

Simonelli, C., Spina, M., Cinelli, R., Talamini, R., Tedeschi, R., Gloghini, A., … & Tirelli, U. Clinical features and outcome of primary effusion lymphoma in HIV-infected patients: a single-institution study. *J. Clin. Oncol., 21*(21), 3948-3954.

Skalsky, R.L., Hu, J., & Renne, R. (2007). Analysis of viral cis elements conferring Kaposi's sarcoma-associated herpesvirus episome partitioning and maintenance. *J. Virol.*, *81*(18), 9825-9837.

Skelding, K.A., Rostas, J.A., & Verrills, N.M. (2011). Controlling the cell cycle: the role of calcium/calmodulin-stimulated protein kinases I and II. *Cell Cycle, 10*(4), 631-639.

Soulier, J., Grollet, L, Oksenhendler, E., Cacoub, P., Cazals-Hatem, D., Babinet, P, … & Sigaux, F. (1995). Kaposi's sarcoma-associated herpesvirus-like DNA sequences in multicentric Castleman's disease. *Blood, 86*(4), 1276-1280.

Staskus, K. A., Zhong, W., Gebhard, K., Herndier, B., Wang, H., Renne, R., …& Haase, A.T. (1997). Kaposi's sarcoma-associated herpesvirus gene expression in endothelial (spindle) tumor cells. *J. Virol.*, *71*(1), 715-9.

Steinbrück, L., Gustems, M., Medele, S., Schulz, T.F., Lutter, D., & Hammerschmidt, W. (2015). K1 and K15 of Kaposi's Sarcoma-Associated Herpesvirus Are Partial Functional Homologues of Latent Membrane Protein 2A of Epstein-Barr Virus. *J. Virol.*, *89*(14), 7248-7261.

Stürzl, M., Gaus, D., Dirks, W.G., Ganem, D., & Jochmann, R. (2013). Kaposi's sarcoma-derived cell line SLK is not of endothelial origin, but is a contaminant from a known renal carcinoma cell line. *Int. J. Cancer, 132*(8), 1954-1958.

Sun, R., Lin, S.F., Gradoville, L., Yuan, Y., Zhu, F., & Miller, G. (1998). A viral gene that activates lytic cycle expression of Kaposi's sarcoma-associated herpesvirus. *Proc. Natl. Acad. Sci. USA, 95*(18), 10866-10871.

Sun, R., Lin, S.F., Staskus, K., Gradoville, L., Grogan, E., Haase, A., & Miller, G. (1999). Kinetics of Kaposi's sarcoma-associated herpesvirus gene expression. *J. Virol.*, *73*(3), 2232-42.

Taylor, J.F., Templeton, A.C., Vogel, C.L., Ziegler, J.L., & Kyalwazi, S.K. (1971). Kaposi's sarcoma in Uganda: a clinico-pathological study. *Int. J. Cancer, 8*, 122-135

Thakker, S., & Verma, S. C. (2016). Co-infections and pathogenesis of KSHV-associated malignancies. *Front. Microbiol.*, *7*, 151.

Thome, M., Schneider, P., Hofmann, K., Fickenscher, H., Meinl, E., Mattmann, C., … & Tschopp, J. Viral FLICE-inhibitory proteins (FLIPs) prevent apoptosis induced by death receptors. *Nature, 386*(6624), 517-521.

Tischer, B.K., von Einem, J., Kaufer, B., & Osterrieder, N. (2006). Two-step red-mediated recombination for versatile high-efficiency markerless DNA manipulation in Escherichia coli. *Biotechniques, 40*(2), 191-197.

Tomkowicz, B., Singh, S.P., Lai, D., Singh, A., Mahalingham, S., Joseph, J., … & Srinivasan, A. (2005). Mutational analysis reveals an essential role for the LXXLL motif in the transformation function of the human herpesvirus-8 oncoproten, kaposin. *DNA Cell Biol., 24*(1), 10-20.

Toth Z., Maglinte, D.T., Lee, S.H., Lee, H.R., Wong, L.Y., Brulois, K.F., … & Jung, J.U. (2010). Epigenetic analysis of KSHV latent and lytic genomes. *PLoS Pathog., 6*(7), e1001013.

Toth, Z., Papp, B., Brulois, K., Choi, Y.J., Gao, S.J., & Jung, J.U. (2016). LANA-mediated recruitment of host polycomb repressive complexes onto the KSHV genome during de novo infection. *PLoS Pathog.*, *12*(9), e1005878.

Trus, B.L., Heymann, J.B., Nealon, K., Cheng, N., Newcomb, W.W., Brown, J.C., … Steven, A.C. (2001). Capsid structure of Kaposi's sarcoma-associated herpesvirus, a gammaherpesvirus, compared to those of an alphaherpesvirus, herpes simplex virus type 1, and a betaherpesvirus, cytomegalovirus. *J. Virol.*, *75*(6), 2879–2890.

Ueda, Y., Hirai, S., Osada, S., Suzuki, A., Mizuno, K., & Ohno, S. (1996). Protein kinase C activates the MEK-ERK pathway in a manner independent of Ras and dependent on Raf. *J. Biol. Chem., 271*(38), 23512-23519.

Umbach, J.L. & Cullen, B.R. (2010). In-depth analysis of Kaposi's sarcoma-associated herpesvirus microRNA expression provides insights into the mammalian micro-RNA processing machinery. *J. Virol., 84*(2), 692-703.

Umene, K. (1999). Mechanism and application of genetic recombination in herpesviruses. *Rev. Med. Virol., 9*, 171-182.

Vallery, T.K., Withers, J.B., Andoh, J.A., & Steitz, J.A. (2018). Kaposi's sarcoma-associated herpesvirus mRNA accumulation in nuclear foci is influenced by viral DNA replication and viral noncoding polyadenylated nuclear RNA. *J. Virol., 92*(13), e00220-18.

Verschuren, E.W., Klefstrom, J., Evan, G.I., & Jones, N. (2002). The oncogenic potential of Kaposi's sarcoma-associated herpesvirus Cyclin is exposed by p53 loss in vitro and in vivo. *Cancer Cell, 2*(3), 229-241.

Vieira, J. & O'Hearn, P. (2004). Use of the red fluorescent protein as a marker of Kaposi's sarcoma-associated herpesvirus lytic gene expression. *Virology, 325*(2), 225-240.

Virgin 4th, H.W., Latreille, P., Wamsley, P., Hallsworth, K., Weck, K.E., Dal Canto, A.J., & Speck, S.H. (1997). Complete sequence and genomic analysis of murine gammaherpesvirus 68. *J. Virol.*, *71*(8), 5894-5904.

Wang, S., Liu, S., Wu, M.H., Geng, Y., & Wood, C. (2001). Identification of a cellular protein that interacts and synergizes with the RTA (ORF50) protein of Kaposi's sarcoma-associated herpesvirus in transcriptional activation. *J. Virol.*, *75*(24), 11961-11973.

Wang, S.E., Wu, F.Y., Yu, Y., & Hayward, G.S. (2003). CCAAT/enhancer-binding protein-alpha is induced during the early stages of Kaposi's sarcoma-associated herpesvirus (KSHV) lytic cycle reactivation and together with the KSHV replication and transcription activator (RTA) cooperatively stimulates the viral RTA, MTA, and PAN promoters. *J. Virol.*, *77*(17), 9590-9612.

Wang, Y., Li, H., Chan, M.Y., Zhu, F.X., David, M., Lukac, D.M., & Yuan, Y. (2004). Kaposi's sarcoma-associated herpesvirus ori-Lyt-dependent DNA replication: cis-acting requirements for replication and ori-Lyt-associated RNA transcription. *J. Virol.*, *78*(16), 8615–8629.

Wang, H.W., Trotter, M.W., Lagos, D., Bourboulia, D., Henderson, S., Mäkinen, T., … & Boshoff, S. (2004). Kaposi sarcoma herpesvirus-induced cellular reprogramming contributes to the lymphatic endothelial gene expression in Kaposi sarcoma. *Nat. Genet., 36*(7), 687-693.

Wang, Y., Tang, Q., Maul, G.G., & Yuan, Y. (2006). Kaposi's sarcoma-associated herpesvirus ori-Lyt-dependent DNA replication: dual role of replication and transcription activator. *J. Virol., 80*(24)**,** 12171-12186.

Wang, Y., Li, H., Tang, Q., Maul, G. G., & Yuan, Y. (2008). Kaposi's sarcoma-associated herpesvirus ori-Lyt-dependent DNA replication: involvement of host cellular factors. *J. Virol.*, *82*(6), 2867–2882.

Wang, L.X., Guobin, K., Pankaj, K., Wuxun, L., Yue, L., Zhou, Y., … & Wood, C. (2014). Humanized-BLT mouse model of Kaposi's sarcoma-associated herpesvirus infection. *Proc. Natl. Acad. Sci. USA, 111*(8), 3146-3151.

Warden, C., Tang, Q., & Zhu, H. (2010). Herpesvirus BACs: past, present, and future. *J. Biomed. Biotechnol., 2011*, 124595.

West, J.A., Wicks, M., Gregory, S.M., Chugh, P., Jacobs, S.R., Zhang, Z., … & Damania, B. (2014). An important role for mitochondrial antiviral signaling protein in the Kaposi's sarcoma-associated herpesvirus life cycle. *J. Virol.*, *88*(10), 5778-5787.

White, I.E. & Campbell, T.B. (2000). Quantitation of cell-free and cell-associated Kaposi's sarcoma-associated herpesvirus DNA by real-time PCR. *J. Clin. Microbiol.*, *38*(5): 1992-1995.

Wu, F.Y., Ahn, J.H., Alcendor, D.J., Jang, W.J., Xiao, J., Hayward, S. D., & Hayward, G. S. (2001). Origin-independent assembly of Kaposi's sarcoma-associated herpesvirus DNA replication compartments in transient cotransfection assays and association with the ORF-K8 protein and cellular PML. *J. Virol.*, *75*(3), 1487–1506.

Xie, J., Pan, H., Yoo, S., & Gao, S.J. (2005). Kaposi's sarcoma-associated herpesvirus induction of AP-1 and interleukin 6 during primary infection mediated by multiple mitogen-activated protein kinase pathways. *J. Virol.*, *79*(24), 15027-15037.

Xu, Y., Rodriguez-Huete, A., & Pari, G.S. (2006). Evaluation of the lytic origins of replication of Kaposi's sarcoma-associated virus/human herpesvirus 8 in the context of the viral genome. *J. Virol.*, *80*(19), 9905-9909.

Yakushko, Y., Hackmann, C., Günther, T., Rückert, J., Henke, M., Koste, L., … & Henke-Gendo, C. (2011). Kaposi's sarcoma-associated herpesvirus bacterial artificial chromosome contains a duplication of a long unique-region fragment within the terminal repeat region. *J. Virol.*, *85*(9), 4612-4617.

Ye, F., Lei, X., & Gao, S.J. (2011) Mechanisms of Kaposi's sarcoma-assciated herpesvirus latency and reactivatiooni. *Adv. Virol., 2011*, 193860.

Yoo, J., Kang, J., Lee, H.N., Aguilar, B., Kafka, D., Lee, S., … & Hong, Y.K. (2010). Kaposin-B enhances the PROX1 mRNA stability during lymphatic reprogramming of vascular endothelial cells by Kaposi's sarcoma herpes virus. *PLoS Pathog.*, *6*(8), e1001046.

Yu D., Ellis, H.M., Lee, E.C., Jenkins, N.A., Copeland, N.G., & Court, D.L. (2000). An efficient recombination system for chromosome engineering in Escherichia coli. *Proc. Natl. Acad. Sci. USA*, *97*(11), 5978-5983.

Zhang, Z. Chen, W., Sanders, M.K., Brulois, K.F., Dittmer, D.P., & Damania, B. (2016). The K1 protein of Kaposi's sarcoma-associated herpesvirus augments viral lytic replication. *J. Virol., 90*(17), 7657-7666.

Zhao, Y., Wang, S., & Zhu, J. (2010). A multi-step strategy for BAC recombineering of large DNA fragments. *Int. J. Biochem. Mol. Biol., 2*(3), 199-206.

Zhong, W., Wang, H., Herndier, B., & Ganem, D. (1996). Restricted expression of Kaposi sarcoma-associated herpesvirus (human herpesvirus 8) genes in Kaposi sarcoma. *Proc. Natl. Acad. Sci. USA, 93*(13), 6641-6646.

Zhu, F.X., King, S.M., Smith, E.J., Levy, D.E., & Yuan, Y. (2002). A Kaposi's sarcoma-associated herpesviral protein inhibits virus-mediated induction of type I interferon by blocking IRF-7 phosphorylation and nuclear accumulation. *Proc. Natl. Acad. Sci. USA, 99*(8)**,** 5573-5578.

Zhu, F.X. & Yuan, Y. (2003). The ORF45 protein of Kaposi's sarcoma-associate herpesvirus is associated with purified virions. *J. Virol., 77*(7), 4221-4230.

APPENDIX A: Supplementary Data

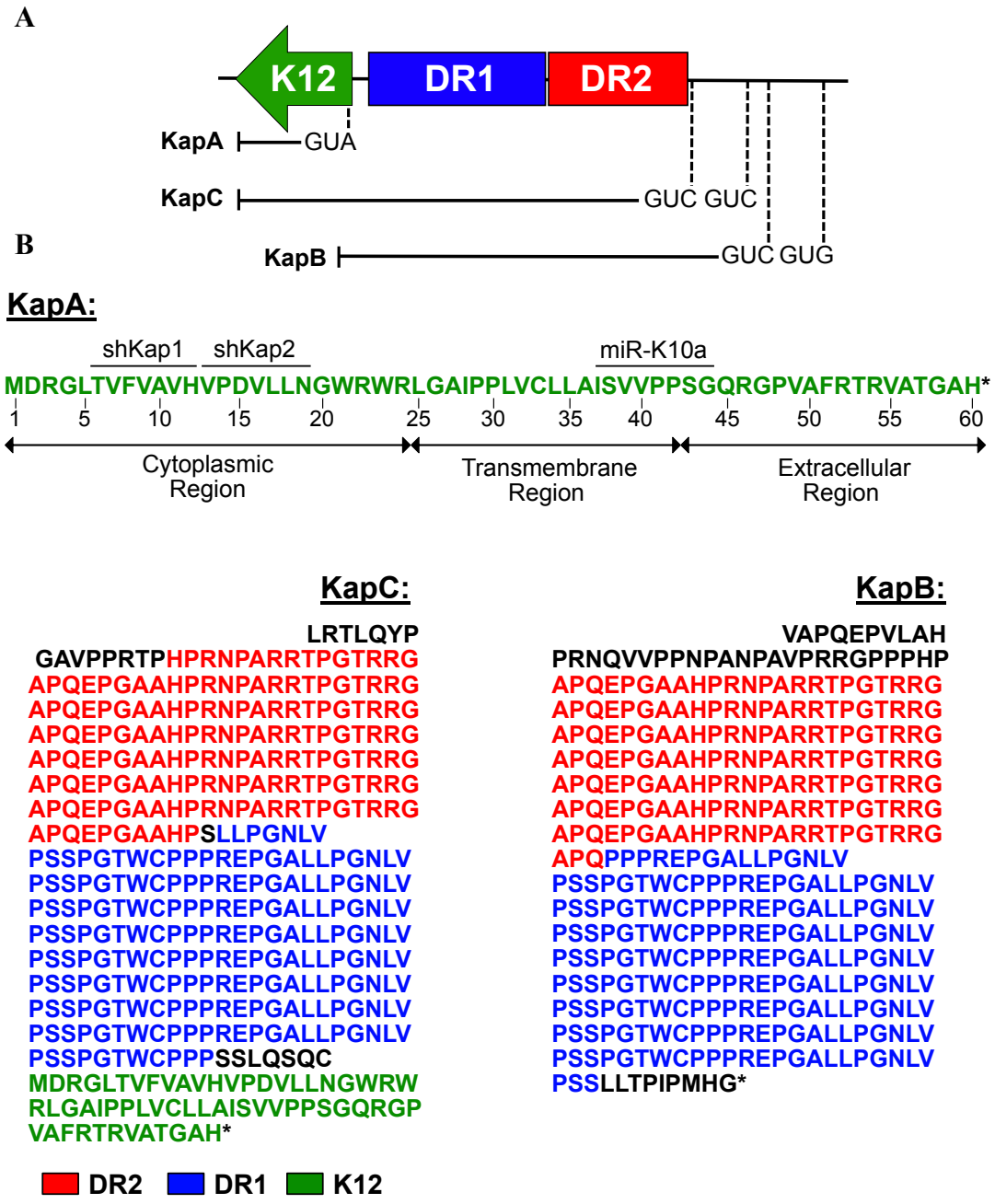

Figure A.1: Translation products of the kaposin locus. (A) Diagram depicting the putative translation initiation codons for the kaposin proteins, Kaposin A (KapA), B (KapB), and C (KapC). (B) Primary amino acid sequences are shown for the three kaposin proteins and their associated domains, direct repeat (DR) regions, DR2 (red), DR1 (blue), and K12 (green). Relative positions for the nucleotide sequences used to generate miR-K10a and the target/seed sequences for shRNAs, shKap1 and shKap2, are indicated. Adapted from Kliche et al., 2001.

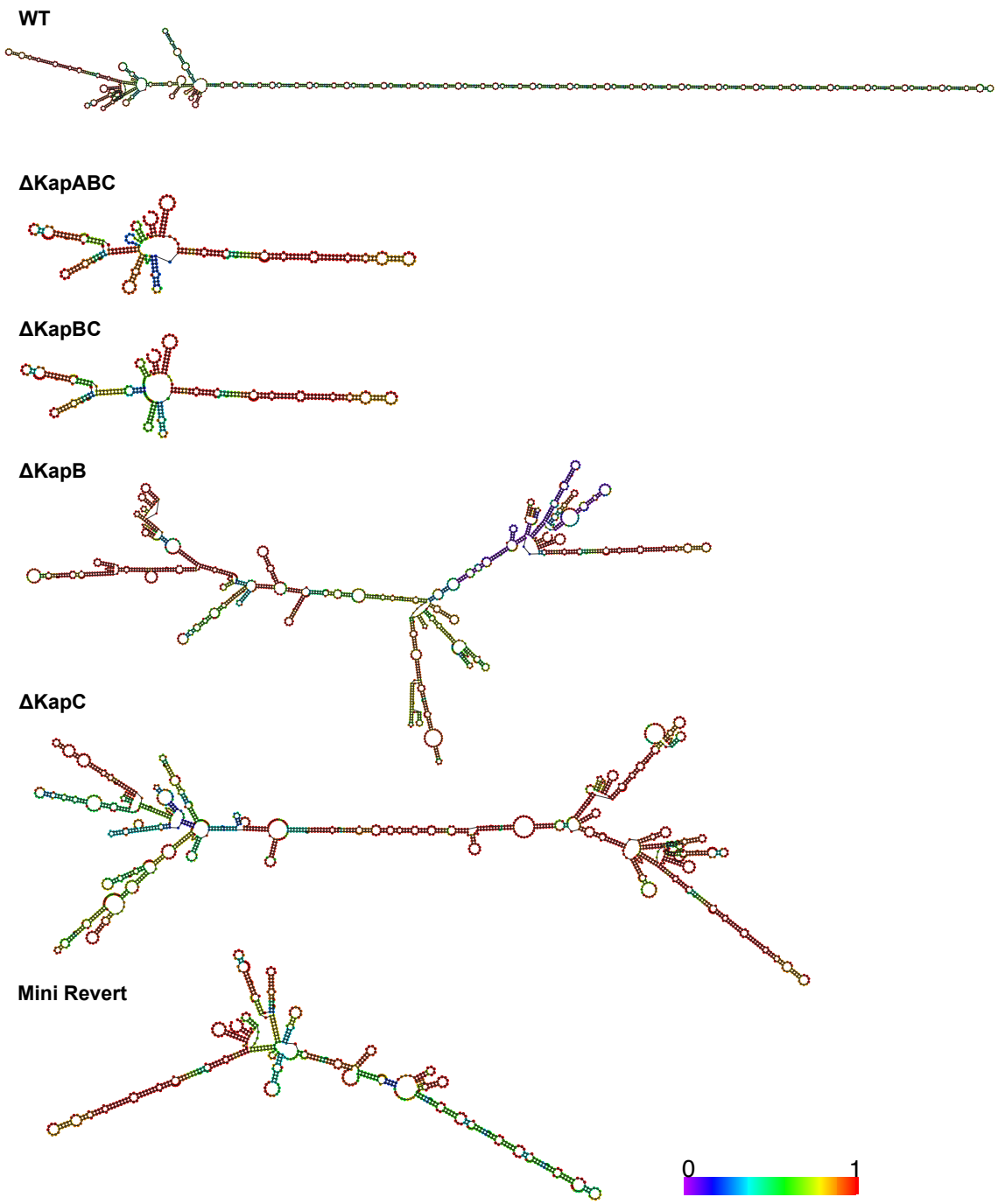

Figure A.2: Alternative coding of the direct repeat regions altered the predicted RNA structure of the kaposin transcript. Nucleotide sequences of the wild-type (WT) and kaposin-mutant transcripts were analysed using RNAfold software, a component of the Vienna RNA package described in Gruber et al., 2008, to obtain predicted minimum free energy RNA secondary structures. Each nucleotide is annotated by colour as a measure of low (purple) to high (red) reliability based on positional entropy and base-pair probability.

Figure A.3: Construction of recombinant BAC16 revertant sequences containing varying number of DR repeats led to partial or incomplete recombination products. (A) PCR primer sets were designed to amplify across the DR regions of the kaposin locus and were tested for their efficiency at amplifying a wild-type (WT) nucleotide sequence. Reaction mixtures were either left untreated or supplemented with either 3% or 5% DMSO. (B) A construct containing the number of repeats corresponding to wild-type DRs (BAC16) or a smaller construct matching the DRs of a KS lung isolate (KS Lung) were electroporated into BAC16-containing GS1783 *E. coli* for Lambda Red recombineering. Antibiotic-resistant bacterial clones were screened by colony PCR using the homology primer identified in (A). (C) Clones containing partial recombination products from (B) were induced to undergo a second recombination event to remove the KanSacB cassette; antibiotic-resistant clones were screened by colony PCR using three sets of primers. Expected sizes of PCR products are indicated in kilobases, kb; PCR products were also screened by Sanger sequencing.

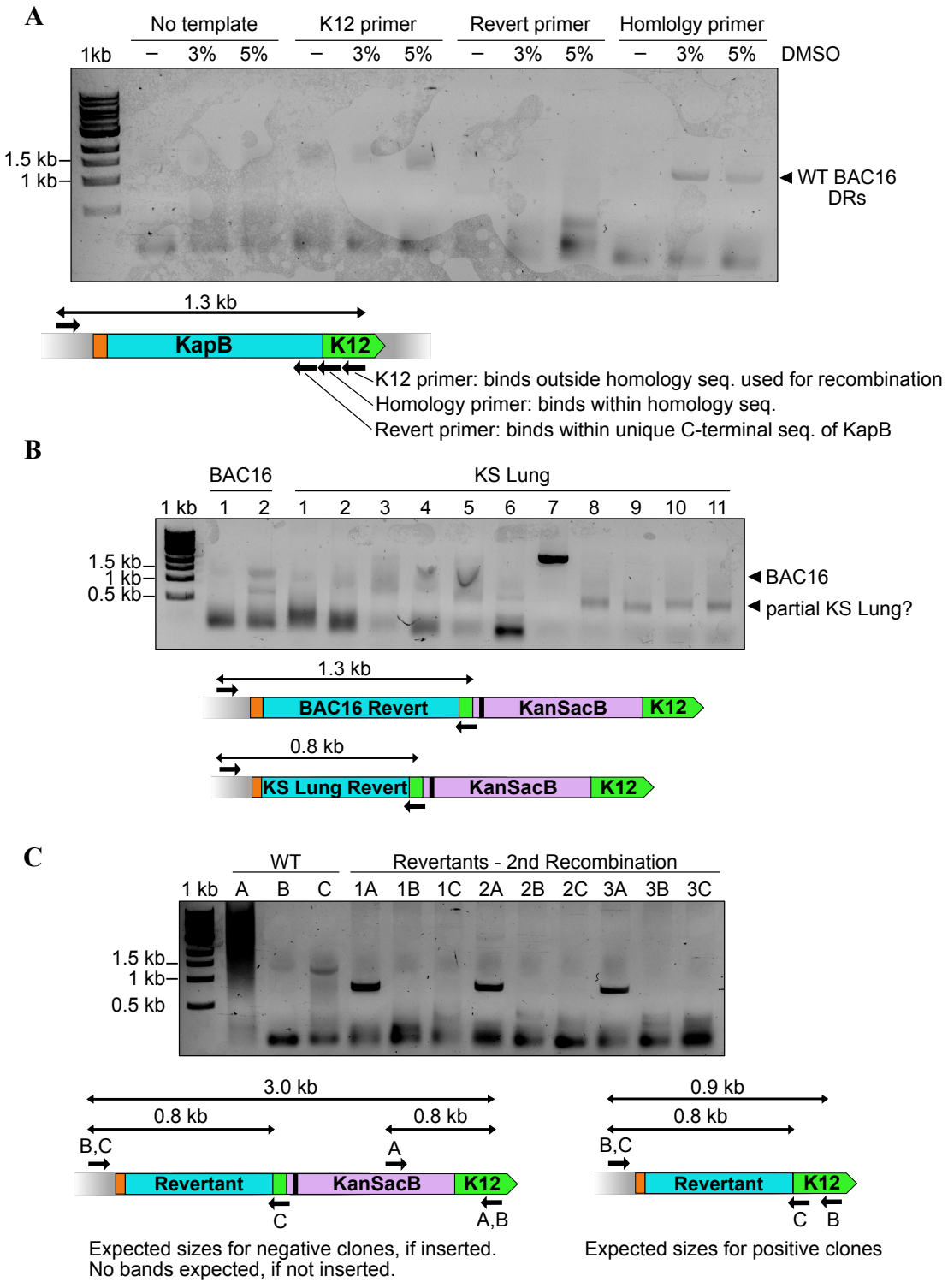

Figure A.3: Construction of recombinant BAC16 revertant sequences containing varying number of DR repeats led to partial or incomplete recombination products.

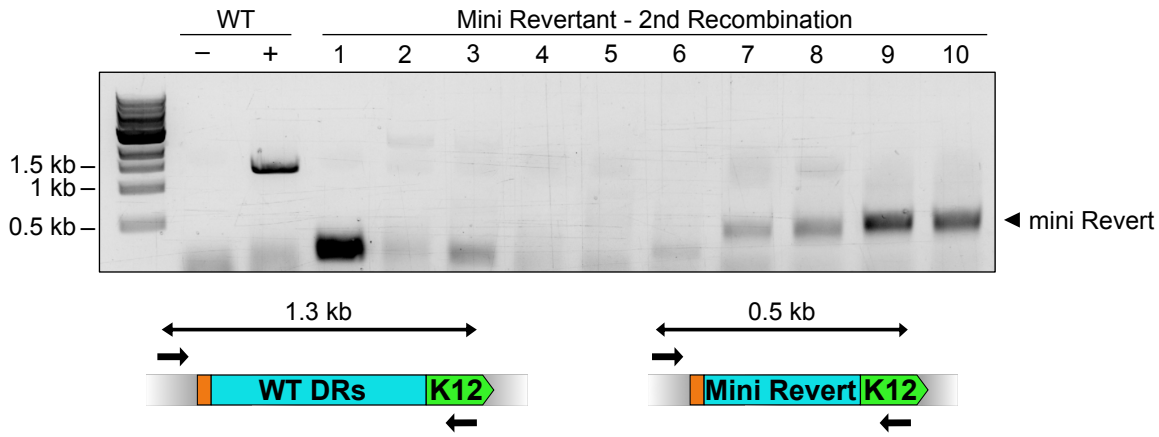

Figure A.4: A kaposin-mutant mini-revertant was constructed in recombinant BAC16 KSHV by Lambda Red recombineering and verified by colony PCR. Colony PCR was conducted on antibiotic-resistant bacterial clones following two rounds of Lambda Red recombination to introduce a miniprotein construct, consisting of one copy each of the direct repeat regions, DR1 and DR2, of the kaposin locus into the KSHV BAC16 genome. Primers designed to amplify regions spanning across the homology ends used for recombination were used to verify the correct size of the insert, in kilobases (kb). PCR amplification using either wild-type BAC16 or no template were used as positive (+) and negative (-) controls, respectively. All PCR products were confirmed by Sanger Sequencing.

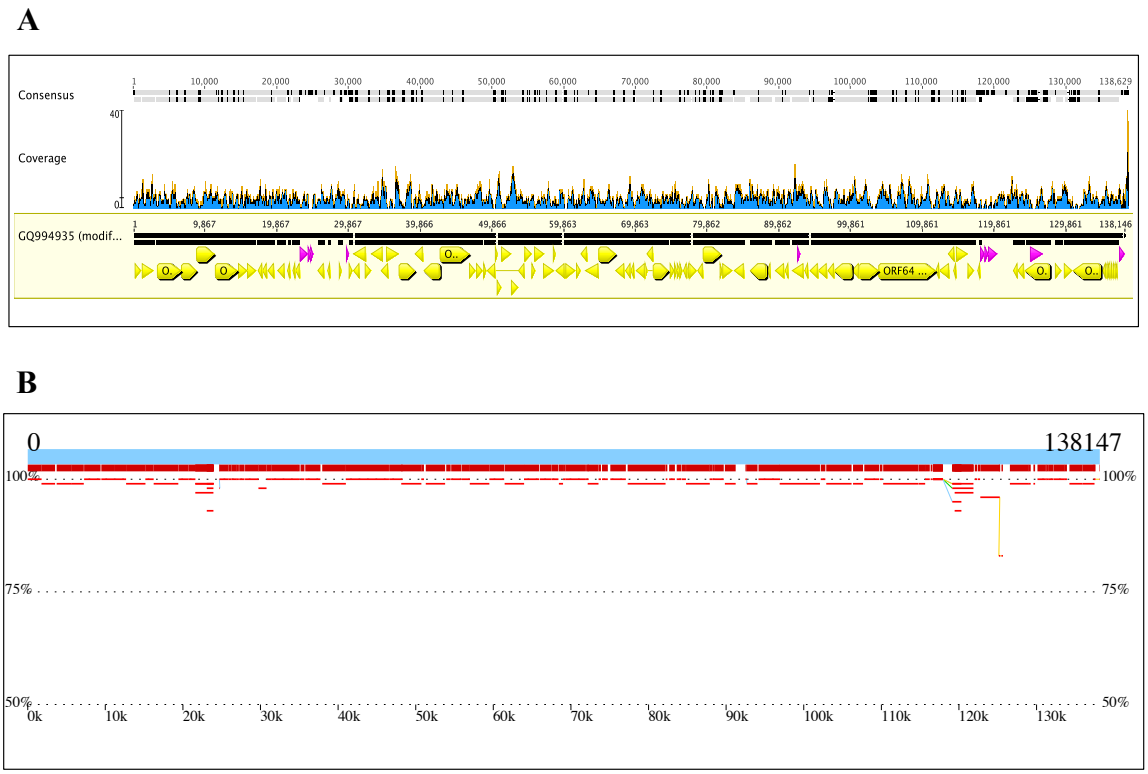

Figure A.5: Next-generation sequencing of BAC16 DNA failed to produce single contiguous pieces of DNA, despite spanning the majority of the KSHV genome. (A) Next-generation sequencing (NGS) reads of wild-type and kaposin-mutant BAC16 DNA were obtained from Illumina MiSeq at the Integrated Microbiome Resource (IMR) at Dalhousie University. Sequencing reads were trimmed based on a quality score >20 and were mapped to the BAC16 KSHV genome (Genbank, accession no. GQ994935, ORFs shown in yellow, repeat regions shown in purple) using Geneious software. A representative image is shown for wild-type BAC16 reads mapping to the consensus sequence with depth of coverage for mapped nucleotides depicted as blue peaks. Gaps in mapped reads are indicated as black bars in the consensus sequence. (B) Paired sequences were trimmed to eliminate base calls with low quality scores and assembled to produce contigs (red bars) matching the ~140-kb Genbank published sequence of BAC16 KSHV by Dr. Bruce Curtis of the Archibald laboratory at Dalhousie University. A representative image is shown for ΔKapBC BAC16 contigs mapped to the consensus sequence with % pairwise identity indicated.

Table A.1: Proportion of reads from Illumina MiSeq of BAC16 DNA mapped to GenBank consensus sequence using Geneious software

BAC16 DNA	No. Total Reads	No. Mapped Reads	Nucleotides Covered in Genome	Mean Coverage Per Nucleotide
Wild-Type	89,458	2,651	88.4 %	4.2 ± 2.9
ΔKapABC	83,247	2,438	86.4 %	3.9 ± 2.7
ΔKapBC	114,387	4,272	94.4 %	6.7 ± 3.7
ΔKapB	70,850	2,485	88.5 %	3.8 ± 2.6
ΔKapC	118,320	3,447	93.6 %	5.6 ± 3.3
Mini-Revert	125,135	3,039	90.6 %	4.8 ± 3.5